eman ta zabal zazu

Universidad del País Vasco
Euskal Herriko Unibertsitatea

Universidad del País Vasco UPV/EHU
Facultad de Medicina y Enfermería
Departamento de Fisiología

The Role of Osteopontin in Liver Fibrosis

Tesis doctoral para optar al grado de Doctor, presentada por:

Wing-Kin Syn

MBChB (Hons) MRCP FRCPE FEBGH FRCP FACP

2017

Directora de la Tesis doctoral:

Patricia Aspichueta Celaá

Table of Contents

Table of Contents

Abbreviations

Abbreviations

AIH: autoimmune hepatitis

ALD: alcoholic liver disease

ALK: activin-like kinase

ALT: alanine aminotransferase

αSMA: α smooth muscle actin

BDL: bile duct ligation

CCL_4: carbon tetrachloride

CD1d: CD1d deficient

CLD: chronic liver disease

CM: conditioned media

DAMP: danger associated molecular pattern

DMP1: dentin matrix protein 1

DSPP: dentin sialophophoprotein

EMT: epithelial mesenchymal transition

ERK: extracellular signal regulated kinase

FFPE: formalin fixed, paraffin embedded

Gli: glioblastoma

GSK3β: glycogen synthase kinase-3β

H&E: hematoxylin and eosin

Hh: hedgehog

HIF-1α: hypoxia-induced factor 1α

HSC: hepatic stellate cell

IBSP: integrin binding sialoprotein or bone sialoprotein

Inh: indian hedgehog

Jα18-/-: Jα18 chain deficient

LMNC: liver mononuclear cell

LPC: liver progenitor cell

LPS: lipopolysaccharide

MAPK: mitogen activated protein kinase

MCD: methionine choline deficient

MEPE: matrix extracellular phosphoglycoprotein

MF: myofibroblast

MMP: matrix metalloproteinase

NAFLD: nonalcoholic fatty liver disease

NASH: nonalcoholic steatohepatitis

NKT: natural killer T

OPN: osteopontin

PBC: primary biliary cholangitis

PCLS: precision cut liver slice

PI3K: Phosphoinositide-3 kinase

PSC: primary sclerosing cholangitis

Ptc: patched

SIBLING: small integrin binding, N-linked glycoprotein

Shh: sonic hedgehog

Smo: smoothened

SR: Sirius red

Src: Src kinase

TGF-β: transforming growth factor β

TIMP: tissue inhibitor of metalloproteinase

TLR: toll-like receptor

TNF-α: tumor necrosis factor α

WT: wild type

Chapter 1: Resumen/Summary

Capítulo 1

El desarrollo de fibrosis en enfermedades hepáticas crónicas (CLD) como las hepatitis víricas B o C, la enfermedad de hígado graso no alcohólica (NAFLD) y la alcohólica supone un reto sin resolver en clínica. Actualmente, no existe ningún tratamiento antifibrótico que reduzca o revierta la progresión de la fibrosis hepática en pacientes con CLD (1). Por tanto, los individuos con fibrosis hepática corren el riesgo de desarrollar cirrosis, y complicaciones como cáncer hepático y fallo hepático, en donde el único tratamiento es el transplante (2, 3). Además, se prevé que la prevalencia de CLD incremente en las próximas décadas, debido principalmente a la epidemia de los factores de riesgo para el desarrollo de NAFLD, que incluye la obesidad, el síndrome metabólico, y la diabetes mellitus tipo 2 (4, 5).

La fibrosis hepática resulta de una reparación fallida después de un daño (6). La reparación involucra los esfuerzos de múltiples tipos celulares (células estelares (HSC) o pericitos hepáticos, células progenitoras (LPCs), células endoteliales, y células inmunes). Durante el daño hepático agudo (como el provocado por fármacos o la resección hepática), se produce la expansión de LPCs y pericitos para reemplazar las células epiteliales que mueren (hepatocitos y colangiocitos), mientras el endotelio sinusoidal regula el tráfico hepático de los distintos subgrupos de células inmunes para eliminar los restos celulares que estimulan la regeneración de nuevas células epiteliales (6, 7). La recuperación se produce cuando el insulto se elimina, y entonces las células muertas se reemplazan con nuevas y funcionales células epiteliales. Por el contrario, esta reparación “restauradora” no tiene lugar durante el daño hepático crónico; la activación sostenida de los pericitos hepáticos y la reprogramación aberrante de las LPCs lleva al depósito y acumulo del exceso de colágeno, induciendo fibrosis. La fibrogénesis es perpetuada, o incluso amplificada porque se produce el reclutamiento de células inmunes con efecto profibrogénico mas que el de subgrupos que resuelvan la fibrosis (8). Estudios recientes muestran que la reparación hepática está finamente regulada por múltiples moléculas de señalización, y que la dicotomía en la respuesta hepática, es decir reparación restaurativa versus reparación desregulada, puede ser explicada en parte por las alteraciones provocadas en estas vías de señalización.

Estas moléculas de señalización incluyen citoquinas, factores de crecimiento y morfogenos.

Previamente, mi investigación se centró en el papel de la vía Hedgehog (Hh), que orquesta la construcción de tejido durante el desarrollo fetal (9, 10). Encontré que en NASH se produce la resurrección de la vía Hh, y que la muerte de hepatocitos provoca la liberación de ligandos Hh, que promueven la viabilidad y la proliferación de las LPC vecinas y la acumulación de miofibroblastos (MF, es decir HSC activadas) (11, 12). En concordancia con los hallazgos en cultivos celulares, animales salvajes que desarrollan fibrosis tras daño hepático también activan la vía Hh. Es de destacar, que animales con excesiva señalización Hh muestran mayor acumulación de MF y LPCs y desarrollan más fibrosis (13, 14). Encontré que la señalización Hh también provoca la reprogramación (transición mesenquimal-epitelial, EMT) de LPCs, que además induce la producción de matriz y fibrosis (15 – 17), y activa la respuesta inmune. Así, el “cross-talk” entre células estromales (HSC y LPCs) y células inmunes dirigido por la señalización Hh regula la respuesta inmune del daño hepático y provoca la activación de MF y LPCs, la desregulación de la reparación hepática y la fibrogénesis. Durante este tiempo, otro grupo de investigación demostró que en el promotor de osteopontina (OPN) hay sitios de unión con Glioblastoma (Gli, factores de transcripción aguas debajo de la vía Hh), y sugirió que la señalización Hh podría regular la transcripción de OPN (18).

OPN es una citoquina pro-inflamatoria y una proteína de la matriz extracelular que se sobreexpresa en inflamación tisular, fibrosis y en malignidad (19). Es de destacar, que los animales deficientes en OPN muestran pobre cicatrización del tejido, es decir menos fibrosis, y están protegidos frente al desarrollo de cáncer, mientras que la sobreexpresión de OPN conduce al exceso de fibrosis y al desarrollo espontaneo de tumores (20, 21). Se han asociado altos niveles de OPN en suero e hígado con la acumulación de neutrofilos en un modelo de steatohepatitis alcohólica (22, 23) y se ha mostrado que la OPN secretada aumenta la activación de NKT y que promueve la acumulación de neutrofilos (24), mientras que los ratones OPN-/- están protegidos frente a la hepatitis inducida por Concavalina A. Todas estas observaciones

me llevaron a hipotetizar que la sobreexpresión de OPN in CLD promueve la fibrinogénesis activando células estromales e inmunes.

En esta tesis primero introduciré el concepto de reparación hepática y presentaré los mecanismos implicados en la fibrosis hepática. A continuación describiré los cuatro estudios planteados para dar respuesta a esta hipótesis.

Para dilucidar el papel de OPN en fibrosis hepática se ha utilizado una combinación de técnicas moleculares e inmunohistoquímicas, cultivos celulares y diferentes modelos animales de daño hepático. La relevancia de estos resultados en la enfermedad humana fue confirmada con estudios de expresión y función de OPN en tejido hepático y HSCs de pacientes que sufrieron transplante hepático por etapa final de enfermedad hepática.

En resumen, el conjunto de estudios que se describen en esta tesis muestran:

1. **Durante el daño hepático crónico, la sobreexpresión de OPN, inducida por la activación de la vía Hh, promueve la fibrosis hepática**

La OPN se sobreexpresa de manera significativa en hígados de pacientes con NASH cirrótico, hígado graso alcohólico (ALD), hepatitis autoinmune (AIH), colangitis biliar primaria (PBC), y colangitis primaria esclerosante (PSC), y en varios modelos murinos de daño hepático incluido el de NASH fibrosis inducido por una dieta deficiente en metionine y colina (MCD). Nosotros mostramos que la OPN derivada de LPC puede actuar de forma paracrina para activar a HSC quiescentes en MF secretoras de colágeno. Las HSC también secretan OPN que auto-regula su fenotipo fibrogénico. Por otro lado, la neutralización de OPN reprime la fibrogenesis de HSC in vitro y reduce la fibrosis hepática in vivo.

A través de experimentos que demuestran que Gli y OPN co-localizan en células hepáticas, y que los niveles de mRNA de OPN incrementan con agonistas de Smoothen, y disminuyen con antagonistas de Smoothen confirmamos la hipótesis de que OPN está regulada por Hh. A través del uso de aptameros para OPN, que neutralizan la OPN circulante, verificamos que OPN es una diana clave aguas debajo de la señalización Hh y no viceversa ya que el neutralizar OPN no ejerce ningún efecto en la expresión celular de Gli2 (diana de Hh), pero reduce de manera significativa la expresión genética fibrogénica, incluso en células deficientes en Ptc con una actividad de la vía Hh incrementada. Los resultados explican porque a la par de evidenciar que los ratones OPN-/- están protegidos frente al desarrollo de NASH fibrosis, observamos que el contenido hepático en células Gli2 (+) y OPN (+) aumentan en paralelo según la fibrosis avanza en pacientes con NAFLD.

2. La OPN interactúa con leptina en NASH.

Al igual que la vía Hh, la OPN es importante como efectora, aguas abajo, de la fibrogenesis inducida por leptina. Es de destacar, que la neutralización de OPN anula la activación de HSC independientemente de la presencia de leptina exógena. Este hallazgo es importante ya que se ha evaluado en distintos estudios la posible utilidad de la administración de leptina a aquellos pacientes con hipoleptinemia y NASH. Sin embargo, si la leptina es directamente pro-fibrogénica, la administración de leptina exógena podría conllevar el empeoramiento de la fibrosis. Mientras que neutralizar la leptina en aquellos pacientes con exceso de leptina y avanzada fibrosis en NASH podría ser una estrategia útil anti-fibrótica, pero al mismo tiempo podría aumentar la ingesta y el peso corporal y con ello el riesgo metabólico, evitando así el efecto beneficioso. Por tanto, en estos casos neutralizar OPN podría ser una atractiva estrategia para afrontar la fibrogénesis inducida por los altos niveles de leptina.

3. La OPN modula la respuesta de LPC

La respuesta de LPC (o la reacción ductular en humanos) es predictiva de fibrosis. Por ello, la respuesta de reparación asociada a las LPC puede ser una diana de gran valor para inhibir la

fibrosis en CLD. Además de inhibir la activación de HSC, el tratamiento con aptameros o anticuerpos anti-OPN atenúa tanto in vivo como in vitro la respuesta de LPC. Nosotros mostramos el mecanismo por el que OPN regula la viabilidad de LPC, y regula directamente el fenotipo de las LPCs, sobreexpresando genes mesenquimales y reprimiendo los epiteliales. La neutralización de OPN inhibe la migración de LPC en el proceso de cicatrización y en ensayos de transmigración. Nosotros mostramos que estos efectores celulares actúan por modulación de la vía TGF-β : La neutralización de OPN reprime los niveles de fosfo-Smad2/3 (indicativos de reducida activación de TGF-β) y mantiene los niveles de los co-represores transcripcionales, ski y SnoN.

4. La OPN derivada de células NKT hepáticas promueve fibrosis en NASH

He reportado en trabajos anteriores que la activación de la vía de Hh en CLD aumenta la acumulación de las células NKT (16). En este trabajo, nosotros confirmamos y ampliamos esos hallazgos mostrando que la fibrogénesis en ratones que desarrollan NASH inducido por la dieta depende directamente de las células NKT y que las acciones fibrogénicas de las células NKT están directamente mediadas por OPN. En comparación con los animales WT, dos cepas de ratones deficientes en células NKT (Jα18-/- and CD1d-/-) mostraron una marcada atenuada fibrosis tras 8 semanas de dieta MCD.

En resumen, estos hallazgos confirman que la OPN promueve la fibrogenesis hepática, y sugieren que la OPN puede ser una atractiva diana anti-fibrótica porque modula distintos mecanismos coordinados.

Relevancia clínica

Numerosas evidencias sugieren que la OPN es un efector clave en alteraciones metabólicas (25). La OPN esta incrementada en tejido adiposo inflamado, en endotelio vascular inflamado, y está sobreexpresada en la enfermedad isquémica de corazón y en diabetes tipo 2 (26 – 29). Los animales deficientes en OPN también muestran mejoría en la sensibilidad periférica a la insulina y en los perfiles metabólicos (mejora el manejo de lípidos y glucosa) (25). Los resultados aquí

mostrados apoyan la idea de que OPN puede ser una diana para beneficiar a pacientes con fibrosis en avanzado NASH. Estos resultados son de alta relevancia en clínica ya que se han desarrollado anticuerpos y aptameros de humano para inhibir las acciones de OPN que podrían ser usados para tratar a pacientes con NASH avanzado.

Chapter 1

The development of fibrosis in chronic liver diseases (CLD) such as viral hepatitis B or C, alcoholic liver disease, autoimmune liver diseases, and nonalcoholic fatty liver disease (NAFLD) presents a vast unmet clinical challenge. At present, there is no effective anti-fibrotic treatment that halts or reverses the progression of liver fibrosis in patients with CLD (1). Individuals with liver fibrosis are therefore, at risk of developing cirrhosis, and complications such as liver cancer and liver failure, for which the only potential treatment is a liver transplant (2, 3). Furthermore, the prevalence of CLD is predicted to increase in coming decades due to the global epidemic of major risk factors for NAFLD including obesity, the metabolic syndrome, and type 2 diabetes mellitus (4, 5).

Liver fibrosis is the result of 'mis-repair' following injury (6). Normal liver repair involves the concerted efforts of multiple cell types (hepatic stellate cells (HSC) or liver pericytes, liver progenitor cells (LPCs), endothelial cells, and immune cells). During acute liver injury (such as following acute drug injury or liver resection), expansion of LPCs and pericytes occur to replace dying epithelial cells (hepatocytes and cholangiocytes), while sinusoidal endothelium regulates the trafficking of immune cell subsets in the liver to remove cellular debris which further stimulates regeneration of new epithelial cells (6, 7). Recovery occurs when the insult is removed, and dying cells are replaced by functioning new epithelial cells. By contrast, such 'restorative' repair does not occur during chronic liver injury; sustained activation of liver pericytes and aberrant reprogramming of LPCs lead to excess collagen deposition and accumulation (i.e. fibrosis). Fibrogenic outcomes are perpetuated, or even amplified by the preferential recruitment of 'effector – profibrogenic' immune cells rather than 'fibrosis-resolving' subsets (8). Recent studies show that liver repair is normally tightly regulated by multiple molecular signals, and that the dichotomy in liver outcomes (i.e. restorative repair vs. deregulated repair) may be explained in part, by perturbations in these signaling pathways.

Some of these cellular signals include cytokines, growth factors, and morphogens. Previously, my research had focus on the role of the Hedgehog (Hh) pathway, which normally orchestrates tissue

construction during foetal development (9, 10). I found that resurrection of the Hh pathway occurs in NASH, and that dying hepatocytes release Hh ligands which promote the viability and proliferation of neighboring LPCs and the accumulation of myofibroblasts (MF; i.e. activated HSC) (11, 12). Consistent with cell culture findings, wild-type (WT) mice which develop liver fibrosis after injury also activate the Hh pathway. Importantly, Patched-deficient (Pt+/-) mice with excessive Hh signaling exhibit even greater accumulation of MF and LPCs and develop more fibrosis (13, 14). I found that Hh signaling also induces the re-programming (epithelial-to-mesenchymal transition, EMT) of LPCs, which further increasing matrix-production and fibrosis (14), and also activates immune responses (15 – 17). Thus, stromal cell (HSC and LPCs) - immune cell cross-talk driven by Hh signaling regulates immune responses to liver injury and drives the activation of MF and LPCs, resulting in dysregulated repair and fibrogenesis. During this time, a group demonstrated Glioblastoma (Gli, downstream transcription factors of the Hh pathway) binding sites in the OPN promoter and suggested that Hh signaling might regulate also OPN transcription (18).

OPN is a pro-inflammatory cytokine and matrix protein which is upregulated during tissue inflammation, fibrosis, and malignancy (19). Interestingly, mice deficient in OPN exhibit poor wound healing (i.e. less fibrosis), and are protected from cancers, while the overexpression of OPN leads to excess fibrosis and spontaneous tumour development (20, 21). Elevated serum and liver OPN are also associated with neutrophil accumulation in a model of alcoholic steatohepatitis (22, 23), and secreted OPN was shown to augment NKT activation and promote neutrophil accumulation (24), while OPN-/- mice are protected from Concavalin-A hepatitis. These observations led me to *hypothesize* that overexpression of OPN in CLD promotes fibrogenesis by activating stromal and immune cells.

In this thesis, I will first introduce the concept of liver repair and summarize mechanisms of liver fibrosis. I will then describe the four studies which were aimed at addressing the hypotheses.

A combination of cell culture, immunohistochemistry, and molecular techniques in association with mouse models of liver injury were used to elucidate the mechanistic roles of OPN in liver fibrosis. Their relevance to human liver disease were confirmed by studies of OPN expression and function in human liver tissues and isolated HSCs from patients who had undergone liver transplant surgery for end-stage liver disease.

In sum, the collective studies described in this thesis show that:

1. **OPN is upregulated by Hh pathway activation during chronic liver injury and promotes liver fibrosis**

OPN is significantly overexpressed in livers from cirrhotic human NASH, alcoholic liver disease (ALD), autoimmune hepatitis (AIH), primary biliary cholangitis (PBC), and primary sclerosing cholangitis (PSC), and in several murine models of liver injury including the methionine choline deficient (MCD) diet model of NASH fibrosis. We show that LPC derived OPN can act in a paracrine fashion to activate quiescence HSC into collagen secreting MF. HSC themselves also secrete OPN which auto-regulate its fibrogenic phenotype. OPN neutralization on the other hand, represses HSC fibrogenesis in vitro and reduces liver fibrosis in vivo.

By demonstrating co-localization of Gli and OPN in liver cells, and proving that expression of OPN mRNA is increased by a Smoothened agonist, and decreased by a Smoothened antagonist, we confirm the hypothesis that OPN is Hh regulated. Using OPN aptamers (which neutralizes circulating OPN), we verify that OPN is a key down-stream target of Hh signaling (rather than vice versa) because neutralizing OPN had no effect on cellular expression of Gli2 (a Hh target), but significantly reduced fibrogenic gene expression, even in Ptc+/- mouse derived cells with supra-normal Hh pathway activity. Coupled with the evidence that OPN-/- mice are significantly protected from NASH fibrosis, the data explain why we observe that hepatic content of Gli2(+) cells and OPN (+) cells increased in parallel as liver fibrosis advanced in patients with NAFLD.

2. OPN interacts with leptin in NASH.

Like Hh, OPN is an important downstream effector of leptin-induced fibrogenesis. Importantly, OPN neutralization abrogates HSC activation despite the presence of exogenous leptin. This finding is clinically informing because studies have evaluated the potential utility of leptin replacement in those with hypoleptinemia-NASH. However, if leptin is directly pro-fibrogenic, the supplementation of exogenous leptin may inadvertently lead to worsening fibrosis. While leptin neutralization in those with advanced NASH-fibrosis (and excess leptin) may be a useful anti-fibrotic strategy, it is also likely to increase food intake and body weight (and metabolic risk), thereby negating any potential clinical benefit. Thus OPN neutralization could be an attractive strategy in the face of high leptin levels.

3. OPN modulates the LPC response

The LPC response (or the ductular reaction in humans) is predictive of subsequent fibrosis hence, targeting the LPC associated repair response may be of value in inhibiting fibrosis in CLD. In addition to inhibiting HSC activation, treatment with OPN aptamers or OPN neutralizing antibodies also attenuated the LPC response in vitro and in vivo. Mechanistically, we show that OPN is an important viability factor for LPCs, and directly regulates LPC phenotype by upregulating mesenchymal genes while repressing epithelial ones. OPN neutralization conversely inhibits LPC migration in both wound healing and transmigration assays. We find that these cellular effects occur via modulation of the TGF-β pathway: OPN neutralization represses phospho-Smad2/3 levels (indicative of reduced TGF-β activation) and maintains levels of transcriptional co-repressors, Ski and SnoN.

4. Liver NKT cell derived OPN promotes NASH fibrosis

I had previously reported that Hh pathway activation in CLD enhances hepatic accumulation of NKT cells (16). Herein, we confirm and extend those findings by showing that fibrogenesis in mice with diet-induced NASH directly depends upon NKT cells and that the fibrogenic actions of NKT

cells are directly mediated by OPN. Compared with WT mice, two strains of NKT cell deficient mice (Jα18-/- and CD1d-/-) exhibited dramatically attenuated fibrosis after 8 weeks of MCD diet.

In sum, these findings confirm that OPN promotes liver fibrogenesis, but also suggest that OPN could be an attractive anti-fibrotic target because it modulates multiple concerted mechanisms.

Clinical Relevance

Accumulating evidence suggest that OPN is a key effector of metabolic outcomes (2). OPN is significantly increased in inflamed adipose tissues, in inflamed vascular endothelium, and is upregulated in patients with ischemic heart disease and type 2 diabetes mellitus (26 – 29). Mice genetically deficient in OPN also exhibit improved peripheral insulin sensitivity and metabolic profiles (improved lipid and glucose handling) (25). The current data support the concept that targeting OPN may be beneficial in patients with advanced (NASH) fibrosis. These results are clinically important because humanized antibodies and aptamers which inhibit OPN actions have been developed, and may be used to treat patients with advanced NASH.

Chapter 2: Introduction

Chapter 2

Fibrosis progression: Putative mechanisms and molecular pathways

Syn WK and Diehl AM. In: Williams R and Taylor-Robinson SD, eds. Clinical Dilemmas in Non-Alcoholic Fatty Liver Disease, 1st edition. John Wiley & Sons, Ltd. 2016; 61 – 71

2.1. The Concept of Liver Repair

Although a significant number of studies have been performed to help characterize NAFLD progression, the concept of repair is applicable across all CLD.

The presence of dying and ballooned hepatocytes distinguishes NASH, a more advanced stage of NAFLD from simple steatosis (30, 31). Excessive free fatty acid influx, de novo lipogenesis, and impaired fatty acid oxidation lead to steatosis. Subsequent oxidative, cytotoxic and immune stresses then promote hepatocyte injury and death. Fat-laden hepatocytes which remain are unable to replicate and replace the lost hepatocytes, thereby triggering an expansion of LPCs (or stem cells) which attempt to restore architecture and function (32, 33). This LPC response is termed the ‘ductular reaction’ in humans, is a harbinger of fibrosis, and is characteristic of progressive liver disease (34).

2.1.1. Hepatocyte Cell Death

Gores and colleagues first reported an increased number of apoptotic hepatocytes in patients with NASH (30), and showed that the magnitude of apoptosis positively correlated with disease grade and stage (35). Mice deficient in caspase-2 (an initiator caspase responsible for long-chain fatty acid-induced cell death) exhibited reduced hepatocyte apoptosis and developed significantly less fibrosis when fed the high-fat (a model of steatosis and early NASH) or the MCD diet (a model of advanced NASH-fibrosis) (36). Pharmacologic approaches using a pan-caspase inhibitor similarly resulted in decreased active caspase-3, cell death, and fibrosis (37). These studies in animal models and in humans show that hepatocyte death is intricately linked to NASH progression.

2.1.2. Tissue Repair and Fibrogenesis

The loss of functioning hepatocytes is accompanied by a compensatory proliferation of LPCs (i.e. liver stem cells) located in the Canal of Hering. These LPCs are surrounded by liver pericytes (referred to as HSC), portal fibroblasts, and an extracellular matrix enriched with endothelial cells forming neovasculature. LPCs, liver pericytes, stromal cells, and extracellular matrix collectively constitute the progenitor niche (38, 39).

For many individuals with CLD, fibrosis (i.e. deregulated repair) is the general outcome. Although the reasons for this remain poorly understood, animal studies show that factors stimulating the progenitor response are pro-fibrogenic, and LPCs themselves are highly reactive and secrete high levels of pro-inflammatory and pro-fibrogenic cytokines. Fate-mapping and immunohistochemistry studies demonstrate that LPCs may be directly re-programmed, from an epithelial to a mesenchymal (EMT) (and possibly fibrogenic) phenotype (40, 41), and recently liver pericytes were identified as multi-potent progenitors capable of secreting collagen matrix as well as giving rise to new epithelial progenitors (i.e. mesenchymal to epithelial phenotype) (42, 43). In addition, the progenitor-derived 'secretome' can act on neighbouring immune and endothelial cells to perpetuate and amplify fibrogenic outcomes (15, 44). Thus, the resultant ductular reaction observed during chronic injury should be considered a fibrogenic repair response (i.e. fibrosis promoting). 'Restorative' repair (where progenitors differentiate into new, functioning epithelial cells) occurs when the injury and pro-fibrogenic / pro-inflammatory stimuli are removed.

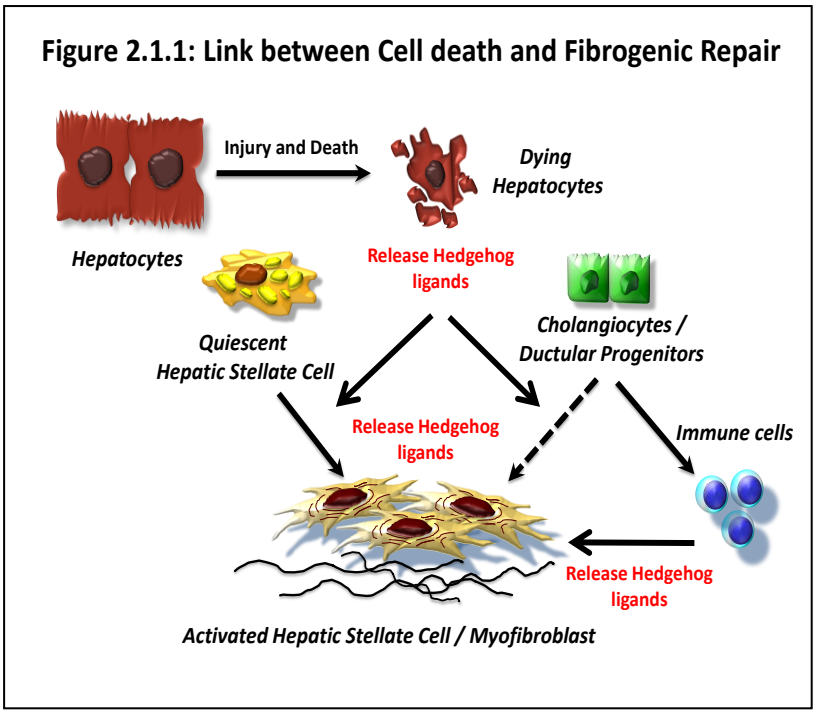

Fig. 2.1.1: Link between cell death and liver fibrosis.
Hepatocyte injury or death leads to the release of signalling factors (such as Hh) which promote the proliferation of ductular progenitors (or LPCs) and HSC as part of the repair response. Activated HSCs transform into collagen secreting myofibroblasts. LPCs secrete chemokines which recruit immune cells into the liver. In turn, recruited immune cells secrete even more cytokines and growth factors that perpetuate the fibrogenic response. LPCs may also undergo EMT into scar-producing myofibroblasts.

(From: Fibrosis progression: Putative mechanisms and molecular pathways by Syn WK and Diehl AM; in Clinical Dilemmas in Non-Alcoholic Fatty Liver Disease, First Edition, 2016. John Wiley & Sons, Ltd.)

2.2. Mechanisms of Liver Fibrosis

Despite ample evidence showing that cell death triggers fibrogenesis, the mechanistic link remains poorly understood. Previously, it was proposed that phagocytosis of apoptotic hepatocytes by macrophages and HSC led to secretion of pro-fibrogenic mediators (45). In turn, these promoted HSC activation and fibrosis (an indirect mechanism). More recently, injury-associated inflammasome activation and release of damage-associated molecular patterns (DAMPs) were reported to promote disease progression (46). Inflammasome activation and DAMP release triggers immune cell recruitment, and RAGE, a receptor for high-mobility group box 1 (an example of DAMP), is required for LPC proliferation (47). Despite this, there is no convincing evidence for DAMPs directly activating HSC.

Recent studies suggest that soluble mediators released by injured and dying hepatocytes are major regulators of repair. Using cell culture and in vivo models, we showed that stressed or dying hepatocytes release Hedgehog (Hh) ligands, a morphogen normally responsible for orchestrating tissue development and cell fate (11). Hh ligands directly stimulate LPC and HSC (i.e. fibrogenic repair) (14, 48), provoke secretion of chemokines which lead to the recruitment of inflammatory cells (i.e. repair-associated inflammation) (15), and promote capillarisation of liver sinusoidal endothelium (44); features characteristic of progressive liver disease. Importantly, the level of Hh pathway activation correlated with the amount of injury and fibrosis (14, 49), suggesting that targeting the Hh pathway could be beneficial in the treatment of fibrosis.

2.2.1. Local Regulation of Fibrogenesis

Liver disease outcomes are dictated by the prevailing microenvironment. For example, an upregulation of pro-fibrogenic molecules would promote scar deposition and accumulation, while an excess of matrix degrading enzymes could facilitate resolution of fibrosis.

Cytokines and growth factors are small soluble proteins secreted by immune cells, progenitor and ductular cells (cholangiocytes), liver pericytes, and endothelial cells, and are responsible for mediating cellular crosstalk (cell to cell communication) and regulating tissue metabolic responses. TGF-β for example, is the prototypical pro-fibrogenic cytokine that is upregulated during CLD, and promotes LPC and pericyte proliferation and activation (50). Other novel mediators include Hh and OPN.

The extracellular matrix is dynamically regulated, even during progressive fibrogenesis. The deposition of fibrillar collagens (especially collagen type 1), elastin, and matrix proteins by liver pericytes is matched by activities of matrix metalloproteinases (MMPs) (endopeptidases responsible for matrix degradation) produced by inflammatory cells and pericytes. MMPs in turn, are inhibited by extracellular inhibitors of metalloproteinases (TIMPs), which bind to active MMPs to inhibit their enzymatic activities (51, 52). The balance between MMPs and TIMPs alters the rate

and pattern of matrix degradation, allowing for the fine regulation of matrix turnover. As an example, mice overexpressing TIMP1 developed more fibrosis, and failed to remodel the matrix during the fibrosis-resolution phase, while rats overexpressing MMP8 developed less fibrosis (53).

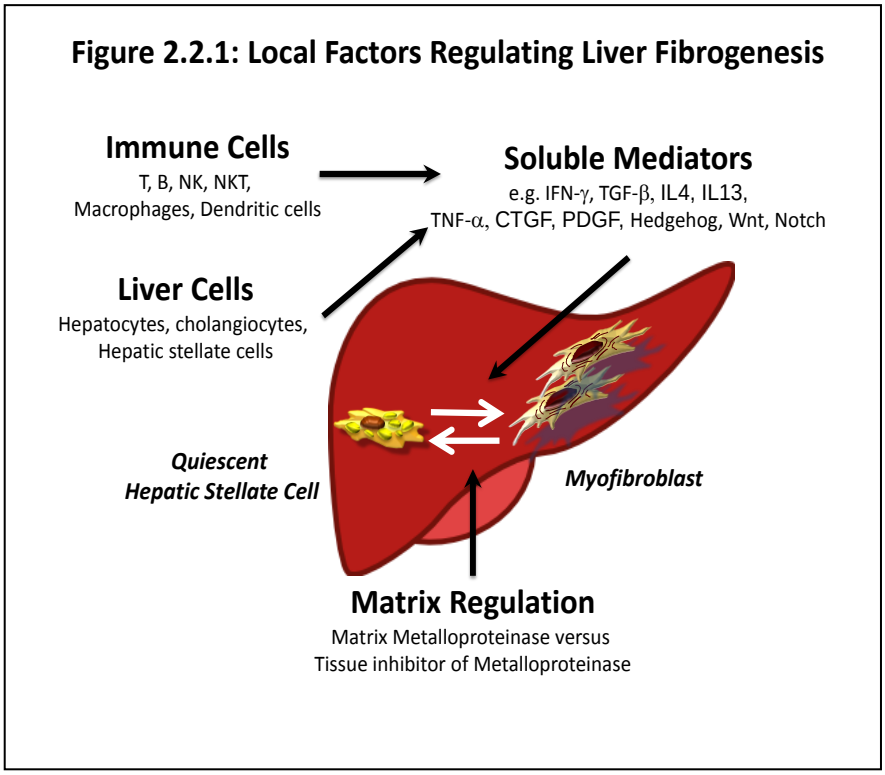

Fig. 2.2.1: Local Factors Regulating Liver Fibrogenesis

HSC activation occurs in the presence of pro-fibrogenic factors. Cytokines (e.g. IFN-γ,TNF-α, TGF-β, IL4, IL13), growth factors (PDGF, CTGF), and morphogens (Hh, Wnt, Notch) are secreted by resident liver cells, as well as recruited immune cells (T cells, NK cells, NKT cells, T regulatory cells, γδT cells, monocytes and macrophages). Matrix composition is dynamically regulated by MMPs responsible for matrix degradation. In turn, MMPs are inhibited by TIMPs.

(From: Fibrosis progression: Putative mechanisms and molecular pathways by Syn WK and Diehl AM; in Clinical Dilemmas in Non-Alcoholic Fatty Liver Disease, First Edition, 2016. John Wiley & Sons, Ltd.)

Chronic liver injury is often associated with the *recruitment of immune subsets (chronic inflammation)* into the liver (54). Activated T and B cells, T-regulatory cells, natural killer and NKT cells, monocyte-macrophage subsets, dendritic and innate lymphoid cells, together constitute the innate and adaptive arms of the immune response. Collectively, these cells are responsible for maintaining liver tolerance on one hand, and for defence on the other (patrolling and clearance of cellular debris). Trafficking of immune cells into the liver is tightly regulated by chemokines (chemotactic cytokines), and expression of specific adhesion molecules on the liver sinusoidal endothelial surface (55). Mice genetically deficient in NKT cells are protected from NASH fibrosis,

while the accumulation of inflammatory macrophages promotes fibrogenesis. The role of macrophages is complex and recent studies suggest that a Ly6C intermediate – low subset is a key source of MMPs during fibrosis resolution (56). Thus, inhibiting recruitment of the 'pro-fibrogenic' subset could prevent fibrosis development, while increasing recruitment of the 'pro-resolution' subset could enhance fibrosis resolution through secretion of MMP12 and MMP13.

2.2.2. Other Factors Regulating Liver Fibrosis

Gut-Liver

The human intestine normally harbours a diverse community of microbes that promotes metabolism and digestion in a symbiotic relationship with the host. Cumulative evidence show that changes to the intestinal microbiota (dysbiosis) lead to adverse liver outcomes. For example, compositional changes may increase energy extraction from food and result in the development of NAFLD (57). Feeding mice with a high-fat diet and inducing dysbiosis (by reducing the ratio between Bacteriodetes and Firmicutes, while increasing gram negative proteobacteria) accelerate fibrogenesis (58). Mechanistically, dysbiosis causes intestinal inflammation, a loss of intestinal barrier, and the translocation of microbial products (such as lipopolysaccharides, LPS). These lead to activation of pattern recognition receptors such as Toll-like receptors (TLR) 4, and perturbations in choline and bile acid metabolism. Interestingly, altered interactions between microbiota and inflammasome sensing may also govern the rate of NAFLD progression. To date, most of these data arise from animal experiments; better designed, longitudinal studies in humans are needed.

Adipose-Liver

The adipose tissue is a metabolically active, 'cytokine factory'. The vast majority of individuals with NAFLD are overweight or obese, and in these individuals, the adipose tissue is enriched with immune infiltrates and secretes high levels of pro-inflammatory, pro-fibrogenic cytokines including leptin and tumour-necrosis factor alpha (TNF-α) (59). Serum leptin levels are significantly upregulated in patients with NASH, and have been shown to directly activate HSC and potentiate TGF-β mediated effects (2, 60). By contrast, adiponectin levels are inversely correlated with fat

mass, and are suppressed in patients with NASH. Adiponectin exerts hepato-protective and anti-fibrogenic effects, and mice with adiponectin deficiency developed more severe liver fibrosis after the high-fat diet (61).

2.2.3. Putative Molecular Pathways

Distinct mechanisms and multiple signals from liver cells, immune cells, and extra-hepatic tissues are integrated to generate a coherent repair response. We will highlight three molecular pathways currently being evaluated as targets for anti-fibrotic treatments.

TGF-β

TGF-β is the most potent pro-fibrogenic cytokine which induces fibrosis by direct activation of HSC and LPC, stimulating the synthesis of extracellular matrix, and inhibiting matrix degradation through the production of TIMPs (50). TGF-β is secreted as an inactivated protein bound to a latency-associated peptide; when activated, TGF-β then signals through its cognate receptors (i.e. activin-like kinase, ALK5), leading to the phosphorylation and nuclear translocation of its transcription factors, Smad2/3.

The overexpression of TGF-β promotes fibrosis while deletion of TGF-β and Smad3 protects against fibrosis. Therefore, targeting this pathway appears to be attractive, and multiple approaches include anti-sense oligonucleotides (which inhibit TGF-β mRNA), specific neutralizing antibodies (that interfere with ligand binding), natural TGF-β antagonists (such as Smad7), and TGF-β receptor - kinase blockers. However, as TGF-β signaling is also important for tumour suppression, immune regulation, and cell differentiation, strategies that selectively target excess matrix deposition and accumulation will need to be developed. In a recent study, investigators described the selective delivery of an ALK5-inhibitor by coupling the compound to mannose-6-phosphate human serum albumin (M6PHSA) which allows selective uptake by HSC (the main liver cell type responsible for matrix deposition) (62). In another, specific blockade or loss of HSC-

expressing αv integrins (by pharmacologic and genetic approaches, respectively) inhibited TGF-β activation and fibrogenesis (63).

Hh signaling

The Hh pathway is critical for tissue development and cellular responses including proliferation, apoptosis, and differentiation (9, 10). Excessive activation of the Hh pathway during development leads to childhood cancers such as medulloblastoma, while inactivity impairs wound healing.

Components of the Hh pathway:

The binding of Hh ligands (Sonic Hh or Indian Hh) to cognate receptor Ptc, on cell surface membranes leads to the depression of a co-receptor Smoothened (Smo). Depressed Smo is responsible for the transduction of signals downstream, and leads to the nuclear translocation of Gli1, 2, 3 transcription factors and expression of Hh-target genes (i.e. canonical Hh signaling). Ptc / Smo-independent activation of the Hh pathway has also been described (i.e. non-canonical Hh signaling).

Relationship between Hh and other pro-fibrogenic factors:

The regulation of the Hh signaling pathway is complex, and future studies will be needed to fully understand the effects of canonical versus non-canonical pathways on liver outcomes. Interestingly, leptin and PDGF effects are mediated by increased secretion of Hh ligands (canonical signaling) (64), while TGF-β and insulin-like growth factor enhances non-canonical Hh signaling (65). TGF-β induces Gli transcription and Gli protein stabilization, while insulin-like growth factor inhibits Gli phosphorylation by glycogen synthase kinase-3β (GSK-3β), preventing its proteosomal degradation (i.e. more pathway activation). More recently, Hh signaling has also been shown to be a regulator of the LPS response, and links hypoxia with fibrosis via hypoxia-induced factor (HIF)-1α.

Summary of Hh actions:

Injured (endoplasmic reticulum stress) or dying hepatocytes (pro-apoptotic stimuli) produce high levels of Hh ligands which act on surrounding liver progenitors, liver pericytes, sinusoidal endothelium, and immune cells (i.e. Hh-responsive cells) (11, 12).

1. Hh ligands stimulate HSC proliferation and promote their transition into collagen-producing MF. In turn, HSC and MF secrete additional Hh ligands that amplify fibrogenesis (48, 64).
2. Hh ligands induce proliferation of LPCs and promote reprograming of epithelial LPCs into mesenchymal (fibrogenic) phenotype (14). They also stimulate the secretion of chemokines such as CXCL16, which recruit inflammatory T and NKT cell subsets into the liver (15)
3. Infiltrating immune cells are Hh-responsive, and activated T cells, NKT cells, and macrophages secrete Hh ligands which perpetuate liver injury (16, 17, 66)
4. Activation of the Hh pathway activates sinusoidal endothelial cells, upregulates expression of key adhesion molecules and induces capillarisation of sinusoidal endothelium (44).

Evidence of the Hh pathway in Human Liver Disease

There is minimal Hh pathway activity in a healthy adult liver. By contrast, Hh pathway activation occurs in CLD (ALD, NAFLD, PBC, and chronic viral hepatitis), and activity of the Hh pathway parallels liver fibrosis stage (13, 14, 49, 67, 68).

Modulating the Hh pathway in vivo:

Activation of the Hh pathway also occurs in models of liver fibrosis (chronic carbon tetrachloride (CCL4), bile duct ligation (BDL), MCD diet (NASH), alcohol-induced injury, and genetic models of biliary fibrosis or NAFLD), and mice genetically engineered to exhibit greater Hh pathway activation developed more liver fibrosis than wild type mice (11, 13, 14, 69). Inhibiting the Hh pathway by pharmacological (i.e. cyclopamine or GDC-0449; both Smo antagonists) or genetic approaches (i.e. conditional deletion of the Smo gene) prevents fibrosis progression (14, 40, 41). The aggregate data in humans and mice suggest that the Hh pathway is a key regulator and integrator of fibrogenic signals (such as LPS-TLR4, leptin, TGF-β, HIF-1α). Hh pathway inhibitors

such as Vismodgib (GDC-0449) are already licensed for use in patients with advanced skin and haematological cancers, and should be evaluated as anti-fibrotic agents.

2.3. Osteopontin (gene: Spp1)

OPN is both a pro-inflammatory cytokine and a matrix protein. It is also known as secreted phosphoprotein 1 or early T cell activation factor, and is an acidic member of the small integrin-binding ligand N-linked glycoprotein (SIBLING) family of proteins. OPN is highly upregulated in inflamed and fibrotic tissues of the skin, lungs, kidneys, and joints, and also in malignancy (19). OPN expression is regulated by cytokines (TNF-α, IL-6, IL-1), growth factors, adipokines, and morphogens (Wnt and Notch). Interestingly, Glioblastoma (Gli, downstream transcription factors of the Hh pathway) binding sites have also been demonstrated in the OPN promoter, suggesting that Hh signaling might regulate OPN transcription (18).

The OPN molecule contains an arginine-glycine-aspartic acid (RGD) sequence which can bind several integrins including $\alpha_v\beta_1$, $\alpha_v\beta_3$, $\alpha v\beta_5$, $\alpha_5\beta_1$, $\alpha_8\beta 1$ (70, 71). Enzymatic (e.g. by thrombin; tOPN) cleavage reveals a SVVYGLR amino-acid sequence in humans (or SLAYGLR in mice) which binds $\alpha_4\beta_1$ and $\alpha_9\beta 1$ (72 – 75). OPN also binds to CD44 via non-RGD domains to regulate migration, adhesion and proliferation, and engagement of OPN with integrins and CD44 leads to the activation of diverse signaling pathways (PI3K, MAPK, ERK, Src) (21, 76).

Figure 2.3.1: Osteopontin and SIBLINGs

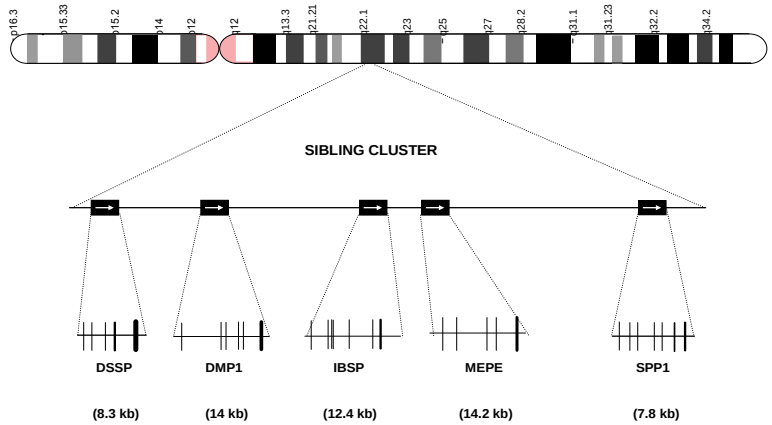

Fig. 2.3.1: Osteopontin and SIBLING family of proteins. OPN (*SPP1*) is located on chromosome 4, specifically in the region 4q22.1. It is part of a cluster of 5 genes that together form the SIBLING family, which contain the following genes: the dentin sialophosphoprotein (*DSPP*), the dentin matrix protein 1 (*DMP1*), the bone sialoprotein (*IBSP*), the matrix extracellular phosphoglycoprotein (*MEPE*), and osteopontin (*SPP1).*

(From: Briones-Orta MA ….Syn WK. Osteopontin splice variants and polymorphisms in cancer progression and prognosis. Biochim Biophys Acta. 2017 Feb 28; 1868(1):93-108)

2.3.1. OPN in the Liver

Elevated serum and liver OPN are associated with neutrophil accumulation in a model of alcoholic steatohepatitis (22, 23), and secreted OPN has been shown to augment NKT activation and promote neutrophil accumulation (24). By contrast, OPN-/- mice are protected from Concavalin-A hepatitis. In the beta-glucan hepatic granuloma model, OPN-/- mice also accumulated fewer liver macrophages, T cells, DC, expressed lower TNF-α, and developed less severe injury (78). Importantly, mice deficient in OPN also exhibit poor wound healing (i.e. less fibrosis), and are protected from cancers, while the overexpression of OPN leads to excess fibrosis and spontaneous tumour development (20, 21).

Chapter 3: Hypothesis and Objectives

Chapter 3

Rationale:

Previously, I had reported that activation of the Hh pathway occurs in CLD and that the degree of Hh pathway activity positively correlated with liver fibrosis stage (13, 14, 49). During CLD, secreted Hh ligands directly activate HSC into collagen-producing MF and stimulate LPC to undergo EMT which enhances fibrogenesis (14). Hh stimulated LPCs also secrete chemokines which recruit immune cells such as NKT cells into the liver (15, 16). NKT cells themselves secrete Hh and other factors which perpetuate the inflammatory response and amplify fibrogenesis.

OPN is a pro-inflammatory cytokine and matrix protein which is highly upregulated in areas of inflammation and fibrosis, and promotes the recruitment of neutrophils in the Concavalin-A model of hepatitis (19, 24). OPN deficiency on the other hand, leads to impaired wound healing (i.e. less fibrosis) (20). These findings suggest that OPN and Hh exhibit similar functions. More recently, a group further described Gli binding sites in the OPN promoter and postulated that Hh signaling might regulate also OPN transcription (18).

These findings therefore, led to me to **hypothesize that OPN upregulation promotes fibrogenesis in CLD**.

Objectives:

1. Evaluate the role of OPN in NAFLD / NASH fibrosis
2. Study the interaction between OPN and Leptin in NASH
3. Evaluate the role of OPN in the LPC response
4. Evaluate the role of OPN in chronic liver inflammation (NASH)

Chapter 4: Experimental Approaches

Chapter 4

4.1. Animal Studies

All animal care and procedures were as per the NIH "Guide for the Care and Use of Laboratory Animals", and approved by relevant institutions: Duke University Institutional Animal Care and Use Committees, and the United Kingdom Home Office approval in accordance with the Animals (Scientific Procedures) Act of 1986 (University of Birmingham, PPL 40/3201).

For study 5.1:

C57BL/6 Patched-deficient (Ptc+/-) and WT (of the same background) mice were obtained from Jackson Laboratories (Bar Harbor, ME). Ptc+/- mice have only 1 copy of patched, a Hh-pathway repressor. Therefore, these mice are unable to silence Hh signaling and exhibit excessive Hh-pathway activity. WT and Ptc+/- mice were fed the MCD diet (MP Biomedicals, Solon, OH) to induce NASH and liver fibrosis or control chow (MP Biomedicals, Solon, OH) (n= 8/group) for 8 weeks. 129 Sv/J Black-Swiss OPN-deficient (OPN-/-) mice or littermate controls were also fed the MCD or control chow (n= 6/group). Because the 129 Sv/J strain was reported to be more sensitive to MCD treatment than the C57BL/6 strain (79), OPN-/- mice and littermate controls were fed the diets for 4, rather than 8, weeks.

For study 5.2:

To induce NASH and fibrosis, lean (WT) and obese (ob/ob) mice (males, C57BL/6; n= 5/group) were fed the MCD diets for 8 weeks. In the control arm, ob/ob and WT mice (n=5/group) were permitted *ad libitum* consumption of water and control chow.

For study 5.3:

Carbon Tetrachloride (CCL_4): WT mice (n= 5/group) received twice-weekly intra-peritoneal injections of CCL_4 (0.5 mg/kg, Sigma-Aldrich) for 6 weeks to induce liver fibrosis (80), or vehicle (mineral oil)

MCD diet: WT mice (n= 5/group) were fed the MCD diet for 5 weeks to induce nonalcoholic steatohepatitis (NASH)-fibrosis, or control chow (14).

3, 5,-Diethoxycarbonyl-1,4-dihydrocollidine (DDC) diet: WT mice (n= 5/group) were fed the DDC-diet for 3 weeks to induce biliary-type fibrosis (81).

Osteopontin neutralization in vivo:

OPN-specific aptamers: Three additional studies were performed (4th study: CCL_4; 5th study: MCD; 6th study: DDC) (n= 10/study; 5/group). OPN aptamers (OPN-R3) (which specifically neutralize circulating or extracellular OPN) or sham aptamers (OPN-R3-2) (its biologically-inactive mutant) (both synthesized by Dharmacon, Lafayette, CO) (82) were administered to mice by tail-vein injections (total of 4 injections per mouse), during the final week of dietary or chemical challenge. A 200ug dose of sham or OPN aptamers (in 100ul of PBS) was used as this was the dose previously shown to exhibit efficacy in vivo (83). All mice were sacrificed 24 hours after the final dose of aptamers.

OPN neutralizing antibodies: MCD-fed mice (n= 5/group) were injected either control (IgG) or anti-OPN (R&D) in the final week, as described above (4 injections; 50ug/injection), using an amount of anti OPN previously shown to be effective in reducing insulin-resistance in obese mice (25), and sacrificed 24 h after the final injection.

For study 5.4:

WT, CD1d-deficient (CD1d-/-), and Jα18-deficient (Jα18-/-) mice (RIKKEN, Japan) of B6 backgrounds were fed MCD diet or control chow for 8 weeks.

For all studies, mice were housed in 12 h-light/dark cycle with food and water ad libitum. Liver samples were obtained for RNA analyses and immunohistochemistry (IHC).

4.1.1. Mouse Liver IHC

Liver tissue was fixed in formalin and embedded in paraffin (FFPE) and serial sections stained with hematoxylin and eosin (H&E). To quantify liver fibrosis, five micron sections were stained with picrosirus red (SR) (Sigma, St. Louis, MO) and counterstained with fast green (Sigma, St. Louis, MO). Immunohistochemical staining to detect OPN and αSmooth muscle actin (SMA) was performed using the DAKO Envision System (DAKO Corporation) according to the manufacturer's protocol. Antigen retrieval was performed by heating in 10 mM sodium citrate buffer (pH 6.0) or incubating with pepsin (00-3009; Invitrogen). Primary antibodies used are listed below in **Table 1.** Polymer-HRP anti-rabbit (Dako; K4003) and anti-goat (Santa Cruz; sc-2768; 1:250) were used as secondary antibodies. Antigens were demonstrated by diaminobenzidine (DAB) (DAKO). Double IHC was performed using Ferangi Blue or Vina Green, according to the manufacturer's recommendation (Bio-Care Medical). Negative controls included liver specimens exposed to 1% bovine serum albumin and isotype matched antibodies. The proportion of tissue stained with SR, αSMA, and OPN were assessed by morphometric analysis with MetaView software (Universal Imaging Corp, Downtownington, PA). For morphometric quantification, 40 to 50 randomly chosen, 20x fields per section (excluding the major bile duct in each portal tract from consideration) were evaluated for each mouse liver section.

Table 1: antibodies for mouse IHC

Specificity	**Antibody**	**Supplier**
OPN (mouse)	AF808	R&D
Sox9	5535	Millipore
αSMA	Ab5694	Abcam
E-Cadherin	31955	Cell Signal
K19	TROMA-3	Iowa Hybridoma Bank
Gli2	18-732-292462	Genway

4.1.2. ALT determination

Serum alanine aminotransferase (ALT) was measured using kits commercially available from Biotron Diagnostics (66-D; Hemet, CA) according to the manufacturers' instructions.

4.1.3. Hydroxyproline Assay

Hydroxyproline content in whole liver specimens was quantified colorimetrically as previously described (80). 30 mg of freeze-dried liver samples were used. Hydroxyproline concentration was calculated from a standard curve prepared with high purity hydroxyproline (Sigma, St. Louis, MO) and expressed as mg hydroxyproline/g liver.

4.1.4. ELISA assays for plasma OPN

Peripheral blood was collected at the time of sacrifice, and plasma obtained and stored at -80^{0}C till analysis. Plasma OPN was measured using the commercially available OPN ELISA kit (R&D; DY441) and in accordance with the manufacturer's instructions. All samples were run in duplicate, and expressed as pg/ml.

4.2. Human studies

Human studies were conducted in accordance with the Declaration of Helsinki (2008), and in accordance with NIH and respective Institutional guidelines for human subject research. Informed consent was obtained from participating subjects. Studies of samples acquired from the Hepatobiliary Unit in Birmingham were done in accordance with local ethical approval 04/Q2708/41 and REC 2003/242 from the South-Birmingham Research Ethics Committee, UK

4.2.1. Liver tissues

De-identified FFPE liver sections of explanted liver tissues from individuals undergoing liver transplantation for NASH, ALD, PBC, or AIH-cirrhosis (n= 6/group) from the Liver and Hepatobiliary Unit, Birmingham, UK and Department of Pathology at Duke University were used. Liver sections from biopsy-proven NASH-related early and advanced fibrosis (n= 10/group) were

also used. Normal tissues were obtained from non-diseased livers removed during resection for colorectal hepatic metastases or from split-liver grafts. Freshly explanted AIH, NASH, ALD, PSC, and PBC-cirrhotic liver tissues (n= 5/group) were also snap-frozen and used for total liver RNA analyses.

4.2.2. Human Liver IHC

This was performed as described for mouse IHC. Primary antibodies used are listed in **Table 2**. Polymer-HRP anti-rabbit (Dako; K4003) and anti-goat (Santa Cruz; sc-2768; 1:250) were used as secondary antibodies. Antigens were demonstrated by diaminobenzidine (DAB) (DAKO). The use of isotype matched control antibodies eliminated staining, demonstrating specificity.

SR staining with quantification by morphometric analysis was performed as described in mouse IHC. For OPN quantification, 15 to 20 randomly selected x20 fields (excluding the major bile duct in each portal tract from consideration) were analyzed with the MetaView software.

Table 2: antibodies for human IHC

Specificity	**Antibody**	**Supplier**
OPN (human)	AF1433	R&D
Gli2	18-732-292462	Genway

4.2.3. Serum or Plasma samples

Plasma was taken from patients with early (n=25) or advanced NASH (n=25) at the time of liver biopsies, and stored at -80^{0}C till analysis.

4.2.4. OPN ELISA

Serum were taken from patients and stored at -80^{0}C till analysis. Serum OPN was measured using the commercially available OPN ELISA kit (R&D; DY1433) and in accordance with the manufacturer's instructions. All samples were run in duplicate, and expressed as pg/ml.

4.3. Cell Cultures – HSC

4.3.1 Human HSCs

The human HSC line, LX-2, was cultured in serum-supplemented DMEM. Primary human HSC were isolated as previously described (80).

4.3.2. Rat or Mouse HSCs

Primary HSCs were isolated from Sprague-Dawley rats, assessed for purity and viability, and seeded at a density of 3 x 10^2 cells/mm^2 in DMEM supplemented with 10% fetal bovine serum (FBS) and penicillin (50 U/ml) /streptomycin (50 ug/ml) (80). A similar isolation/culture protocol was used for studies involving mouse primary HSC (16). Day 4 HSCs were used in all experiments. The mouse HSC line (GRX) was maintained in DMEM, 5% FBS, and 1% penicillin/streptomycin (84).

4.3.3. Experiments using HSC:

Studies of Hh and OPN in cultured HSC

To evaluate the effects of Hh signaling on HSC, day 4 HSC cultures were grown for an additional 24 h in medium containing either exogenous Hh agonist (SAG) at a concentration of 0.3uM, 5uM cyclopamine (Toronto Research Chemicals Inc., Toronto, Canada), an inhibitor of Hh-signaling, or 5uM tomatidine (Calbiochem, San Diego, CA), a catalytically inactive analog of Cyclopamine (48, 80) (tomatidine serves as a control for cyclopamine).

In separate experiments, recombinant OPN (rOPN) or vehicle was added to cultures to assess their effects on HSC activation. 100ng/ml dose was used in this study because it stimulated

greatest effects in vitro (85). The effects of neutralizing circulating or extracellular OPN were assessed by treating HSC with OPN RNA aptamer or sham aptamer (82). Aptamers (6.66 ug/ml or 100 nmol/l) were added to medium for 48 h prior to harvest. This concentration of OPN aptamer was shown to inhibit adhesion, migration and invasion in the MDA-MB-231 breast cancer cell line (which highly expresses OPN and is a standard tool for evaluating OPN actions).

4.3.4 OPN knockdown

HSCs were seeded in 24-well plates, $5x10^4$ per well, serum-starved (0.1% FBS/DMEM), and treated with 5 µg/ml polybrene (Santa Cruz, Dallas TX) in low-serum media (0.1% FBS/DMEM) 24 h prior to infection. Cells were trypsinized and suspended in 250 µl media, and treated with 4 µl lentiviral particles ($2x10^4$ IFU) containing shRNA constructs specifically targeting OPN (Santa Cruz sc-36130-V) or non-targeting scrambled control shRNA (Santa Cruz sc-108080). The plates containing cell and viral particle suspensions were immediately centrifuged at 750 x g for 30 min at 25ºC, and placed in the incubator for 48 hr. After the infection period, cells were then split, allowed to recover for 24 hr, then subjected to 8 µg/ml puromycin selection for 72 hr.

4.3.5. Leptin in HSC

For studies that involved treatments with leptin (100ng/ml; R&D systems, Minneapolis, MN) and/or adenoviral vectors, day 7 HSC cultures were cultured overnight in serum-depleted medium (0.1% FBS) before treatments were initiated.

Cells were treated with recombinant leptin (100ng/mL; R&D systems, Minneapolis, MN) for 48 h. For PI3K inhibition, LY294002 (25 uM; Cell Signalling Technology, Danvers, MA) was applied to cells 30 mins prior to treatment.

4.3.6. Adenoviral Transduction of Primary Rat HSC

Ad5GFP, which contains the GFP gene driven by the cytomegalovirus promoter, was used as a control virus. The Ad5dnAkt and Ad5myrAkt viruses express the dominant negative and activated

forms of Akt, respectively (60). Pilot studies demonstrated that maximally efficient transduction occurred at a multiplicity of infection of 100. Subsequent experiments were carried out with this multiplicity of infection for 24 h; virus-containing medium was then aspirated and replaced with fresh medium.

All cell experiments were performed at least in duplicate. Total RNA and protein were harvested before and at the end of the treatments, and analyzed by QRTPCR and immunoblotting, respectively.

4.3.7. Co-culture experiments:

Cholangiocyte – HSC

The immortalized, but non-transformed, murine immature cholangiocyte cell line, 603B was maintained in 6-well, cell-culture plates (Costar 3516, Corning Incorporated) in standard culture media as previously described (86, 87). At 90% confluence, cholangiocyte-conditioned media (CM) were harvested and added to primary HSC cultures together with OPN aptamers or sham aptamers; HSC were harvested 2 days later and mRNA expression was analyzed by QRTPCR. Experiments were performed in duplicate wells and repeated twice.

NKT – HSC

Primary liver mononuclear cells (LMNC) were isolated as previously described (17, 88), and cultured in complete NKT media, with or without the NKT cell ligand, αGalactosylceramide (αGC) (100 ng/ml; Axxora, Cat no 306027, CA), for 24 hours. αGC specifically activates iNKT cells (16, 89). αGC-activated LMNC CM (LMNC-CM) were then added to primary murine HSC, in the presence or absence of the Hh neutralizing antibody, 5E1 (10ug/ml; Iowa Hybridoma Bank), the Smoothened antagonist GDC-0449 (Selleck, Houston), or vehicle for 48 h and RNA was harvested for QRTPCR. Experiments were performed in duplicate wells and repeated twice. In separate experiments, LMNC-CM was added to primary murine HSC with either sham aptamers (100nmol/l) or OPN aptamers (100nmol/l) for 48 h, and RNA harvested as above.

4.3.8. Transmigration and wound healing assays

For transmigration assays, cells were cultured in the upper chamber of a 24-well transwell system (3 µm membrane, Nunc™ Polycarbonate Membrane Inserts, Thermo Fisher Scientific, Loughborough, UK). After 24 h, the upper side of the membrane was gently wiped with a cotton bud to remove non-migrated cells, and the membrane was stained with crystal violet solution (1% crystal violet, 25% methanol) for 10 minutes, washed in PBS and allowed to air dry. Cells migrated to the bottom side of the membrane were visualized on an inverted microscope, and quantified using the average number of migrated cells per 15 randomly-selected fields.

Standard wound healing assays were performed by growing cells to a confluent monolayer, and making a manual scratch using a P200 pipette tip. A reference mark was made on the wound and photographed at time 0, and compared 12 h later. Wound diameters were quantified using NIH Image J version 1.48v (Rasband, W.S., ImageJ, U. S. National Institutes of Health, Bethesda, Maryland, USA, http://imagej.nih.gov/ij/, 1997-2012]).

4.3.9. Precision Cut Liver Slice Organ Culture

In order to study the impact of OPN neutralization in the intact liver we used a Krumdieck Tissue Slicer (TCS Biologicals) to cut aseptic, 250 µm thick slices of live liver tissue, which could be studied for up to 48 h *ex-vivo*. Liver tissue was incubated in Williams E media (Sigma) supplemented with 2% FCS, 0.1µM dexamethasone (Sigma) and 0.5µM insulin (Novo-Nordisk). Tissues were stimulated with recombinant leptin, in the presence of sham aptamers or OPN aptamers. At the end of treatment, liver slices were collected for RNA analysis by QRTPCR. Cell viability was evaluated by measuring the content of ATP with the ATP Bioluminescence Assay Kit CLS II (Roche, Basel, Switzerland), normalized against the total amount of proteins quantified by Pierce BCA Protein Assay Kit (Thermo Fisher Scientific, Waltham, MA). The threshold of viability is 4 nmol/mg protein of ATP measured 2 h after recovery (i.e. time 0 h in Fig 5A).

4.3.10. Semi-quantitative real-time PCR (QRTPCR)

Total RNA was extracted from cell cultures using TRIzol® (Life Technologies, Carlsbad, CA) according to manufacturer's instructions. RNA (1 µg) was reverse transcribed to cDNA templates using iScript cDNA synthesis kit (Bio-Rad, Hercules, CA). For semiquantitative RT-PCR, cDNA (25 ng) was amplified using SYBR® Green PCR Master Mix (Life Technologies) and oligonucleotide primers for specific targets sequences on an Applied Biosystems 7500 Real-Time PCR system. RT-PCR parameters were as follows: denaturating at 95°C for 10 minutes, followed by 40 cycles of denaturing at 95°C for 15 seconds and annealing/extension at 60°C for 60 seconds. Threshold cycles (Ct) were automatically calculated by the system software. Target gene levels were determined relative to the S9 ribosomal protein house-keeping gene using the 2–ΔΔCt method. Primers used are listed in **Table 3.**

Table 3: primers for QRTPCR

Target	Forward 5'->3'	Reverse 5'->3'
Mouse		
S9	AGCCGGCCTAGCGAGGTCAA	CGAAGGGTCTCCGTGGGGTCA
OPN	TGGCAGCTCAGAGGAGAAGAAGC	GGGTCAGGCACCAGCCATGTG
Col1a1	AATGGCACGGCTGTGTGCGA	AGCACTCGCCCTCCCGTCTT
E-Cadherin	CCGCGGCGCACTACTGAGTT	CACTGAGCTCGGGTGCGGTC
Id2	CCCGGTGGACGACCCGATGA	TCTGGGGGATGCTGGGCACC
Snail	GGACCCCCAGTCGCGGAAGA	GGCAGCGTGTGGCTTCGGAT
K19	GTGAAGATCCGCGACTGGT	AGGCGAGCATTGTCAATCTG
αSMA	GATGAAGCCCAGAGCAAGAG	CTTTTCCATGTCGTCCCAGT
TGFβ	GACAGCCCTGCTCACCGTCG	CCCGAGGGCTGGTCCGGAAT
Sox9	CGACTACGCTGACCATCAGA	GACTGGTTGTTCCCAGTGCT
Gli2	ACCATGCCTACCCAACTCAG	CTGCTCCTGTGTCAGTCCAA
InH	ACAGATGGAATGCGTGTGAA	CCGAACCTTCATCTTGGTG
Rat		
S9	AGCCGGCCTAGCGAGGTCAA	CGAAGGGTCTCCGTGGGGTCA
αSMA	GTGGATCACCAAGCAGGAGGAGT	CATAGCACGATGGTCGATTG
Col1a1	CTGCATACACAATGGCCTAA	GGGTCCCTCGACTCCTA
OPN	ATG GCT TTC ATT GGA GTT GC	GAG GAG AAG GCG CAT TAC AG
Human		
S9	GACTCCGGAACAAACGTGAGGT	CTTCATCTTGCCCTCGTCCA
Beta actin	TGGCATCCACGAAACTACCT	ACGGAGTACTTGCGCTCAG
Col 1a1	CGTCGGAGCAGACGGGAGTT	TCCGCTCATGCGTGGCCTCA
αSMA	AGGAGAGCAGGCCAAGGGGCTA	CTTGGCTGGGCTGCTCCACAC
OPN	AGGCATCACCTGTGCCATACCA	TGGCCACAGCATCTGGGTATTTGT
Sox9	TTCAGTGGCGCGGAGACTCG	GCAAAAGTGGGGGCGCTTGC
TGFβ	GTGCTGCTCCACTTTTAACT	AACCCACAACGAAATCTATG

4.3.11 Western blot

Whole cell proteins were homogenized using standard RIPA buffer (Tris-buffered saline [TBS], 1% NP-40, 0.1% SDS) containing Protease Inhibitor Cocktail Tablets from Roche (Indianapolis, IN). Protein concentration was measured using BCA Protein Assay Kit from Pierce Biotechnology (Rockford, IL). 20 to 40 µg of protein were separated by polyacrylamide gel electrophoresis and transferred to nitrocellulose membranes (0.45 µm; Invitrogen). After blocking with 5% non-fat milk (Carnation, Swampscott, MA) in TBS (20mmol/L Tris, pH 7.5, 150 mmol/L NaCl) containing 0.1% Tween-20 (TBS-T), nitrocellulose membranes were incubated with primary antibodies. SuperSignal West Pico Chemiluminescent Substrate (Pierce, Rockford, IL) was used to detect specific antibody-HRP complexes. The band density was measured using the Alphalmager 3400 Analysis System (Alpha Innotech, San Leandro, CA). Primary antibodies used are listed in **Table 4.**

Table 4: antibodies for western blot

Specificity	**Antibody**	**Supplier**
OPN (mouse)	AF808	R&D Systems
OPN (human)	AF1433	R&D Systems
pSMAD2	138D4	Cell Signaling
SnoN	H-317	Santa Cruz
Ski	H-329	Santa Cruz
SMAD7	B-8	Santa Cruz
Keratin 19	ab15463	Abcam
Sox9	AB5535	Millipore
β-actin	AC-74	Sigma

4.3.12 FACS analysis

Primary LMNC

Isolated LMNCs were stained with FITC-conjugated CD3 (BD; 561806), Pacific blue-conjugated CD56 (Biolegend), and PE-conjugated OPN (R&D, IC14331P), and analyzed using the BD^{TM} LSR II (BD Biosciences) at the flow cytometry core facility at the Duke Human Vaccine Institute Flow Cytometry Core Facility, Duke University Medical Center.

4.3.13 Statistical Analysis

Results are expressed as means ± SEM. Significance was established using the Student's t-test and analysis of variance. Differences were considered significant when $p < 0.05$.

Chapter 5: Results

Chapter 5

5.1 Role of OPN in NASH and Liver Fibrosis

Osteopontin is induced by Hedgehog Pathway Activation and Promotes Fibrosis Progression in Nonalcoholic Steatohepatitis
(Syn WK et al. Hepatology. 2011 Jan; 53(1):106-15.)

NASH is a potentially serious form of chronic liver injury because it increases the risk of developing cirrhosis and primary liver cancer. The mechanisms that lead to these outcomes have not been fully elucidated, but appear to involve responses that are triggered by hepatocyte apoptosis (30, 31) and MF accumulation (90). Certain apoptotic stimuli were recently reported to induce hepatocyte production of Hh ligands (11). Hh ligands, in turn, elicit a number of fibrogenic actions by engaging their receptors on Hh responsive liver cells, such as ductular type cells, HSC, and NKT cells. In HSC, for example, Hh pathway activation functions in a cell-autonomous fashion to promote transition of quiescent (Q)-HSC to MF-HSC, enhance MF-HSC proliferation, and inhibit MF-HSC apoptosis (48). Activating Hh signaling in other types of liver cells (e.g., ductular cells and NKT cells) also causes these cells to generate factors that promote MF-HSC accumulation by paracrine mechanisms (14, 16).

OPN, a pro-inflammatory cytokine and integrin-binding ligand (21, 91, 92), is highly expressed in many inflamed tissues and plays a critical role in wound healing (93 – 95). Recently, Gli binding sites were demonstrated in the OPN promoter, prompting speculation that Hh signaling might regulate OPN transcription (18). This concept is potentially relevant to NASH-related liver fibrosis because Hh pathway activity increases in parallel with fibrosis stage in NASH. Moreover, in other tissues, OPN is secreted by the types of cells (e.g., NKT cells and fibroblasts) that mediate fibrogenic repair in NASH (24, 96). Evidence that OPN mRNA increases during culture-related activation of Q-HSC to MF-HSC (96) and correlates with fibrosis severity in biliary atresia (97) further support a potential role for OPN in cirrhosis pathogenesis.

We manipulated Hh pathway activity in mice and cultured cells to determine effects on OPN production, and examined whether or not reducing OPN impacted Hh signaling or fibrogenesis. The results support and advance the concept that OPN is a Hh-target gene and reveal a previously-unsuspected role for OPN as a proximal mediator of Hedgehog's fibrogenic actions in NASH.

5.1.1. Upregulation of OPN parallels Hh pathway activation during MCD diet-induced NASH.

WT mice (n= 8/group) develop hepatic necro-inflammation, accumulate markers of MF-HSC, and exhibit liver fibrosis after 8 weeks of MCD diet. Ptc+/- mice (with haplo-insufficiency of Ptc, a factor that constrains Hh signaling) exhibit worse liver fibrosis than WT mice after MCD diet exposure **(Fig 5.1.1).** This suggests that Hh pathway activation promotes fibrosis progression in this model of NASH, but the exact mechanisms involved need to be determined.

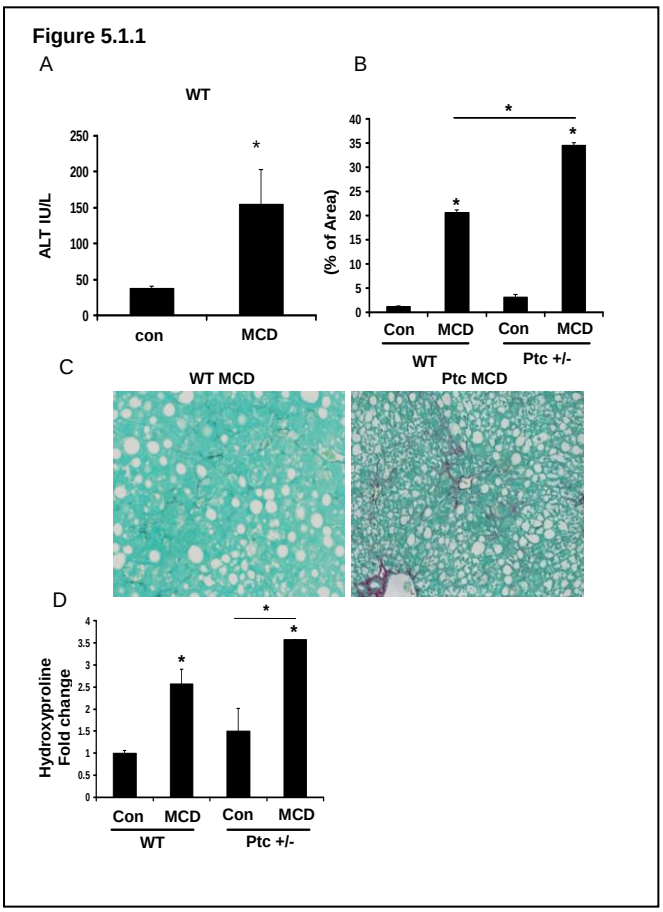

Fig. 5.1.1: Hh pathway activation worsens liver fibrosis during diet-induced NASH.
WT and Ptc+/- mice were fed control chow or the MCD diet for 8 weeks, and then sacrificed to assess serum ALT and severity of liver fibrosis. (A) Serum ALT levels in WT mice fed control or the MCD diet (IU/L; mean ± SEM). (B) SR quantification by morphometric analysis and (C) representative SR staining after MCD diet. Sections from 4 animals were used per group and 10 randomly selected, 200X fields chosen for analysis by the Metaview software. (D) Hepatic hydroxyproline content in both WT and Ptc+/- mice. *P<0.05 vs. control-chow fed mice

Hh pathway activation results in nuclear accumulation of Gli proteins (downstream targets of Hh signaling) (98), and Gli proteins may regulate transcription of OPN, a potential pro-fibrogenic factor (78, 99, 100). Therefore, we compared OPN expression in WT mice that were fed either control or MCD diets for 8 weeks. In WT mice, MCD diets caused a significant induction of OPN mRNA (>10-fold) and protein (about 2-fold) expression **(Fig 5.1.2A, B).** Ptc+/- mice exhibited even greater up-regulation of OPN expression when fed MCD diets **(Fig 5.1.2B, C).** The latter finding supports the concept that Hh signaling increases OPN expression. In both strains, the OPN-immunoreactive cells were mostly ductular in appearance **(Fig 5.1.2D)**. Double immunostaining for Gli2 and OPN in liver samples from NASH patients demonstrated that Gli2-(+) ductular cells that co-expressed OPN localized within fibrous septae **(Fig 5.1.2E).**

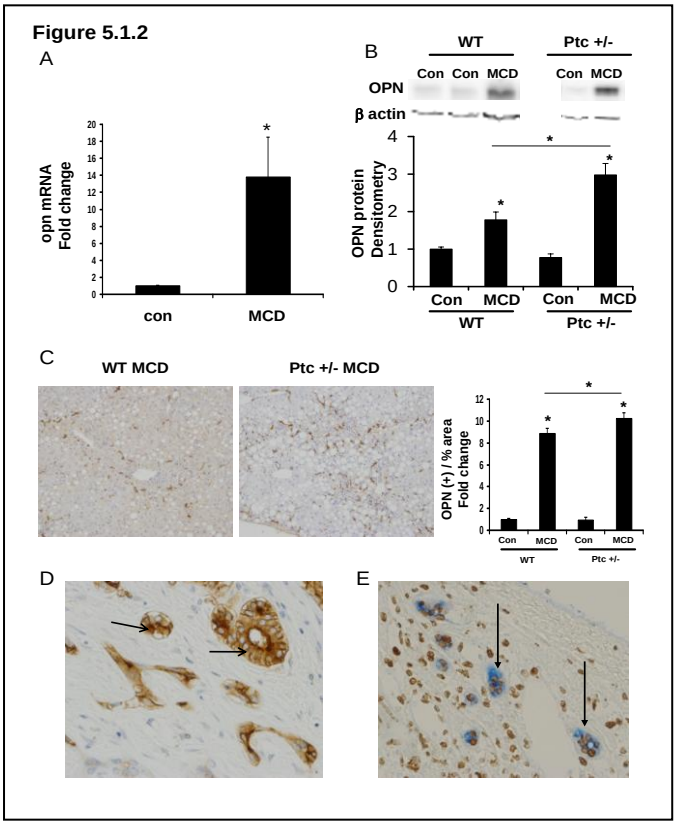

Fig. 5.1.2: Osteopontin (OPN) expression parallels Hedgehog (Hh) pathway activation during diet-induced NASH.
WT and Ptc+/- mice were fed as described in Fig. 5.1.1. (A) OPN mRNA in WT mice fed control or MCD diet. Results are expressed as fold change relative to control-chow fed mice; mean ± SEM. *P<0.05 vs. control-chow fed mice. (B) Total hepatic OPN expression by Western blot and densitometry. (C) Representative OPN immunostaining after MCD treatment in WT and Ptc+/- mice (final magnification 400X), and quantification by morphometry. Sections from 4 animals were used per group and 8 randomly selected 200X fields. Results are expressed as fold change (% positive staining) relative to chow-fed control mice, and graphed as mean ± SEM. *P<0.05 vs. control mice. (D) Representative OPN (+) biliary ductular cells in murine NASH-fibrosis (630X). (E) Representative OPN (blue) and Gli2 (brown) double-positive ductular cells in human NASH-cirrhosis (400X).

5.1.2. MCD diet-fed OPN-deficient mice developed less fibrosis

To evaluate whether or not OPN directly contributed to the fibrogenic response evoked by MCD diets, and gain further insight into the relationship between OPN and the Hh pathway, OPN-/- mice (n=12) and littermates (n=12) were fed MCD or control diets for 4 weeks. OPN deficiency had no obvious effect on expression of the Hh-target gene, Gli2, because both OPN-/- and littermates

showed similar induction of Gli2 mRNA (data not shown) and protein **(Fig 5.1.3A)** after 4 weeks of MCD diet. Despite apparent similarities in Hh pathway activity, however, the fibrogenic responses of OPN-/- mice were markedly attenuated when compared to that of their littermate controls. After MCD diet feeding, for example, OPN-/- mice accumulated 50% fewer αSMA+ cells **(Fig 5.1.3B)** and significantly fewer SR stained fibrils **(Fig 5.1.3C)** than comparably-treated littermates. These results suggest that the Hh pathway mediates its fibrogenic effects, at least in part, by inducing expression of OPN.

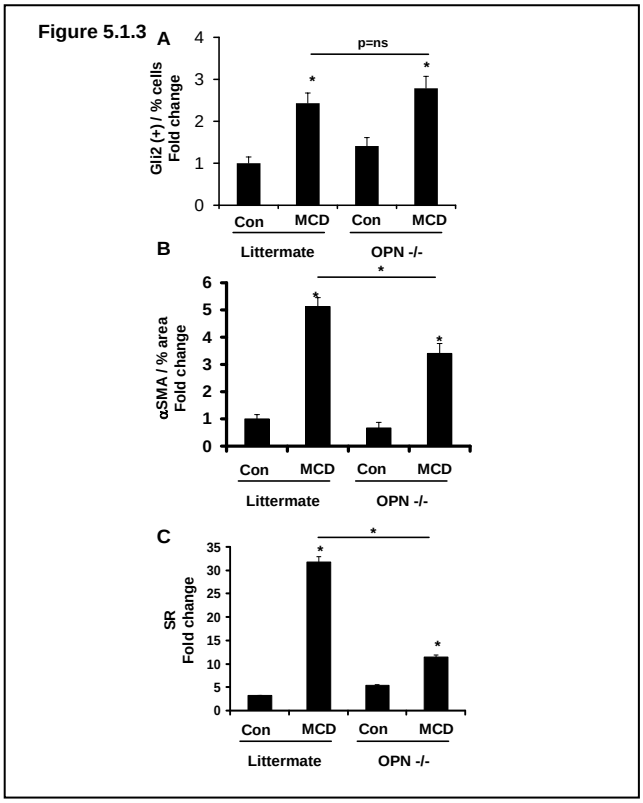

Fig. 5.1.3: OPN-/- mice develop less fibrosis after MCD diet treatment
129Sv/J OPN-deficient and littermates were fed MCD diet or control chow (n=6 mice/group/dietary treatment) for 4 weeks. At the end of treatment, mice were sacrificed. (A) Accumulation of Gli2 (+) cells in OPN-/- and littermates. Sections from 6 animals were used, and 8 randomly selected, 200X field chosen for cell counting. (B) αSMA morphometry. Sections from 3 animals were used at each time point and 10 randomly selected, 200X fields chosen for analysis. (C) SR quantification by morphometric analysis. Sections from 6 animals were used and 10 randomly selected 200X field chosen for analysis. Results are expressed as fold change relative to chow-fed littermates and graphed as mean ± SEM. *P<0.05 vs. littermate control.

5.1.3. Paracrine/Autocrine OPN stimulates HSC expression of fibrogenic genes

Hh responsive bile ductular cells are major sources of OPN **(Fig 5.1.2D)**. Therefore, we treated primary cultures of rodent HSC with CM from monocultures of a cholangiocyte cell line, and assessed effects on HSC gene expression. To determine if HSC responses were mediated by OPN, studies were repeated using cholangiocyte-CM plus OPN aptamers. Cholangiocyte-CM augmented HSC expression of α-sma **(Fig 5.1.4A)** and collagen **(Fig 5.1.4B)**; OPN aptamer treatment repressed α-sma induction by 50% and returned collagen expression to basal values, proving that paracrine signaling involving OPN promoted fibrogenic gene expression in HSC. In

separate studies, other primary HSC cultures were treated with recombinant OPN (rOPN, 100ng/ml) or vehicle for 24 h, and RNA was analyzed by QRTPCR **(Fig 5.1.4C-D)**. rOPN also augmented expression of αsma and collagen Ia1 expression**.** These findings support the concept that exogenous OPN can function as a paracrine factor to promote fibrogenic gene expression in HSC.

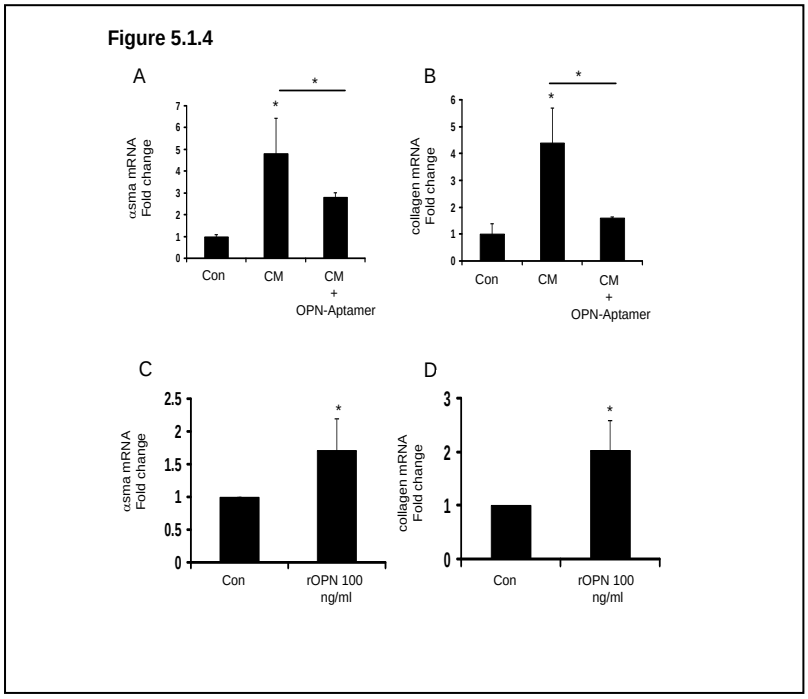

Fig 5.1.4: Paracrine OPN stimulates HSC activation and collagen expression
(A-B) Isolated mouse primary HSC were cultured for 4 days, and then treated with conditioned media (CM) from cholangiocytes, with or without OPN RNA aptamers for 48 h. (C-D) In separate experiments, primary HSC were directly treated with recombinant OPN (rOPN: 0 or 100ng/ml) for 24 hrs, and then harvested for QRTPCR analysis. (A, C,) αsma, (B, D) collagen mRNA. Mean ± SEM of duplicate experiments are graphed. *P<0.05 vs. vehicle treated stellate cells.

Because another group has reported that MF-HSC themselves also express OPN (96), we next investigated changes in endogenous OPN gene expression during "spontaneous" culture-related activation of Q-HSC to MF-HSC. We confirmed that HSC expression of OPN mRNA and protein increased significantly as Q-HSC transitioned to become MF-HSC **(Fig 5.1.5A, B).** Addition of OPN aptamers to day 4 cultures significantly repressed α-sma and collagen gene expression, providing novel evidence that HSC-derived OPN may help to maintain the myofibroblastic phenotype of cultured HSC **(Fig 5.1.5C, D).** As HSC become MF-HSCs, they repress expression of the Hh inhibitor, Hhip, induce expression of Hh ligands, and up-regulate various MF genes, while down-regulating markers of quiescence (48). To clarify the relationship between Hh pathway activation and OPN expression, day 4 culture-activated MF-HSC were treated with cyclopamine to selectively inhibit Hh signaling. Cultures were harvested 24 h later, RNA was

isolated, gene expression was assessed by QRTPCR, and results were compared to parallel cultures that had been treated with tomatidine, an inactive cyclopamine analog. Inhibiting Hh signaling with cyclopamine attenuated induction of OPN gene expression **(Fig 5.1.5E).** Conversely, addition of the Hh agonist, SAG, augmented OPN gene expression significantly **(Fig 5.1.5F).** Thus, endogenous OPN gene expression in MF-HSC is regulated, at least in part, by the Hh pathway.

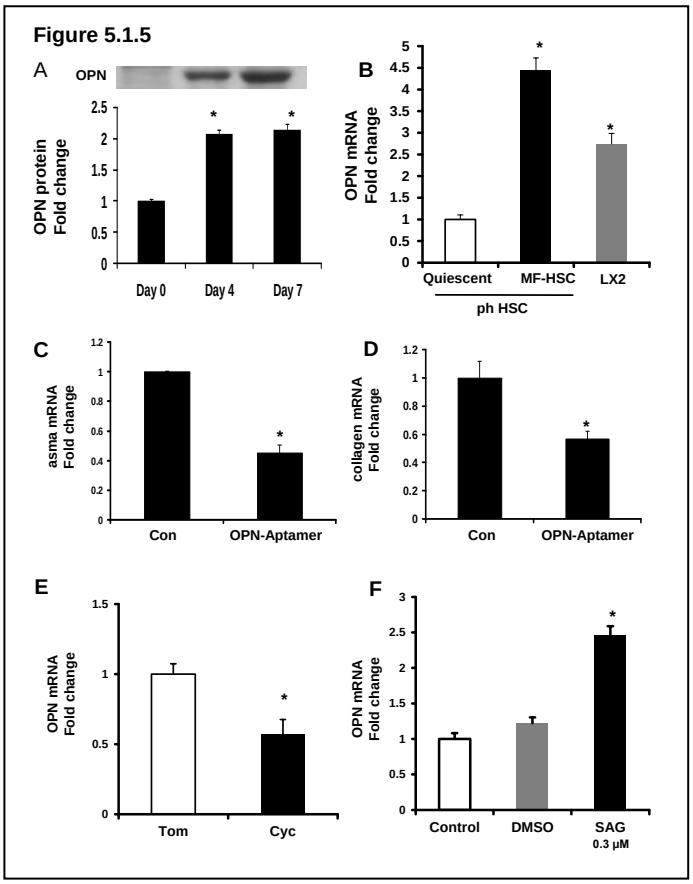

Fig. 5.1.5: Hh regulated OPN overexpression promotes HSC activation in an autocrine fashion
Primary rat HSC were isolated and cultured for 0, 4 and 7 days. At the end of treatment, HSC were washed and cell lysates obtained for Western blot analysis. (A) OPN Western blot and densitometry. Primary human HSC (ph HSC) were also isolated and maintained till culture-activated to myofibroblasts (MF-HSC) and then harvested for RNA and analyzed by QRTPCR. The human HSC line LX2 was used as comparison. (B) OPN mRNA Q-HSC, MF-HSC, and LX2. In separate experiments, day 4 HSC cultures were treated with OPN aptamers or sham aptamers (control) for 48 h and RNA isolated for QRTPCR (C-D). (C) αsma, (D) collagen mRNA. To assess if OPN expression is Hh-regulated, day 4 HSC were treated with Cyclopamine (Cyc), Tomatidine (Tom), or SAG for 24 h, and then harvested for RNA analysis (E-F). (E-F) OPN mRNA. Mean ± SEM of duplicate experiments are graphed. * $p<0.05$ vs. control (vehicle) treated or quiescent stellate cells.

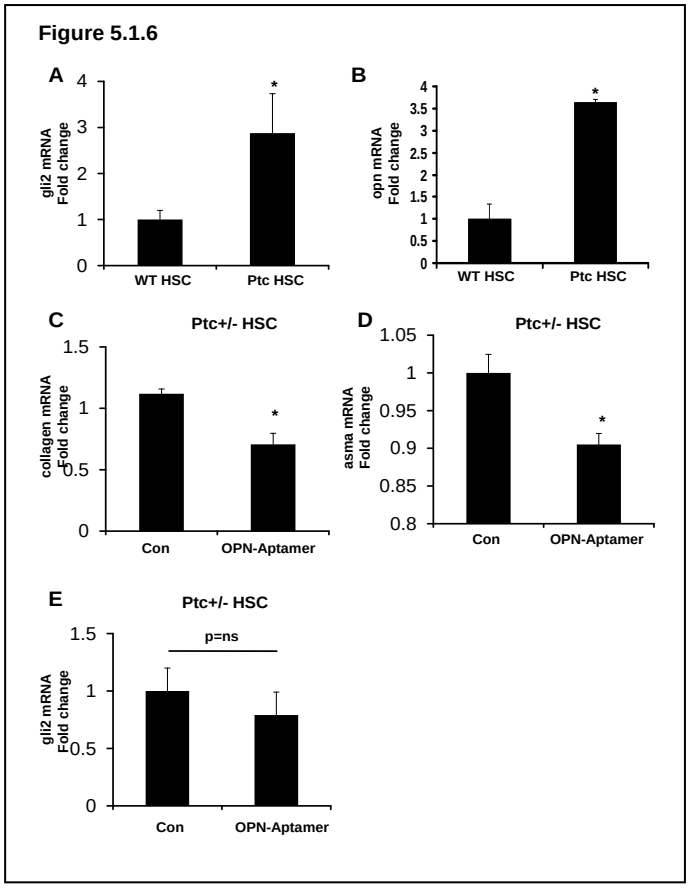

Fig. 5.1.6: OPN is a downstream target of the Hh pathway

WT and Ptc+/- primary HSC were placed in culture for 4 days and then harvested for RNA analysis by QRTPCR. (A) gli2, (B) opn mRNA; mean ± SEM of duplicate experiments are graphed. *p<0.05 vs. WT HSC. In separate experiments, Ptc+/- HSC were treated with OPN aptamers or sham aptamers (control) for 48 h, and effects on fibrogenesis assessed by QRTPCR. (C) collagen, (D) αsma, and (E) gli2 mRNA. Mean ± SEM of triplicate experiments are graphed. * p<0.05 vs. sham aptamer (control) treated HSC

To determine the relative importance of OPN as a down-stream target of the Hh pathway in HSC, day 4 primary MF-HSC from Ptc+/- mice were incubated with OPN aptamers for 48 h. At baseline, HSC from Ptc+/- mice expressed 3-fold more gli2 mRNA than WT HSC, confirming that Ptc-deficiency enhances Hh signaling **(Fig 5.1.6A)**. Consistent with in vivo findings **(Fig 5.1.1)**, Ptc+/- HSC also expressed more OPN mRNA than WT HSC **(Fig 5.1.6B).** Neutralizing OPN significantly reduced collagen and α–sma mRNA levels in the Ptc-deficient HSC **(Fig 5.1.6C-D),** but had little effect on gli2 mRNA expression **(Fig 5.1.6E)**. These findings suggest that the Hh pathway mediates induction of certain fibrogenic genes indirectly, via up-regulation of the Hh responsive gene OPN.

5.1.4. Evidence of OPN overexpression in humans with progressive NAFLD

Because the mouse model of MCD diet-induced NASH differs in several regards from human NASH (101), it was important to determine if OPN overexpression occurred in patients with NAFLD. Coded liver sections from 11 patients with well-characterized NAFL (n = 3), NASH (n = 3), and NASH-related cirrhosis (n=5) were stained to demonstrate OPN, and then analyzed by computer-assisted morphometry. Expression of OPN was lowest in patients with NAFL and highest in patients with NASH-cirrhosis **(Fig 5.1.7A-B)**. To further validate the association between NAFLD-fibrosis stage and OPN expression, total liver RNA was isolated from a separate cohort of 36 individuals with early (Fibrosis stage F0-1) or advanced (F3-4) NASH-fibrosis (n=18/group) and analyzed by QRTPCR. In livers with advanced -fibrosis OPN gene expression was double that of livers with early fibrosis **(Fig 5.1.7C).** Additional analysis was conducted using RNA and protein harvested from explanted livers with NASH-cirrhosis and residual tissue from non-diseased donor livers (n=6 per disease). Livers with NASH-cirrhosis contained over 10x more OPN protein **(Fig 5.1.7D)** and 5x more OPN mRNA compared with non-diseased controls **(Fig 5.1.8A).** Interestingly, OPN was also significantly increased in livers from individuals with ALD **(Fig 5.1.8A, B),** PBC **(Fig 5.1.8A, C)**, AIH**,** and PSC **(Fig 5.1.8A)**, suggesting that OPN induction is a conserved response to chronic liver injury.

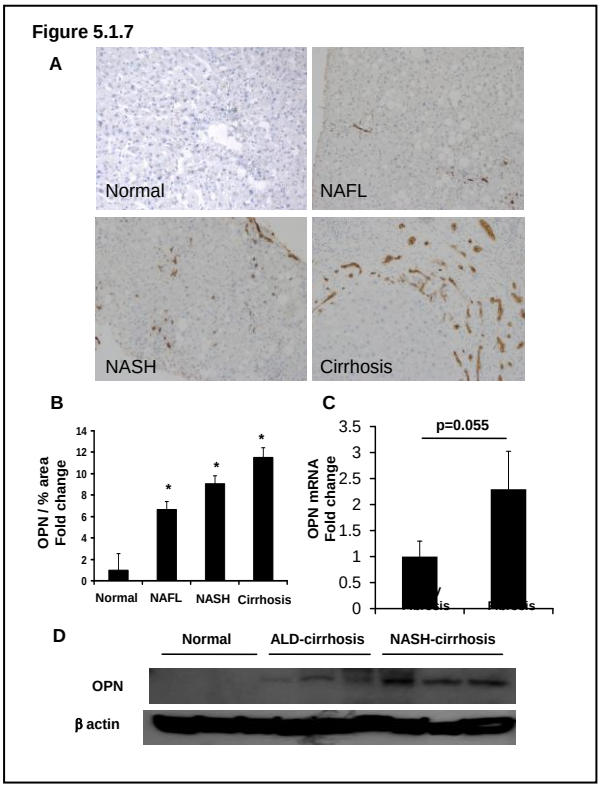

Fig. 5.1.7: OPN overexpression in NAFLD patients
Coded liver sections from patients with NAFL, NASH, and NASH-cirrhosis were stained for OPN and analyzed by computer-assisted morphometry. (A) Representative photomicrographs of liver sections from patients with NAFLD and normal liver from excess donor tissues (200X). (B) Quantitative analysis of OPN in all patients. Amount of OPN is expressed as percentage of stained cells per high-powered field. **P <0* .05 vs. normal. Total liver RNA was isolated from individuals (n=18/group) with early or late NASH-fibrosis and analyzed by QRTPCR. (C) OPN mRNA. Mean ± SEM are graphed * p<0.05 vs early fibrosis. (D) Hepatic OPN protein from normal, ALD-cirrhosis and NASH-cirrhosis individuals

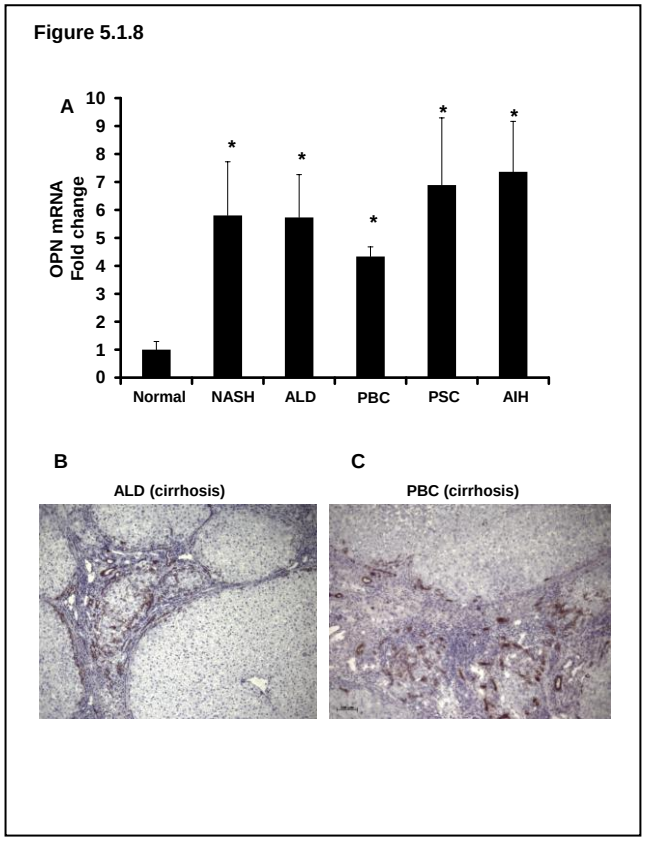

Fig. 5.1.8: Enrichment of hepatic OPN in patients with CLD

RNA were harvested from explanted ALD-, NASH-, PBC-, PSC- and AIH-cirrhotic livers and analyzed by QRTPCR. Liver sections from ALD and PBC-cirrhosis were immunostained for OPN. (A) OPN mRNA (n= 6/group); results expressed as fold change relative to normal donor livers, mean ± SEM. *p<0.05 vs. normal. (B) Representative OPN immunostaining in ALD-cirrhosis (100X), and (C) PBC-cirrhosis (100X).

5.2. Interaction between OPN and Leptin in NASH Fibrosis

Osteopontin is a proximal effector of leptin-mediated non-alcoholic steatohepatitis (NASH) fibrosis
(Coombes JD ….Syn WK. Biochim Biophys Acta. 2016 Jan; 1862(1):135-44)

The HSC is the major source of extracellular matrix, and thus, the key effector of the repair response (3). When activated by cytokines (e.g. TGF-β), growth factors (connective tissue growth factor), or morphogens (Hh, Wnt), quiescent HSC transition into motile, collagen-secreting MF (102). HSCs are also capable of responding to circulating neurotransmitters and hormones (103, 104). Leptin is an adipocyte-derived hormone which, not only controls energy balance and food intake, but also modulates the liver repair response (105 – 107). Binding of leptin to HSC surface receptors for instance, upregulates key fibrogenic genes αSMA and collagen 1α1, while mice deficient in leptin (i.e. ob/ob mice) are protected against liver fibrosis (105, 108, 109). In humans, serum and tissue leptin levels are highly elevated in the obese (110, 111), helping to explain at least in part, why obese, NAFLD individuals are more at risk of developing liver fibrosis.

Recently, we reported that leptin-induced liver fibrosis occurs via activation of the Hh pathway (60) and that upregulation of the Hh ligand and downstream target genes requires induction of the PI3K/Akt signaling. Hh pathway activation promotes transition of quiescent HSC into activated myofibroblasts (25), while inhibition of Hh reverses this phenotype. Similarly, the addition of LY294002 (a PI3K inhibitor) or cyclopamine (a specific Hh pathway inhibitor) to leptin-treated HSC blocked all actions of leptin, thus revealing that the PI3K – Hh axis is necessary for leptin to exert its fibrogenic effects.

OPN is highly expressed in a variety of inflamed tissues, and plays a critical role in tissue repair (19, 112), thus functionally resembling Hh. Interestingly, mice with excessive Hh pathway activity express more liver OPN and develop worse liver fibrosis, while inhibition of Hh signaling (with cyclopamine) in HSC represses OPN levels **(Results: 5.1).** These results demonstrate that OPN is a downstream effector of Hh, and led us to hypothesize that OPN and leptin may interact in

HSC to promote NASH progression. Using a combination of HSC cultures and diet-induced model of NASH, we confirm that OPN is a downstream effector of leptin, and is required for fibrotic outcomes in NASH.

5.2.1. Leptin-deficient (ob/ob) livers contain less OPN and are less fibrotic than control (WT) livers after MCD treatment

Chronic exposure to the MCD diet induced comparable epithelial cell injury in WT (leptin-intact) and ob/ob (leptin-deficient) mice (113, 114). WT mice developed significant liver fibrosis in response to the MCD diet, as evidenced by ~6-fold accumulation of SR stained collagen fibrils **(Fig. 5.2.1A - C),** ~2.5-fold increase in hepatic hydroxyproline content **(Fig. 5.2.1D)**, and a 4-fold upregulation in collagen 1α1 mRNA **(Fig. 5.2.1E).** Collagen deposition was accompanied by the accumulation of αSMA+ cells **(Fig. 5.2.2A, B),** and induction of key fibrogenic genes, αSMA (~4-fold) **(Fig. 5.2.2C),** TGF-β1 (~3-fold) **(Fig. 5.2.2D).** OPN+ cells and OPN mRNA **(Fig 5.2.3A - C)** were significantly increased (greater than 10-fold).

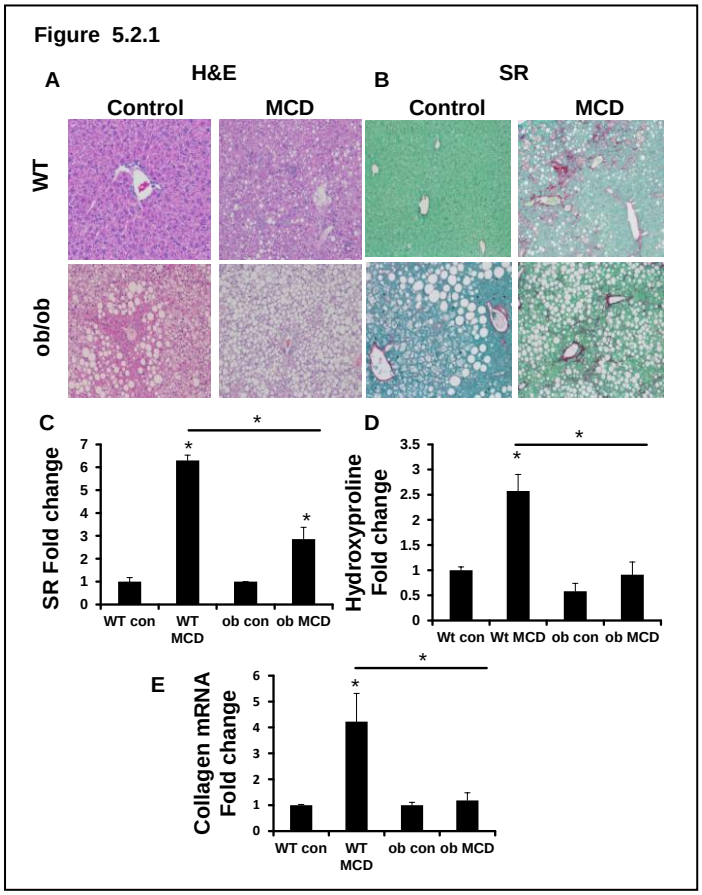

Fig. 5.2.1: Leptin-deficient (ob/ob) mice develop less NASH-fibrosis than leptin-intact (WT) mice
WT and ob/ob mice were fed control chow or the MCD diet for 8 weeks. Livers were harvested for IHC, QRTPCR, and biochemical analysis. Representative staining are shown. (A) H&E. (B) SR staining. (C) SR morphometry. (D) Liver hydroxyproline measurements. (E) Collagen 1α1 mRNA. Results are expressed as fold changes relative to WT control, and graphed as mean ± SEM. *p<0.05 vs. WT control

By contrast, fibrosis was significantly less in ob/ob mouse livers after the MCD diet **(Fig. 5.2.1)**: ob/ob livers contained nearly 50% fewer SR stained collagen fibrils **(Fig. 5.2.1B, C)**, ~2.5-fold less liver hydroxyproline **(Fig. 5.2.1D),** ~50% less TGF-β1 mRNA, and exhibited minimal induction of collagen 1α1, αSMA and OPN mRNA **(Fig. 5.2.1E, 5.2.2C, D, and 5.2.3C)**. The degree of weight loss however, was similar between (WT and ob/ob) MCD-fed groups. These findings confirm that leptin directly promotes fibrogenesis in MCD-induced NASH (60,105, 113).

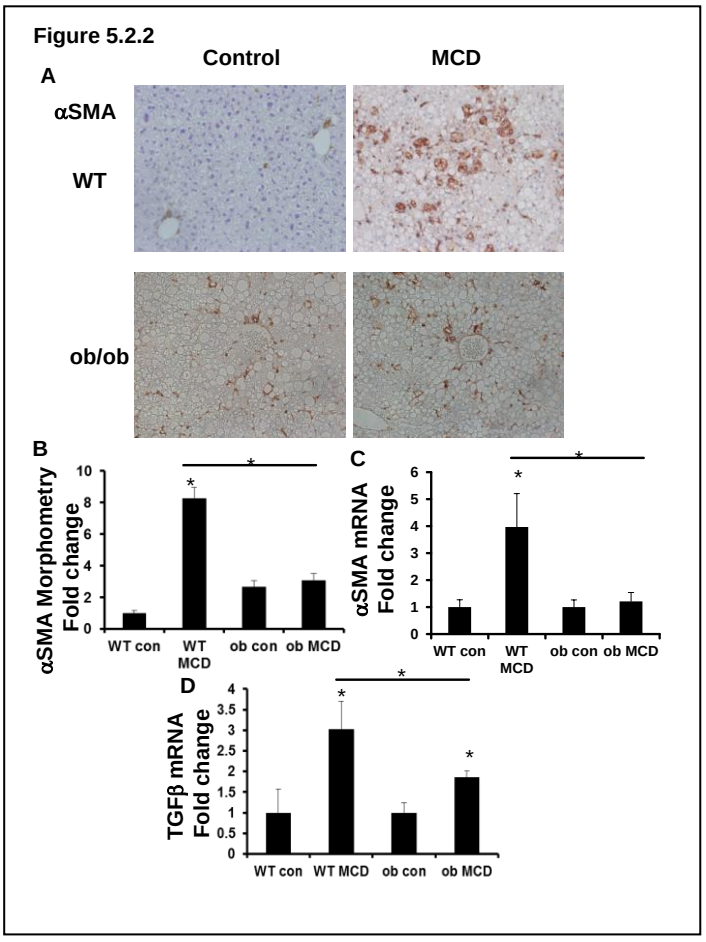

Fig. 5.2.2: ob/ob mice exhibit repressed fibrogenesis in response to the MCD diet
(A) αSMA staining. (B) αSMA morphometry. (C) αSMA mRNA. (D) TGFβ mRNA. Results are expressed as fold changes relative to WT control, and graphed as mean ± SEM. *p<0.05 vs. WT control

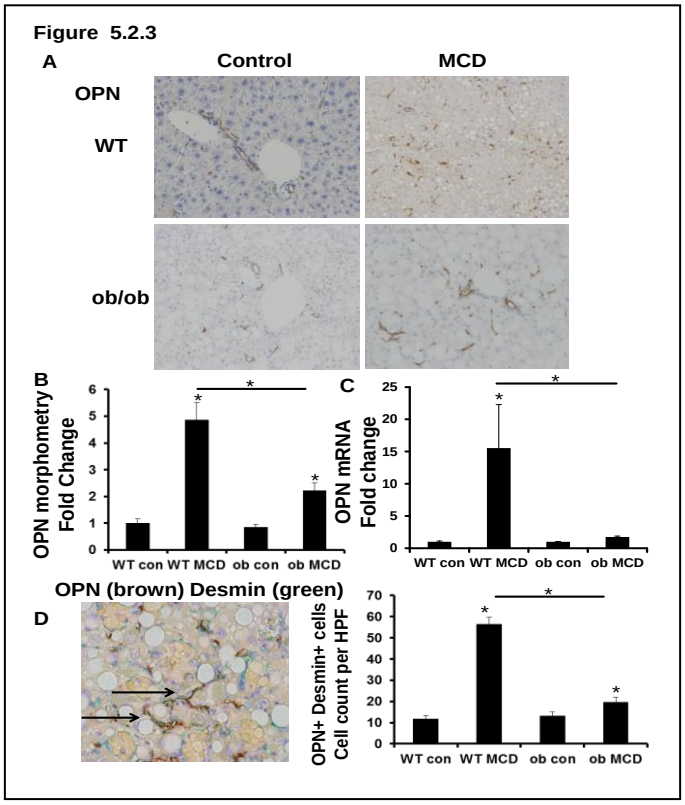

Fig. 5.2.3: OPN expressing HSC accumulate in NASH fibrosis

WT and ob/ob mice were fed control chow or the MCD diet for 8 weeks. Livers were harvested for IHC and QRTPCR. Representative staining are shown. (A) OPN staining. (B) OPN morphometry. (C) OPN mRNA; results are expressed as fold change relative to WT control mice. (D) OPN (brown) and Desmin (marker of HSC) (green) – double immunostaining (magnification x400); graph shows number of OPN / Desmin double-positive cells per HPF (quantified by cell counting); black arrows indicate cells which co-express OPN and Desmin. All results are graphed as mean ± SEM; *p<0.05 vs. WT control mice or otherwise indicated.

5.2.2. OPN is a downstream effector of Leptin in HSC

Leptin is a pro-fibrogenic adipokine which directly activates HSC (105, 106). Recently, we reported that OPN also promotes HSC activation **(Results: 5.1).** In this study, the loss of circulating leptin was directly associated with repressed liver OPN **(Fig 5.2.3A - C)**, and attenuated liver fibrogenesis **(Fig. 5.2.1, 5.2.2)**. These observations led us to hypothesize that leptin could regulate OPN expression in HSC. Herein, we confirm by double immunohistochemistry that desmin (+) HSC co-expressed OPN **(Fig 5.2.3D).** Importantly, the number of desmin / OPN double (+) HSC accumulated by more than 5-fold in MCD-fed mice, but this increase was almost abolished in ob/ob-MCD mice.

To determine if leptin was directly influencing OPN expression in HSC, we treated the mouse HSC line, GRX, with recombinant leptin (rleptin) for 48 h; cells were then harvested for RNA analysis by QRTPCR. rLeptin activated HSC, upregulated OPN, and key fibrogenic markers, αSMA, collagen 1α1, TGFβ (~2-fold) **(Fig 5.2.4A – D).** We next investigated if loss of OPN would inhibit leptin fibrogenic effects. To this end, GRX were treated with lentiviral particles which containin shRNA constructs specifically targeting OPN (GRX-shOPN). Compared with control (GRX-shScr) (GRX infected with lentiviral particles containing non-targeting scrambled shRNA), OPN knockdown (~80%) **(Fig 5.2.5)** significantly abrogated leptin fibrogenic effects by >90% **(Fig 5.2.4).** As increased cell migration is an important feature of activated HSC, we further examined if OPN knockdown (under leptin-stimulated conditions) would impair HSC migratory properties. Migration was assessed by semi-quantitating the dimensions of a wound dividing the confluent monolayer 12 h after the scratch. OPN knockdown led to ~15% less wound healing compared with controls ($p<0.05$) **(Fig 5.2.4E)**. Comparable results observed in the modified cell-invasion assay **(Fig 5.2.4F).** OPN knockdown led to 50% fewer GRX cells invading across the insert membrane.

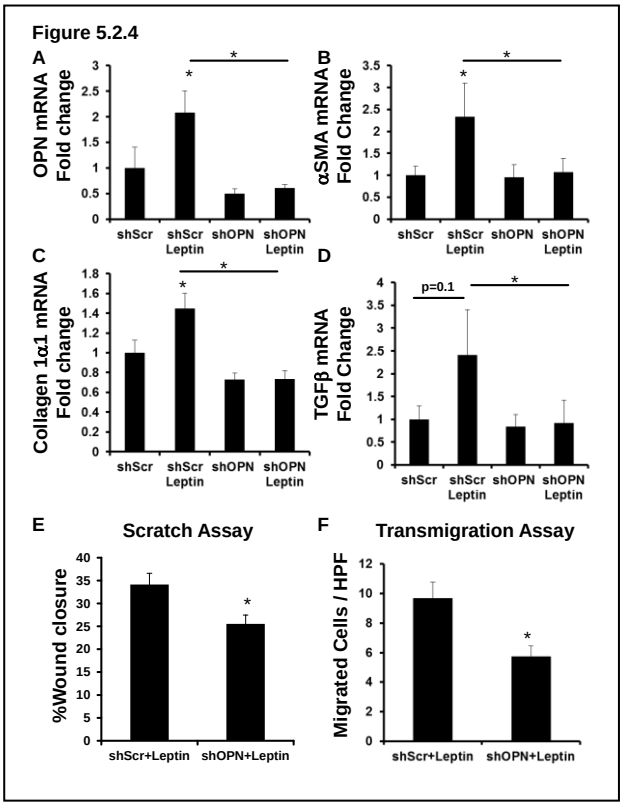

Figure 5.2.4: OPN loss abrogates leptin fibrogenic effects in HSC
HSC (mouse GRX line) with OPN knockdown (shOPN) and control HSC (shScr) were treated with recombinant leptin (or vehicle) for 48 h. Cells were then harvested and RNA analyzed by QRTPCR. (A) OPN mRNA. (B) αSMA mRNA. (C) Collagen 1α1 mRNA. (D) TGFβ mRNA. Results are expressed as fold changes relative to shScr, and graphed as mean ± SEM. Wound-healing and transmigration studies in shOPN or shScr HSC were performed under leptin-treated conditions (E-F). (E) Wound healing; migration was quantified by measuring the distance dividing the two sides of the monolayer. Mean (% wound closure) ± SEM were graphed. (F) Transmigration was evaluated 24 h after seeding of cells, by counting crystal violet-stained cells on the underside membrane in 15 random HPF. Mean cell numbers ± SEM were graphed. *p<0.05 vs shScr or otherwise indicated.

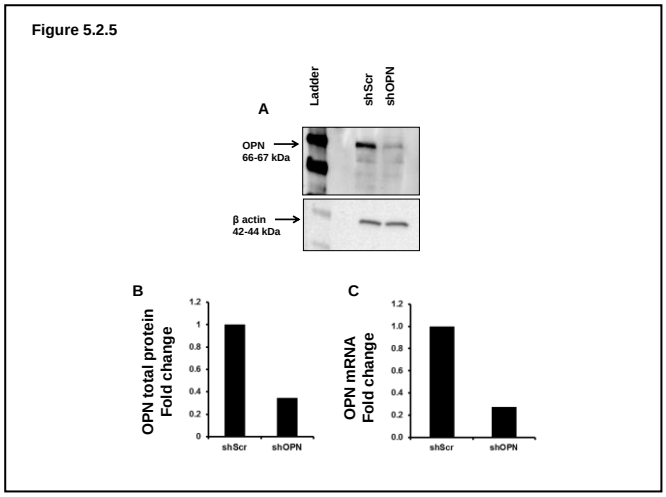

Fig. 5.2.5: OPN knockdown in GRX HSC
Mouse HSC line (GRX) was infected with lentiviral particles containing non-targeting scrambled shRNA (shScr) or OPN-targeting shOPN (shOPN). (A) Western blot and (B) densitometry showing OPN knockdown using lenti-shOPN compared with control lenti-shScr. (C) OPN mRNA. Results were expressed as fold change relative to shScr. *p<0.05 vs. shScr

We verified these results using OPN-specific aptamers which neutralize circulating OPN (82, 83), in the presence of rleptin. OPN neutralization blunted αSMA expression **(Fig. 5.2.6A)**, and significantly repressed collagen 1α1 and TGFβ mRNA (~50%) **(Fig. 5.2.6B, C)**. Similar to knockdown experiments, OPN neutralization also inhibited migratory properties of HSC, leading to impaired wound healing (~30%) and transmigration (~50%) across membranes **(Fig. 5.2.6D, E).** In aggregate, these results demonstrate that OPN is a downstream effector of leptin induced fibrogenesis, and that OPN is a potential anti-fibrotic target.

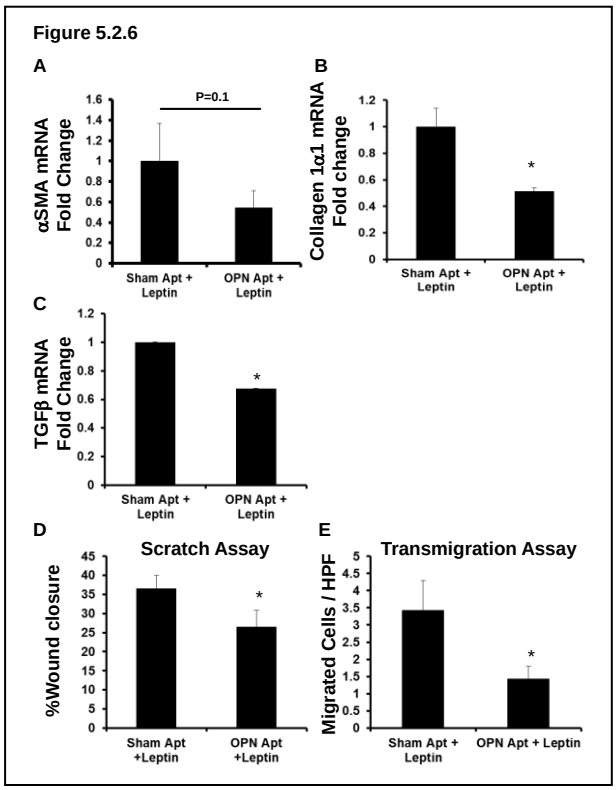

Fig. 5.2.6: OPN neutralization inhibits fibrogenic effects of leptin in GRX HSC
HSC were treated with sham aptamers (100nM) or OPN aptamers (100nM) under leptin-stimulated (100ng/ml) conditions, for 48 h. Cells were then harvested and RNA analyzed by QRTPCR. (A) αSMA mRNA. (B) Collagen 1α1 mRNA. (C) TGFβ mRNA. Results are expressed as fold changes relative to sham-aptamer and graphed as mean ± SEM. Wound-healing and transmigration studies in sham or OPN aptamer-treated HSC were performed under leptin-treated conditions (D-E). (D) Wound healing; migration was quantified by measuring the distance dividing the two sides of the monolayer. Mean (% wound closure) ± SEM were graphed. (E) Transmigration was evaluated 24 h after seeding of cells, by counting crystal violet-stained cells on the underside membrane in 15 random HPF. Mean cell numbers ± SEM were graphed. *p<0.05 vs sham-aptamer

5.2.3. OPN expression is regulated by Leptin-PI3K/Akt signaling in HSC

Leptin receptors couple with PI3K and activate Akt, which is required for leptin-associated fibrogenic effects (115, 116). Leptin activates the Hh pathway in HSC, but this is blocked by LY294002, a PI3K inhibitor (60). Because OPN is a downstream target of the Hh pathway **(Results: 5.1),** we investigated if OPN could similarly be regulated by the PI3K/Akt pathway. GRX HSCs were treated with leptin in the presence or absence of LY294002. LY294002 significantly repressed OPN mRNA by >50% **(Fig 5.2.7A),** and downregulated fibrogenic genes αSMA, collagen 1α1, and TGFβ by up to 60% **(Fig 5.2.7B – D).** OPN knockdown in combination with LY294002 further enhanced repression of fibrogenic genes by an additional ~20% **(Fig 5.2.7).**

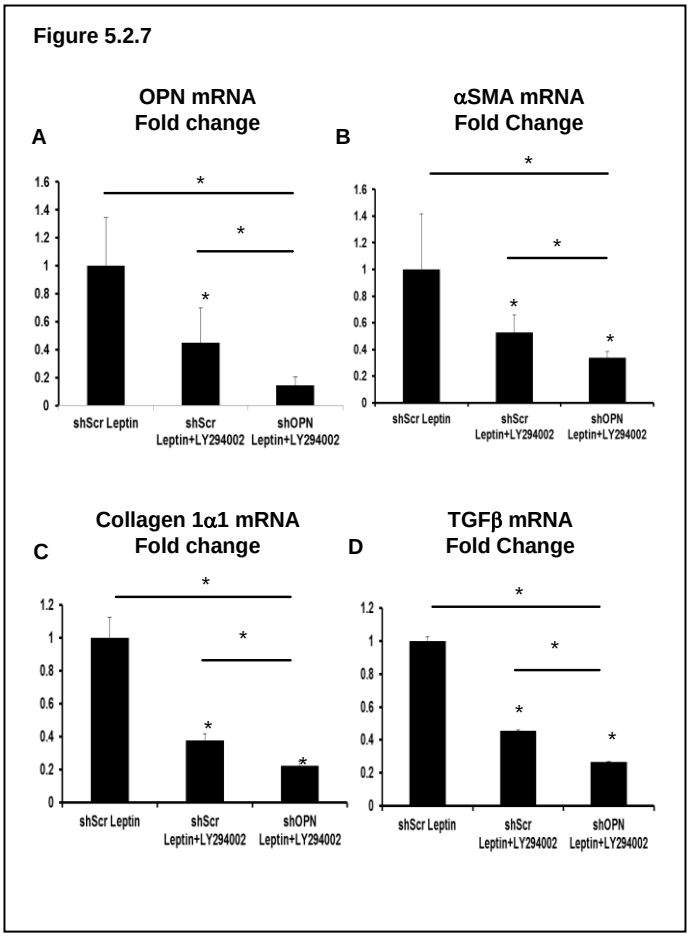

Fig. 5.2.7: OPN is PI3K regulated and enhances fibrogenesis in GRX HSCs
HSC with OPN knockdown (shOPN) and control HSC (shScr) were treated with recombinant leptin, with or without LY294002 (a PI3K inhibitor). Cells were then harvested and RNA analyzed by QRTPCR. (A) OPN mRNA. (B) αSMA mRNA. (C) Collagen 1α1 mRNA. (D) TGFβ mRNA. Results are expressed as fold changes relative to shScr-Leptin, and graphed as mean ± SEM. *p<0.05 vs. shScr-Leptin

To exclude the possibility that observed responses were GRX specific, we repeated experiments using freshly isolated rat HSC. Comparable with GRX HSCs, leptin treated, primary rat HSC upregulated OPN, αSMA, and collagen 1α1 mRNA by ~2-fold **(Fig 5.2.8A – C),** but this effect was completely blocked in the presence of LY294002. OPN mRNA in particular, was repressed below basal expression. Adenoviral-mediated transfer of dominant negative Akt (dnAkt) similarly inhibited leptin mediated changes in OPN, αSMA, and collagen 1α1 mRNA **(Fig 5.2.8A – C)**, but infection with mock adenoviral vectors (AdGFP; control) did not. By contrast, infection with the constitutively active Akt vector (Ad5myrAkt) induced OPN, αSMA, and collagen 1α1 mRNA to levels comparable with leptin-treated cells**.**

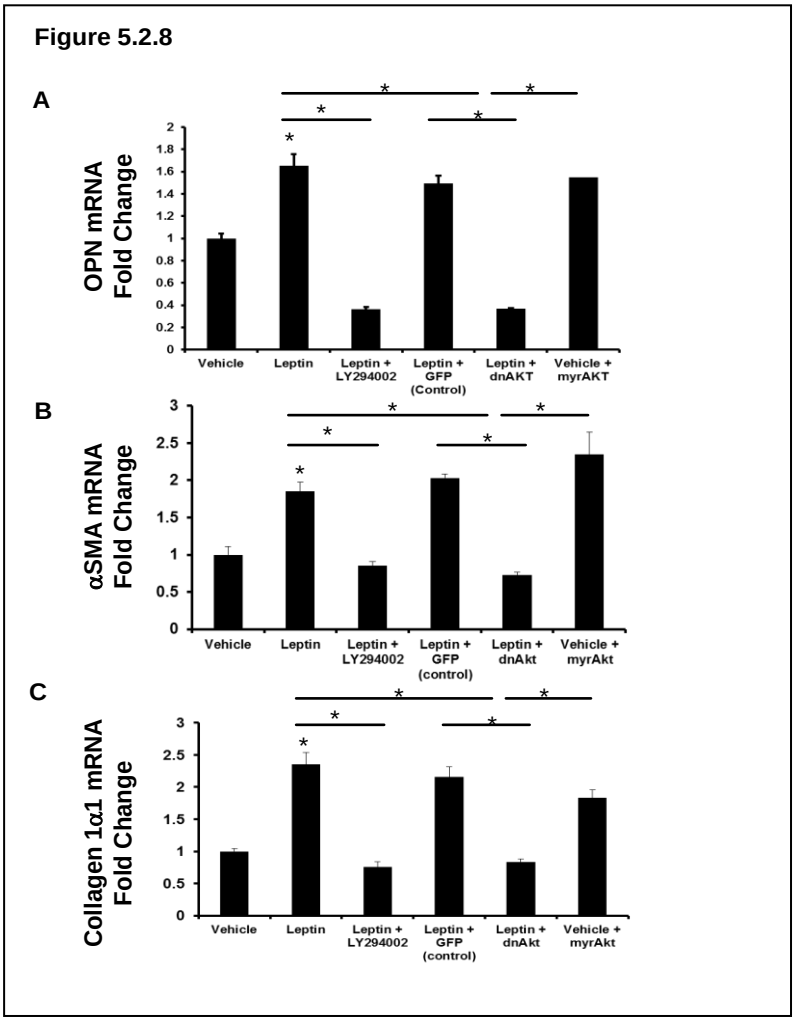

Fig. 5.2.8: OPN is a downstream target of leptin and is PI3K/Akt regulated in primary HSC
Freshly isolated HSC were treated with leptin (or vehicle), with or without LY294002. Additional HSC were also pre-treated with Ad5dnAkt (or Ad5GFP) prior to treatment with leptin (100 ng/mL) or Ad5mryAkt alone. RNA was isolated and changes in gene expression evaluated by QRT-PCR. (A) OPN mRNA. (B) αSMA mRNA. (C) Collagen 1α1 mRNA. Results are expressed as fold changes relative to vehicle-treated HSC, and graphed as mean ± SEM. *p<0.05 vs. vehicle.

5.2.4. OPN neutralization inhibits leptin-associated fibrogenesis in precision-cut liver slices

To validate *in vitro* findings, we used an established liver organ culture system in which precision-cut, viable mouse liver slices (PCLS) were stimulated with leptin, in the presence of sham or OPN aptamers. PCLS are useful because they can be cultured for several days and better reflect the multicellular *in vivo* conditions (3, 117). Liver slice viability was maintained as evidenced by the ATP assay **(Fig 5.2.9A)**. Treatment with exogenous leptin upregulated liver slices OPN mRNA by ~2-folds **(Fig 5.2.9B),** and induced αSMA and collagen 1α1mRNA by ~20% **(Fig 5.2.9C, D).** Conversely, neutralizing OPN significantly repressed OPN and collagen 1α1mRNA**,** even beyond basal levels. No change in total slice αSMA mRNA was detected.

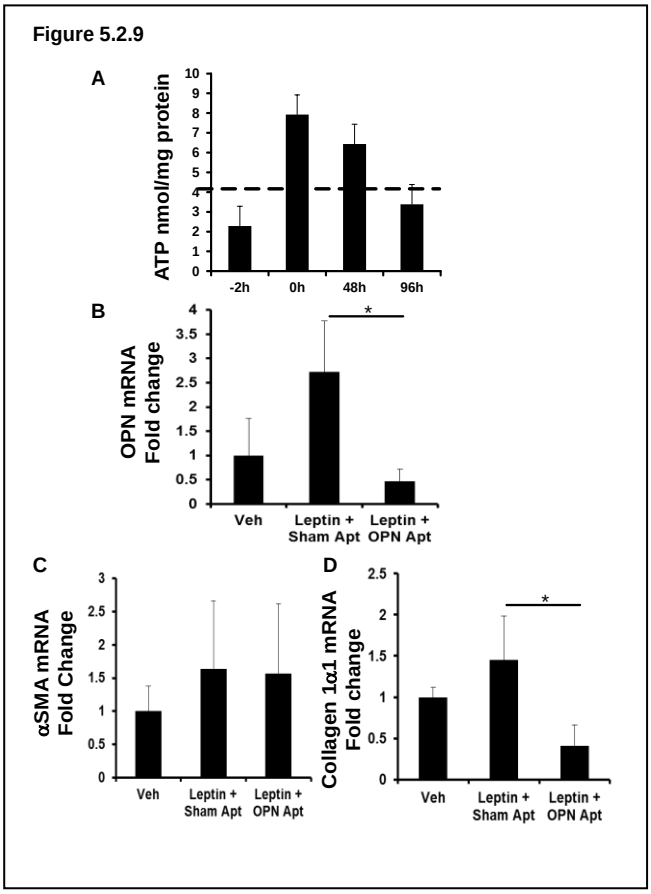

Figure 5.2.9: OPN neutralization abrogates fibrogenesis in PCLS
Precision-cut, viable mouse liver slices (PCLS) (a liver organ culture system) were stimulated with leptin (or vehicle), in the presence of sham or OPN specific aptamers for 48 h. At the end of treatment, liver slices were harvested, viability assessed by ATP content, and RNA analyzed by QRTPCR. (A) ATP content (viability) in nmol/mg protein; hashed line denotes the accepted viability threshold. (B) OPN mRNA. (C) αSMA mRNA. (D) Collagen 1α1 mRNA. Results are expressed as fold changes relative to vehicle-treated PCLS, and graphed as mean ± SEM. *p<0.05 vs. vehicle.

5.3. Role of OPN in the Liver Progenitor Cell Response and Fibrosis

Osteopontin Neutralization Abrogates the Liver Progenitor Cell Response and Fibrogenesis in Mice
(Coombes JD ….Syn WK. Gut. 2015 Jul; 64(7):1120-31)

During CLD, restoration of liver mass and function in response to hepatocyte loss involves activation of liver progenitors within the liver (i.e. progenitor-associated repair response or ductular reaction) (32, 33, 34), which proliferate and differentiate into new hepatocytes and cholangiocytes (118,119). This pool of progenitors is heterogeneous, compromising the resident LPC or oval cell residing in the Canals of Hering (38), bone marrow-derived progenitors (120, 121), as well as HSC (41). HSC are liver fibroblasts which normally transition into collagen-producing MFs when activated (51, 52), but have recently been recognized as a multi-potent progenitor that interacts with the liver progenitor pool (41); thus, providing an explanation for the fibrogenic outcomes which accompany progenitor-cell expansion during persistent liver injury (i.e. fibrogenic-repair). These cell culture and mouse observations are supported by longitudinal human studies, which show that the ductular reaction is predictive of subsequent fibrosis (34,122). Hence, targeting the progenitor-associated repair response may be of value in inhibiting fibrosis in CLD.

Progenitor-cell activation is driven by a milieu of growth factors, and cytokines which accompany CLD (8, 123). Recently, we reported that injury-related re-activation of the Hh induces liver progenitors to proliferate, undergo EMT (i.e. upregulating mesenchymal, while repressing epithelial genes), and secrete factors that activate neighboring progenitors and matrix-producing cells (13 – 15, 48). OPN is a Hh-target, and a matricellular protein that is highly upregulated in fibrotic skin, lungs, kidneys, and joints (20, 124 – 126). Mice genetically deficient in OPN develop less fibrosis after certain injuries, suggesting that OPN may be a direct effector of the fibrotic process. Not surprisingly, HSC express high levels of OPN to auto-regulate their fibrogenic phenotype **(Results: 5.1).** However, the highest expression of OPN is seen in cells located in the liver periportal regions, and recent studies show that OPN is a key regulator of bone-marrow progenitor/stem-cell fate (127). These led us to hypothesize that OPN modulates the progenitor-associated fibrogenic repair response during liver injury.

Despite prevailing data giving credence to OPN being an attractive anti-fibrotic target, and humanized antibodies to OPN being developed for inflammatory-joint diseases (126), no study has yet evaluated the impact of OPN neutralization in the treatment of fibrosis complicating CLD. Therefore, to evaluate these hypotheses, we studied the direct effects of OPN in cultures of LPCs, examined the effects of OPN neutralization (by OPN aptamers or OPN neutralizing antibodies) in three murine models of liver fibrosis, and corroborated findings with analysis of liver tissues from patients with CLD.

5.3.1. OPN is upregulated in human CLD and is expressed by Sox9+ liver progenitors

Coded liver sections from patients with NASH-cirrhosis (n= 5), ALD-cirrhosis (n= 5), and PBC (n= 5) were stained to demonstrate OPN**,** Sox9, and K19**.** Compared with healthy livers, cirrhotic livers exhibit up to 15-fold more OPN protein **(Fig 5.3.1A, Fig 5.3.2A)** and 10-fold more OPN mRNA **(Fig 5.3.2F).** The highest level of OPN is expressed by cells located in the peri-portal regions**.** As expected, cirrhotic livers express more TGF-β mRNA than healthy livers (**Fig 5.3.2F**)

Because Sox9+ cells are bi-potent liver progenitors that arise from peri-portal Canals of Hering (128), we examined this LPC (oval cell) marker. As expected, cirrhotic livers contain up to 10-times more Sox9+ cells (**Fig 5.3.1B, Fig 5.3.2B**) and upregulate Sox9 mRNA by up to 5-fold (**Fig 5.3.2F**). Sox9+ cells also express K19 (another ductular progenitor marker) (**Fig 5.3.2D**). Compared with healthy control livers, cirrhotic livers accumulate up to 20-fold more Sox9/K19 double-positive liver progenitors (**Fig 5.3.2D, E**)**.** Interestingly, the highest amount of OPN is expressed by liver progenitors (**Fig 5.3.1C – E**). Double IHC confirm that OPN+ cells co-localize with Sox9+ cells (**Fig 5.3.1C, D**), and cirrhotic livers are enriched with OPN/Sox9 double positive progenitors by over 15-fold (**Fig 5.3.1E**).

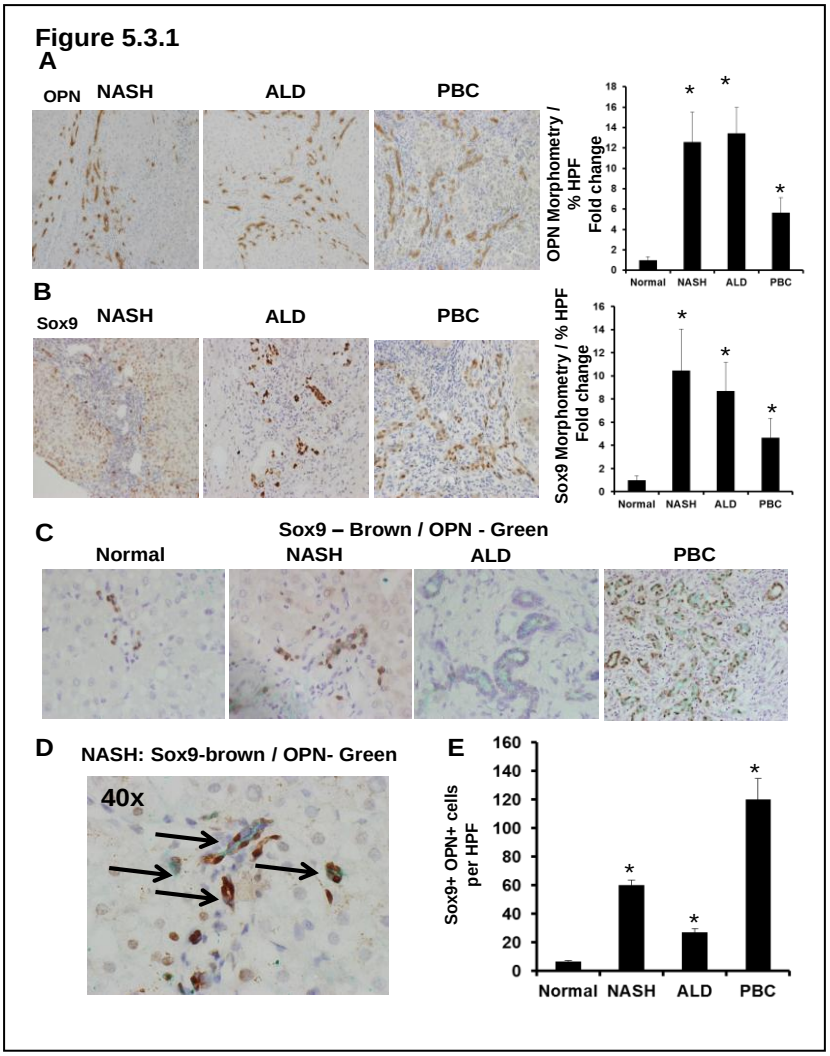

Fig. 5.3.1: OPN is upregulated in human CLD and is expressed by Sox9+ liver progenitors

Liver sections from patients with NASH-cirrhosis (n = 5), ALD-cirrhosis (n = 5), PBC (n = 5), and excess normal donor livers (n = 3), were stained for OPN, and Sox9. OPN-staining was analyzed by morphometry; the number of Sox9+ cells (stained nuclei) was counted in 20 randomly-chosen high-power fields (HPF)/section. Representative photomicrographs are shown. (A) OPN staining and OPN morphometry. (B) Sox9 staining and Sox9 morphometry. (C) Sox9 (Brown) and OPN (Green)–double-immunostaining. (D) High magnification of Sox9 / OPN–double-immunostaining in NASH-cirrhosis (black arrows) (x400). Sox9 / OPN quantification by cell counting; number of double positive cells per HPF. Results are expressed as fold change relative to normal liver and graphed as mean ± SEM. *p<0.05 vs. normal liver

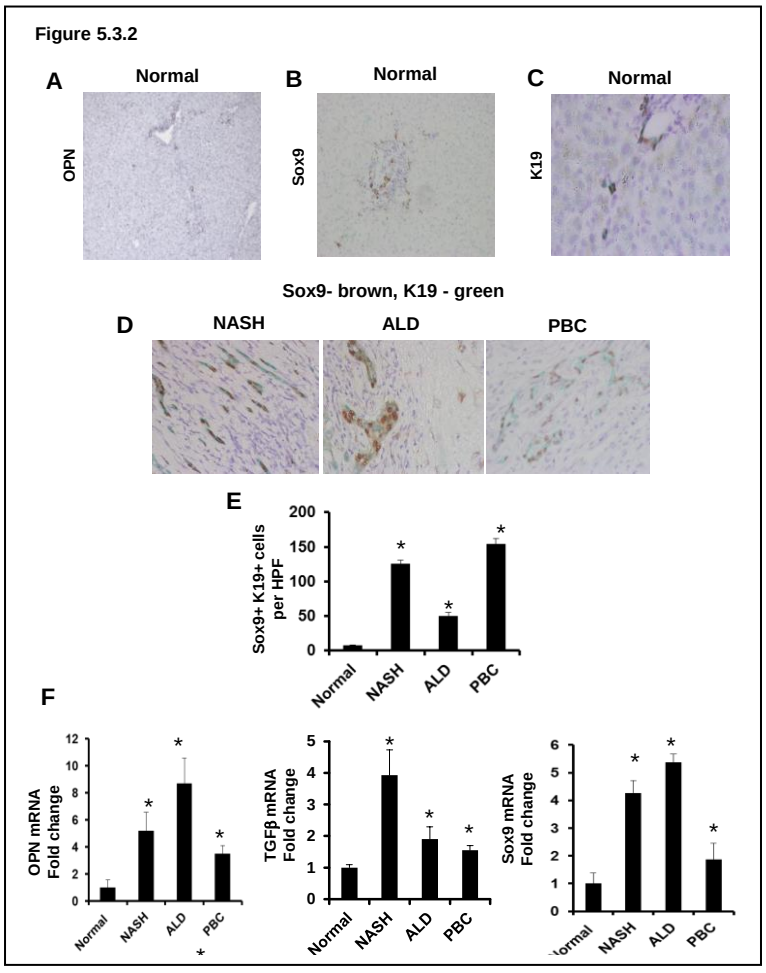

Fig. 5.3.2: Progressive human CLD is associated with upregulated fibrogenic markers and an enhanced liver progenitor response

Excess donor (healthy) livers were stained for OPN, or the LPC markers, Sox9 and K19. Coded liver sections from patients with NASH, ALD, and PBC were also double stained for Sox9-K19. Representative photomicrographs are shown. (A) OPN in healthy liver. (B) Sox9 in healthy liver (C) K19 in healthy liver. (D-E) Sox9 (brown) - K19 (green) double IHC with Sox9/K19 quantification by cell counting; number of double positive cells per HPF. The number of Sox9/K19 double positive cells was counted in 20 randomly-chosen HPF/section. Total liver RNA was also isolated from individuals with NASH, ALD, and PBC (n = 4 / group) and analyzed by qRTPCR. (F) OPN, TGFβ, and Sox9 mRNA. Mean ± SEM are graphed * p<0.05 vs. normal liver.

5.3.2. OPN regulates viability/proliferation of liver progenitors

As the highest amounts of OPN were expressed by Sox9+ LPC in vivo **(Fig 5.3.1)**, we evaluated the importance of OPN in LPC viability/proliferation. We utilized 603B cells (ductular LPCs) (14, 87), which co-express Sox9, K19 (both markers of LPC), and OPN **(Fig 5.3.3A).** 603B supernatants contain high levels of OPN (**Fig 5.3.4**). Treating 603B with OPN aptamers or OPN neutralizing antibodies lowered OPN levels in culture supernatants (**Fig. 5.3.4A, B**). OPN aptamers reduced cell viability by 24 h, but this was most pronounced at 72 h (up to 2-fold reduction) when quantified by the CCK8 assay **(Fig 5.3.3B).** Because liver fibrosis and cirrhosis is associated with upregulated TGF-β **(Fig 5.3.2F)** (and TGF-β modulates progenitor-cell differentiation (129)), we repeated OPN neutralizing experiments under conditions of TGF-β stimulation. OPN neutralization under pro-fibrogenic stimulation led to greater suppression of cell proliferation **(3-fold; Fig 5.3.3C),** and markedly increased 603B apoptosis, as measured by the caspase 3/7 assay **(Fig 5.3.3D);** sub-G1 analysis by FACS (detecting DNA fragmentation) confirmed comparable increases in 603B apoptosis **(3-fold; Fig 5.3.3E-F).**

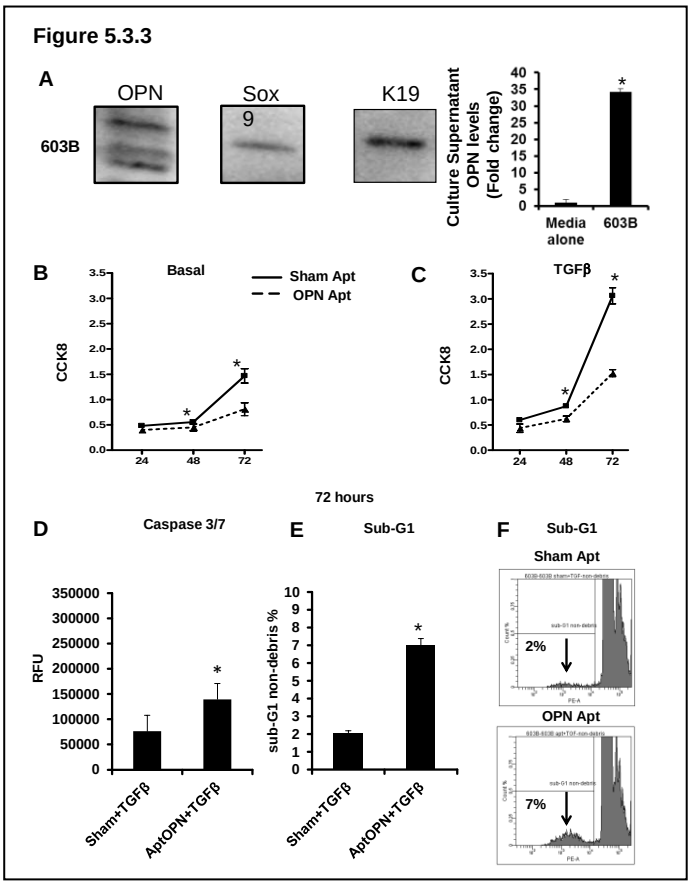

Fig. 5.3.3: OPN promotes LPC viability
LPC were analyzed for OPN, Sox9 and K19 by western blot, and LPC-CM assayed using OPN ELISA. In separate experiments, LPC were treated with sham or OPN aptamers, in the presence or absence of TGF-β. Viability/proliferation was assessed using the CCK8 assay, and apoptotic activity evaluated by caspase-3/7 activity and by sub-G1 analysis (A) OPN, Sox9, and K19 protein expression; OPN levels in 603B-CM. (B) Cell numbers under basal (non-TGF-β) conditions; 24-72 h. (C) Cell numbers under TGF-β conditions; 24-72 h (solid line: sham aptamer-treated; dashed line: OPN aptamer-treated). Mean ± SEM (O.D) are graphed. (D) Caspase-3/7 under TGF-β conditions; 72 h. Mean ± SEM (RFU) are graphed. (E) Sub-G1 analysis under TGF-β conditions; 72 h. % of cells in sub-G1 are graphed (F) Representative sub-G1 histograms from sham or OPN-aptamer treated 603B at 72 h. All experiments were performed in triplicate. *p<0.05 vs. respective baseline

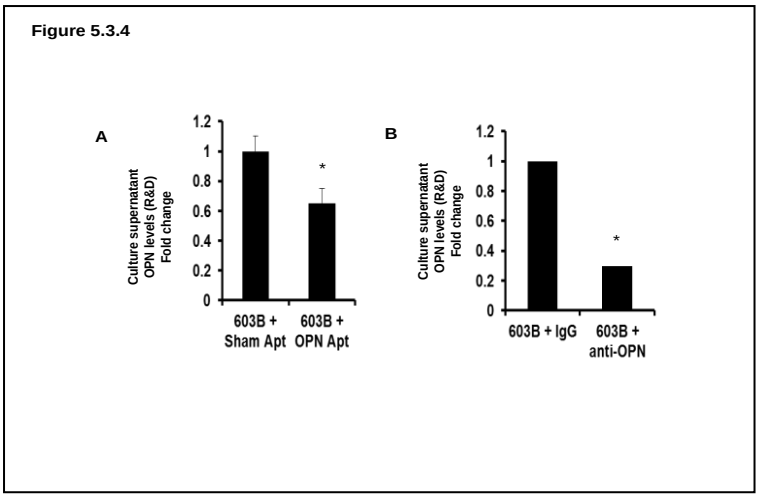

Fig. 5.3.4: LPC secrete high levels of OPN Sham aptamers or OPN aptamers (or anti-OPN or isotype-matched control antibodies) were added to LPC-CM; LPC-CM was then assayed using the OPN ELISA kit (R&D). (A) OPN protein levels in LPC-CM treated with sham aptamers or OPN aptamers, and (B) OPN protein levels in 603B-CM treated with anti-OPN antibody or isotype-matched antibody. Results were expressed as fold change relative to sham-aptamer or isotype-matched control. *p<0.05 vs. respective baseline

5.3.3. OPN enhances progenitor-associated wound healing

OPN effects on LPC

Cumulative data suggest that liver progenitors are capable of re-programming into MF (13, 14, 40). Therefore, we evaluated if changes in OPN levels would lead to similar alterations in progenitor phenotype. 603B-LPCs were treated with recombinant OPN or OPN aptamers**.** OPN neutralization led to a decrease in progenitor associated fibrogenic genes, Snail and Collagen 1αI **(Fig 5.3.5A),** while upregulating epithelial genes, E-Cadherin and Id2 **(Fig 5.3.5B)**. Increased cell-motility and migration are key phenotypic changes that accompany EMT (13, 130). Therefore, we compared 603B migration in OPN neutralizing or control conditions. Migration was assessed by semi-quantitating the dimensions of a wound dividing the confluent monolayer 12 h after the scratch. OPN neutralization led to over 50% less wound healing **(Fig 5.3.5C).** Comparable results were observed in the modified cell-invasion assay **(Fig 5.3.5D).** OPN neutralization led to nearly 70% fewer 603B cells invading across the insert membrane**.**

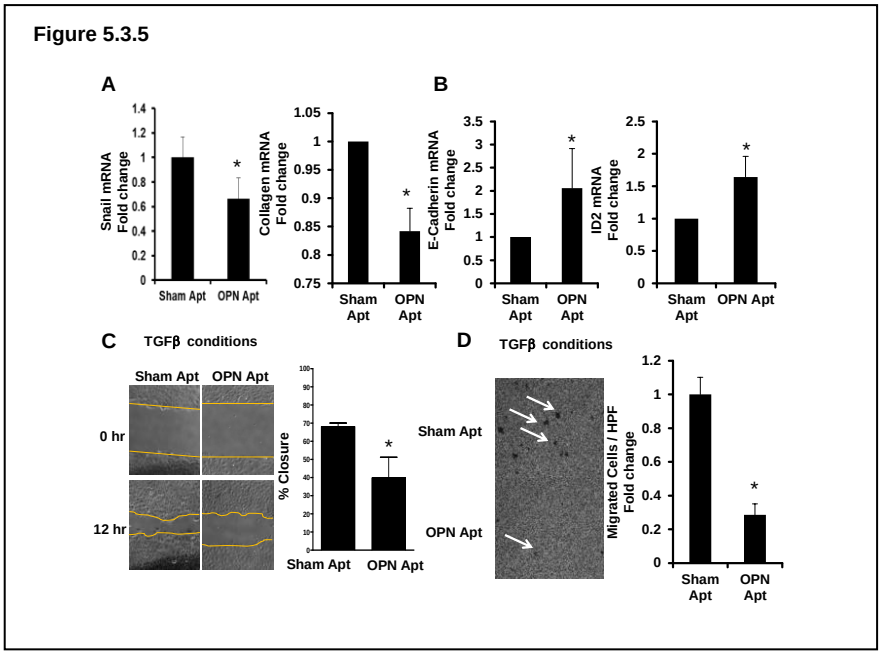

Fig. 5.3.5: OPN enhances LPC associated wound healing responses

603B-LPC were treated with sham or OPN aptamers, in the presence of TGF-β for 48 h. Cells were analyzed for EMT markers. (A) Snail and Collagen 1αI mRNA. (B) E-cadherin and Id2 mRNA. Mean ± SEM were graphed. Wound healing and transmigration studies were performed using conditions described (C-D). (C) Wound-healing under TGF-β conditions at time 0 (time of scratch) and 12 h later; migration was quantified by measuring the distance dividing the two sides of the monolayer. Mean (% wound closure) ± SEM were graphed. (D) Transmigration under TGF-β conditions was evaluated 24 h after seeding of cells, by counting crystal violet-stained cells on the underside membrane in 15 random HPF. Mean cell numbers ± SEM were graphed. *p<0.05 vs sham aptamer.

OPN is a complex molecule which consists of intracellular and extracellular/soluble OPN isoforms, which exhibit overlapping, but also different and opposing functions (19). OPN aptamers neutralize only soluble OPN isoforms. We evaluated if additional loss of intracellular OPN by RNAi might reproduce OPN aptamer effects on LPC phenotype. Compared with control (603B-shScr) (603B infected with lentiviral particles containing non-targeting scrambled shRNA), OPN knockdown (~50%) (603B-shOPN) was associated with a 2-3 fold reduction in cell proliferation under basal and TGF-β conditions (**Fig 5.3.6A-D**), with minimal changes in LPC apoptosis. shOPN abrogated 603B-LPC transmigration by 50% (**Fig 5.3.6E**), but did not affect wound healing response even under TGF-β conditions (data not shown), thus indicating functional differences between extracellular and intracellular OPN.

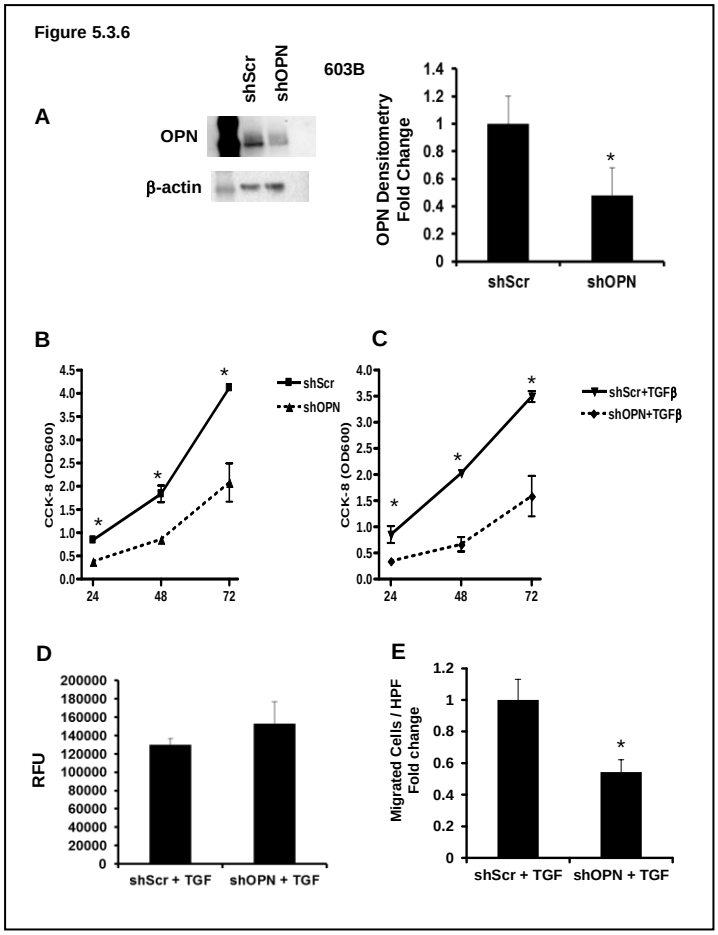

Fig. 5.3.6: OPN knockdown reduces LPC proliferation and transmigration
603B-LPC were infected with lentiviral particles containing non-targeting scrambled shRNA (shScr) or OPN targeting shOPN (shOPN). Viability/proliferation, apoptosis, and transmigration studies were performed. (A) Western blot and densitometry showing OPN-knockdown using lenti-shOPN compared with control lenti-shScr. Results were expressed as fold changes relative to shScr (B) CCK8 assay; cell numbers under basal and TGF-β conditions; 24-72 h (solid line: 603B-shScr cells; dashed line: 603B-shOPN cells). Mean ± SEM (O.D) are graphed. (D) Caspase-3/7 under TGF-β conditions; 48 h. Mean ± SEM (RFU) are graphed. (E) Transmigration under TGF-β conditions was evaluated 24 h after seeding of cells, by cell-count in 15 random HPF. Results were expressed as fold change relative to shScr. *p<0.05 vs. shScr

OPN modulates TGF-β signaling

Because the fibrotic liver is enriched with high levels of TGF-β**,** we next evaluated if OPN effects on LPC were mediated by modulating TGF-β signaling. Treating 603-LPC with TGF-β led to the accumulation of phospho-Smad-2/3 proteins **(Fig 5.3.7A, B),** and to the preservation of Ski and SnoN **(Fig 5.3.7A, B)**, transcriptional co-repressors which inhibit transcriptional activity of TGF-β-dependent Smad-2/3-complexes under basal conditions (131). Both Smad phosphorylation and Ski and SnoN levels were unaffected by the addition of the sham aptamers. In contrast, treatment with OPN aptamers led to reduced levels of phospho-Smad-2/3 proteins **(Fig 5.3.7A, B),** while protecting Ski and SnoN from TGF-β-induced degradation**.** No changes were observed with Smad7 protein, another negative feedback mechanism that regulates the TGF-β signal (132). To better define how OPN modulates TGF-β signaling, we targeted (putative extracellular OPN-receptors on progenitor cells) (133), treating 603B-LPC with CD44 neutralizing antibody, and αvβ3 antagonist XJ735. CD44 and αvβ3 blockade resulted in a 30% reduction in phospho-Smad-2/3

expression (**Fig 5.3.7C**), resembling the effects of OPN neutralization with OPN aptamers. However, general depletion of OPN (intracellular) using shOPN (i.e. 603B-shOPN) did not repress phospho-Smad-2/3 expression (data not shown), implying that widespread OPN knockdown could only recapitulate some effects of OPN neutralization with OPN aptamers, and reinforcing the concept that extracellular OPN is different from intracellular OPN.

Figure 5.3.7

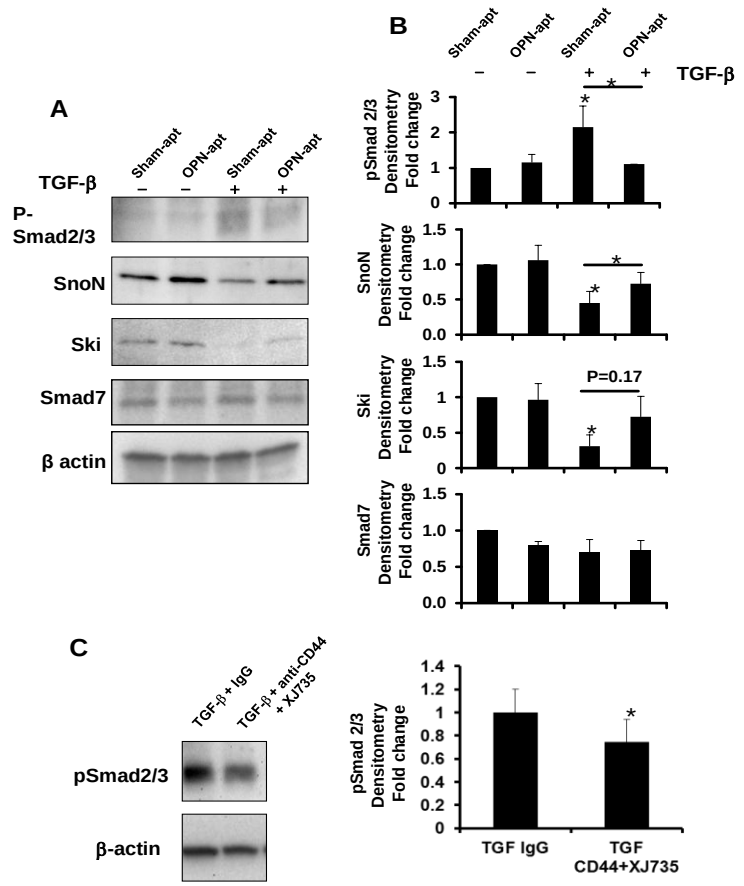

Fig. 5.3.7: OPN aptamers inhibits TGF-β signaling
603B-LPCs were treated with sham aptamers or OPN aptamers, in the presence or absence of TGF-β (5ng/ml) for 48 h. In separate studies, 603B-LPCs were treated with a CD44 neutralizing antibody, and XJ735, a selective αvβ3 antagonist, in the presence of TGF-β for 48 h. At the end of experiments, protein was harvested and analyzed by western blot. (A) Representative western blot: phospho-Smad 2/3, SnoN, Ski, Smad 7, and beta-actin. (B) Protein densitometry for phospho-Smad 2/3, SnoN, Ski, and Smad 7. (C) Western blot and corresponding densitometry for phospho-Smad 2/3. Results are expressed as fold change relative to respective baseline control, and graphed as mean ± SEM. *p<0.05 vs. baseline control

.

OPN effects on HSC

Liver progenitors comprise not only of LPC (oval cell), but HSC, a fibroblast and recently recognized multi-potent progenitor (41). When activated, HSC undergo transition to become MF (40, 48). LPC and HSC are in close proximity, suggesting that both progenitor cell populations are capable of crosstalk. We therefore evaluated whether reduced levels of OPN in the microenvironment alters the 'LPC- secretome' that influences HSC phenotype. 603Bs were treated with OPN aptamers or sham aptamers, in the presence of TGF-β for 48 hours; 603B-CM were

then harvested and added to primary HSC for 24 hours. As expected, the addition of 603B-CM to HSC resulted in activation of HSC by upregulating αSMA and collagen 1α1 mRNA by 2 fold (**Fig 5.3.8A, B**). HSC activation was enhanced when treated with TGF-β–stimulated 603B-CM. The addition of OPN aptamers to 603B resulted in a significantly altered secretome: CM from OPN aptamer-treated 603B induced a significantly attenuated fibrogenic-response in HSC (to almost quiescent) compared with CM obtained from sham aptamer-treated 603B, with 4-fold and 5-fold less αSMA and collagen 1α1 mRNA under basal and TGF-β–stimulated conditions, respectively (**Fig 5.3.8A, B**). Experiments repeated using the human liver myofibroblast line (Lx2) revealed comparable findings: CM from OPN aptamer-treated 603B had diminished activating capacity on Lx2 cells (lower αSMA mRNA by 40% and lower collagen 1αI mRNA by 50%) **(Fig 5.3.8C, D).** To address concerns that effects on HSC could be related to residual OPN aptamers in the 603B-CM, we used CM obtained from 603B-shOPN (OPN knockdown) and 603B-shScr (control) cells, treated with or without TGF-β (**Fig 5.3.8A, B**). Under basal conditions, CM derived from 603B-shOPN activated primary HSC (αSMA and collagen 1α1 mRNA) approximately 2-fold less than CM-603B-shScr (**Fig 5.3.8A, B**). These differences in CM-effects were reduced under TGF-β conditions (~1.5 fold). In a further experiment, 603B-shOPN and 603B-shScr were treated with either sham aptamers or OPN aptamers for 48 hours, and respective CMs collected to treat HSC. The addition of OPN aptamers virtually abolished HSC activation (αSMA and collagen 1α1 mRNA levels were lower than untreated HSC). In aggregate, these data implicate the importance of OPN in modulating the LPC response.

Finally, to confirm that OPN neutralization has a direct impact on HSC, we treated primary HSC directly with sham aptamers or OPN aptamers. OPN neutralization with OPN aptamers led to 50% decrease in αSMA and collagen 1α1 mRNA under basal conditions (**Fig 5.3.8E, F**), but up to 4-fold downregulation under TGF-β stimulation.

In sum, OPN is a critical factor that modulates the LPC niche, by modulating progenitor-cell and HSC responses, via direct and indirect mechanisms.

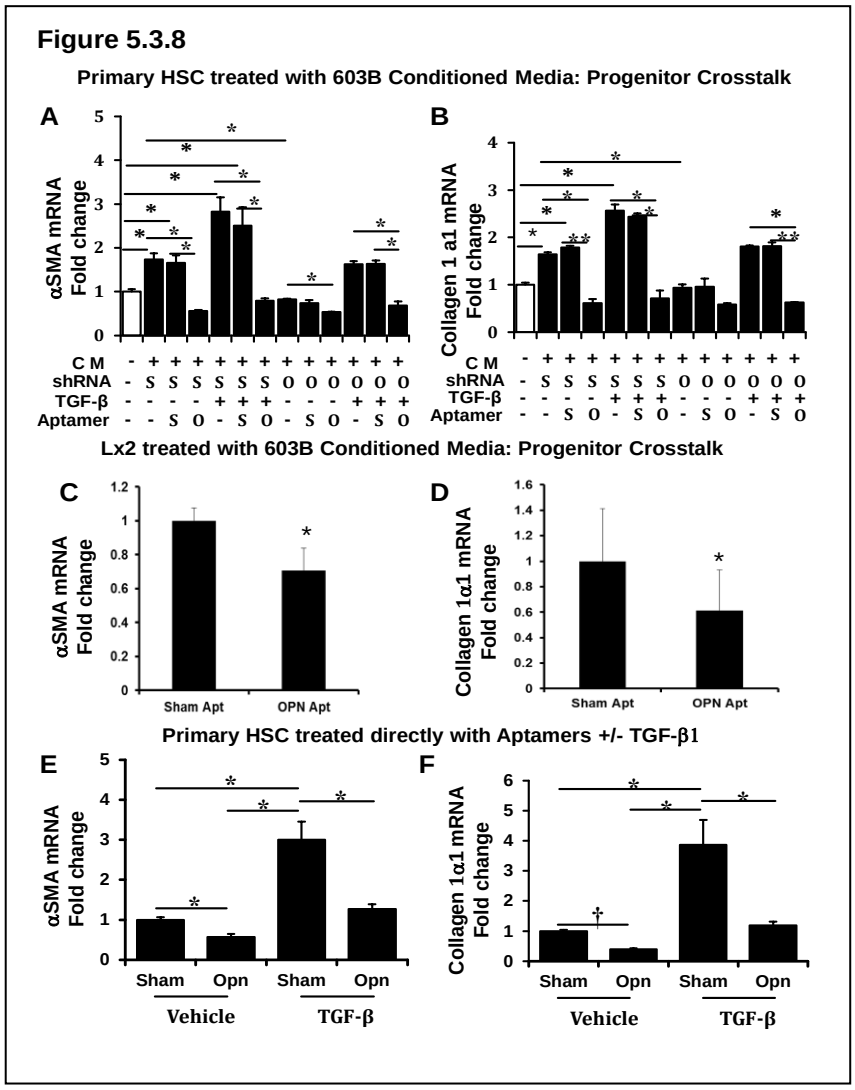

Fig. 5.3.8: OPN modulates LPC secretome and influences HSC activation

603B-LPCs were treated with sham aptamers or OPN aptamers, in the presence or absence of TGF-β (5ng/ml) for 48 h. In a parallel experiment, OPN-knockdown 603B-LPC (603-shOPN) and control (603B-shScr) cells were treated with sham aptamers or OPN aptamers, in the presence or absence of TGF-β. 603B-CM were then harvested, and added to cultures of primary HSC or Lx2 for a further 48 h. HSC or Lx2 RNA was harvested for QRTPCR. (A) αSMA mRNA in primary HSC (B) Collagen 1α1 mRNA in primary HSC (C) αSMA mRNA in Lx2 (D) Collagen 1α1 mRNA in Lx2. Separately, primary HSC cultures were treated directly with sham aptamers or OPN aptamers, in the presence or absence of TGF-β. RNA was harvested after 48 h for QRTPCR. (E) αSMA mRNA in primary HSC (F) Collagen 1α1 mRNA in primary HSC. Results are expressed as fold change relative to untreated HSC or sham aptamer-treated HSC, respectively, and graphed as Mean ± SEM. *p<0.05 vs. respective baseline as indicated, or vs. sham-aptamer-treated 603B conditions. CM: conditioned medium, -: absent, +: present

5.3.4. OPN neutralization ameliorates the LPC response and fibrogenesis in Mice

Accumulation of OPN+ (Sox9+) LPC in liver fibrosis (validation)

CCl_4 and MCD models

Fibrosis:

CCl_4 and MCD-treated mice developed significant liver fibrosis **(Fig 5.3.9, Fig 5.3.10).** This was demonstrated by increased SR staining (8-fold) **(Fig 5.3.9A, B)** and hepatic hydroxyproline quantification. Collagen deposition was accompanied by the accumulation of αSMA+ cells (10-fold) **(Fig 5.3.9C, D),** and induction of key fibrogenic genes, αSMA, Collagen 1αI, and TGF-β1 **(Fig 5.3.10).**

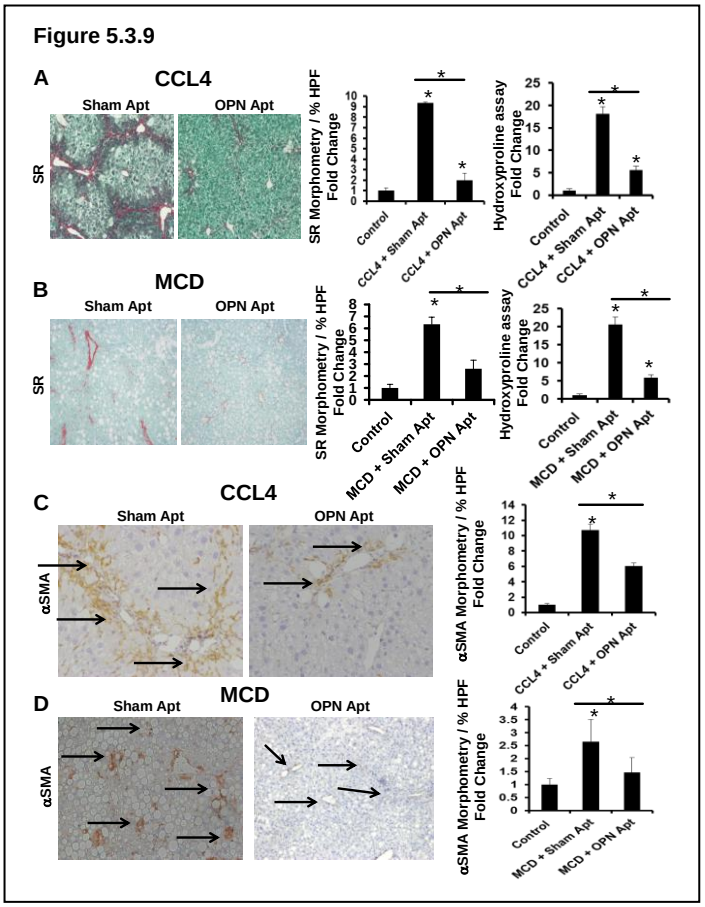

Fig. 5.3.9: OPN aptamers ameliorate fibrogenesis in CCL_4 and MCD diet-treated mice
CCL_4: In one group, mice received twice-weekly injections of olive oil (control) or CCL_4 for 6 weeks. In another group, mice receiving CCL4 were administered sham or OPN aptamers during the final week of CCL4. MCD: one group of mice was fed control-chow or the MCD diet for 5 weeks. Another group fed the MCD diet was treated with sham or OPN aptamers in the final week of dietary-challenge. Mice (n= 5/group) were sacrificed 24 h after final dose of aptamers, and livers analyzed. Representative staining are shown. (A-B) SR staining with morphometry and liver hydroxyproline measurements in CCL_4-treated (A), and MCD-fed (B) mice. (C-D) αSMA immunoreactivity (black arrows) and morphometry (20x fields for analysis) in CCL_4-treated (C), and MCD-fed (D) mice. Results were expressed as fold change relative to control mice and graphed as mean ± SEM. *p<0.05 vs. control mice

Figure 5.3.10

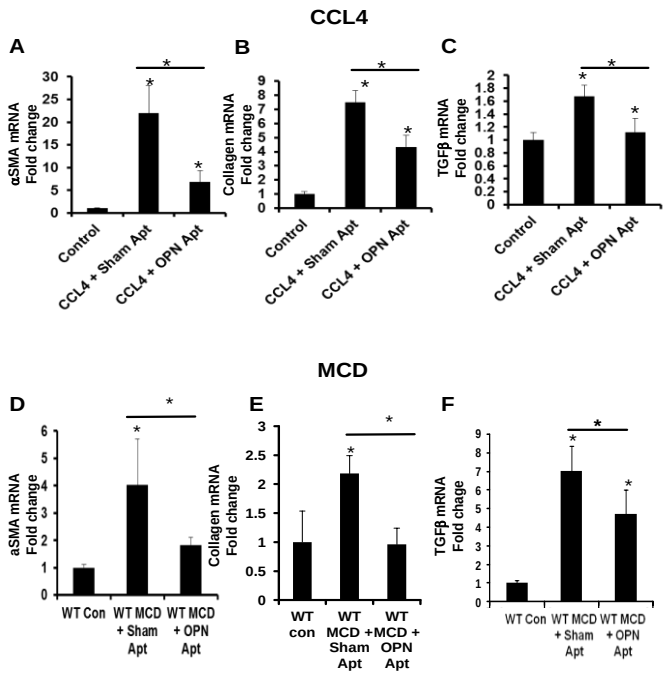

Fig. 5.3.10: OPN neutralization represses fibrogenic genes *in vivo*

Mice were treated as described in 5.3.9., and total liver RNA harvested for QRTPCR. CCL_4: (A) αSMA mRNA (B) Collagen 1α1 mRNA (C) TGF-β mRNA. MCD: (D – F). Results are expressed as fold change relative to control mice and graphed as mean ± SEM. *p<0.05 vs. control mice, or as indicated.

Figure 5.3.11

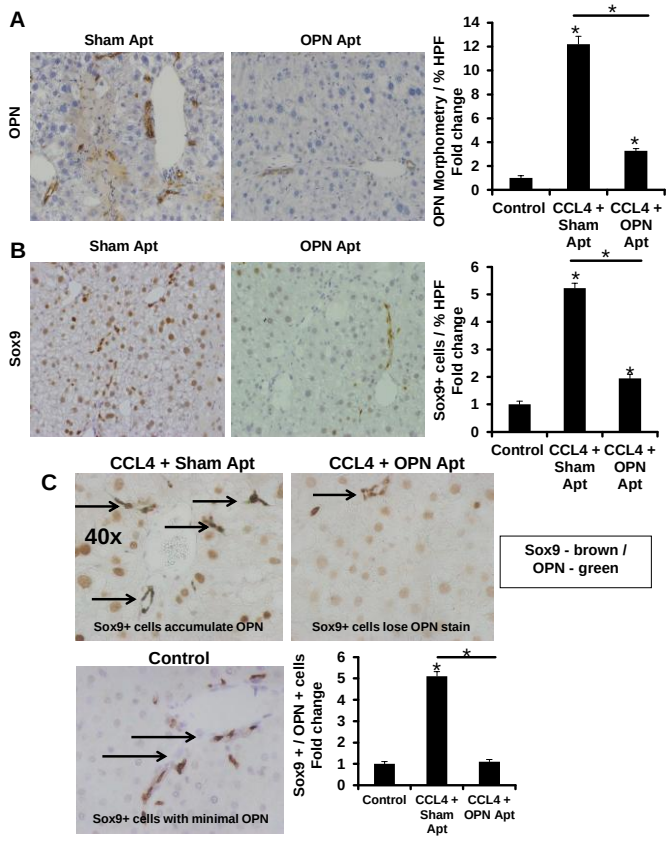

Fig. 5.3.11: OPN aptamers attenuate LPC response in CCL_4-treated mice

Mice were treated as described in Figure 5.3.9. Livers were harvested for IHC. Representative staining displayed. (A) OPN staining and OPN quantification; (B) Sox9 staining and Sox9 quantification; % of positive cells per HPF. (C) Double IHC for Sox9 (Brown) and OPN (Green). (Bottom left panel) Sox9 / OPN double staining in control mice. (Top left panel) Sox9 / OPN double staining (accumulation of Sox9 / OPN double staining) in CCL_4 treated mice receiving sham aptamers. (Top right panel) Sox9 / OPN double staining (loss of OPN staining) in CCL_4 treated mice receiving OPN aptamers. (Bottom right) Sox9 / OPN quantification by cell counting; number of double positive cells per HPF. Results are expressed as fold change relative to control mice and graphed as mean ± SEM. *p<0.05 vs. control mice. Black arrows indicate Sox9 positive cells which co-express (or should co-express) OPN.

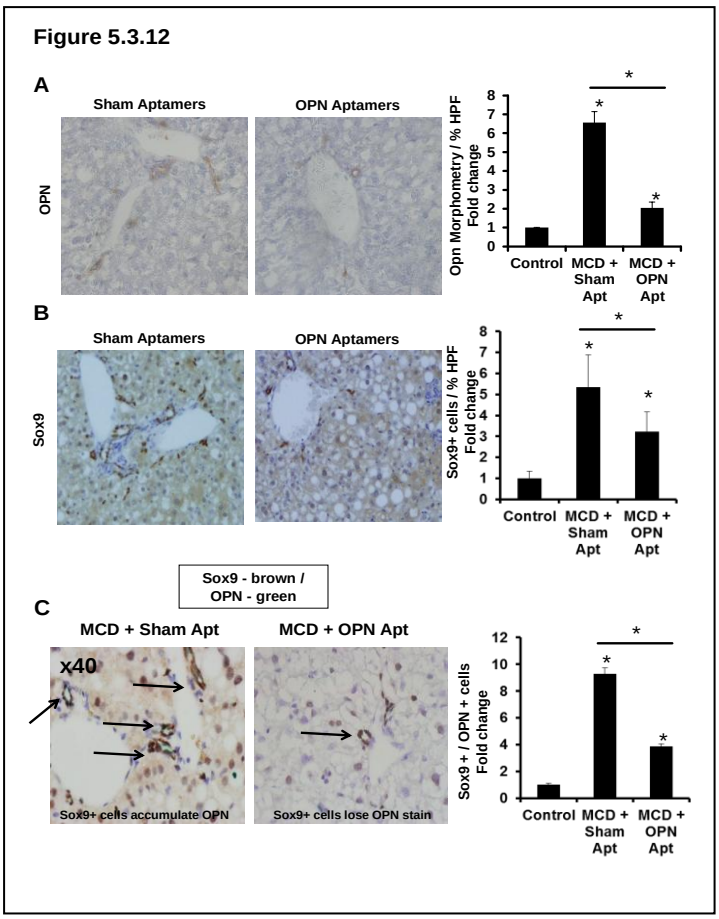

Fig. 5.3.12: OPN aptamers attenuate LPC response in MCD diet-fed mice
Mice were fed control chow or the MCD diet for 5 weeks, in the presence of sham or OPN aptamers, as described in Figure 5.3.9. Livers were harvested for IHC. Representative staining are shown. (A) OPN staining and OPN quantification by morphometric analysis. (B) Sox9 staining and Sox9 quantification by cell counting; % of positive cells per HPF. (C) Sox9 (Brown) and OPN (Green) – double IHC (magnification x400). (Left panel) Accumulation of Sox9 / OPN double positive cells in MCD-fed mice receiving sham aptamers; (Right panel) Fewer Sox9 / OPN double positive cells in MCD-fed mice receiving OPN aptamers. Graph shows Sox9 / OPN quantification by cell counting; number of double positive cells per HPF. Results are expressed as fold change relative to control mice and graphed as mean ± SEM. *p<0.05 vs. control mice. Black arrows indicate Sox9 positive cells which co-express (or should co-express) OPN.

Liver progenitors:

Liver fibrosis was associated with a 6-10 fold increase in OPN+ cells **(Fig 5.3.11A, 5.3.12A),** and an exuberant progenitor-response: 5-fold more Sox9+ LPC **(Fig 5.3.11B, 5.3.12B)**, 4-fold more Sox9 mRNA **(Fig 5.3.13A, C)**, and ~2-fold more K19 mRNA **(Fig 5.3.13B, D).** Specifically, there was a 5 to 10-fold enrichment of OPN+ cells which co-expressed Sox9, the LPC marker **(Fig 5.3.11C, Fig 5.3.12C).**

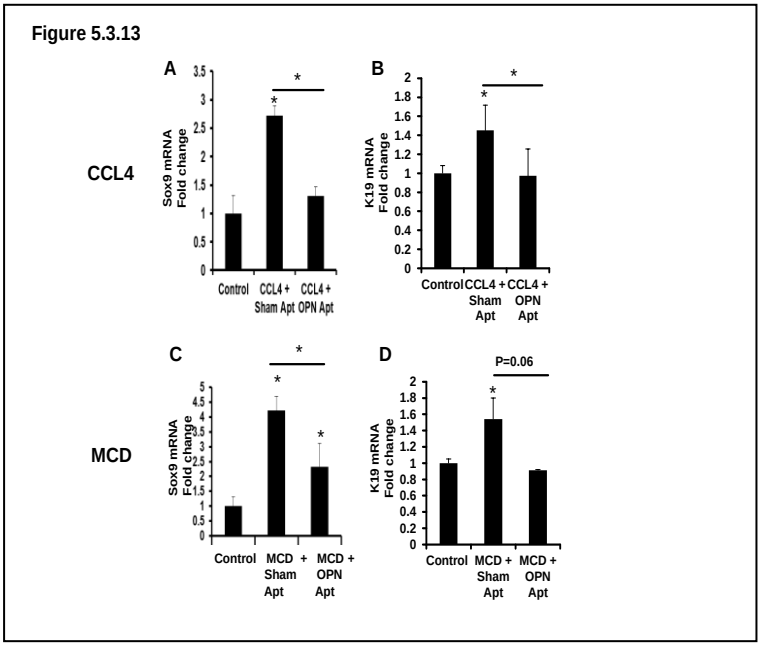

Fig. 5.3.13: OPN aptamers repress Sox9 and K19 mRNA in CCL_4-treated and MCD diet-fed mice
Mice were treated as described in Figure 5.3.9 (A-B) CCL_4: Sox9 and K19 mRNA. (C-D) MCD: Sox9 and K19 mRNA. Results are expressed as fold change relative to control-treated mice and graphed as Mean ± SEM. *p<0.05 vs. control mice, or as indicated.

Liver progenitor re-programming:

Liver fibrosis was accompanied by the upregulation of mesenchymal markers, OPN and Snail **(Fig 5.3.14A, B; Fig 5.3.15A, B),** and a downregulation of epithelial markers, E-cadherin and Id2 **(Fig 5.3.14C, D; Fig 5.3.15C, D).** Double IHC identified Sox9+ LPC which co-expressed E-Cadherin **(Fig 5.3.14E, F; Fig 5.3.15E, F)** under basal conditions; expression of E-Cadherin was significantly repressed during fibrogenesis.

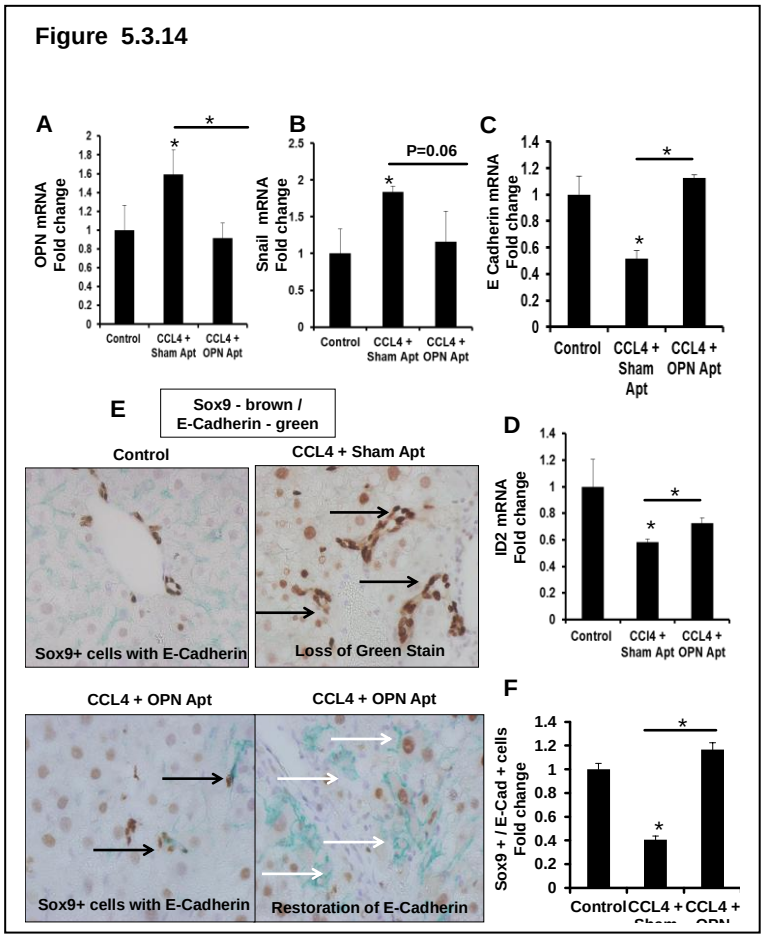

Fig. 5.3.14: OPN aptamers upregulate epithelial and repress mesenchymal genes in CCL_4-treated mice

Mice were treated as described in Figure 5.3.9 (A) OPN mRNA. (B) Snail mRNA. (C) E-Cadherin mRNA. (D) Id2 mRNA. Results were expressed as fold change relative to control-treated mice and graphed as mean ± SEM. Livers were stained for Sox9 (Brown) and E-Cadherin (Green) (E-F). (E) (Top left) Sox9/E-Cadherin double-staining in control mice; (Top right) Loss of E-Cadherin staining in CCL_4 mice with sham aptamers; (Bottom left) Re-expression of E-Cadherin in Sox9+ cells in OPN aptamer-treated mice; (Bottom right) Re-expression of membranous-E-Cadherin in OPN-aptamer-treated mice. (F) Sox9/E-Cadherin quantification by cell counting; number of double positive cells/HPF. Results are expressed as fold change relative to control mice and graphed as mean ± SEM. *p<0.05 vs. control mice. Black arrows indicate Sox9 positive cells which co-express (or should co-express) E-Cadherin. White arrows indicate membranous-expression of E-Cadherin.

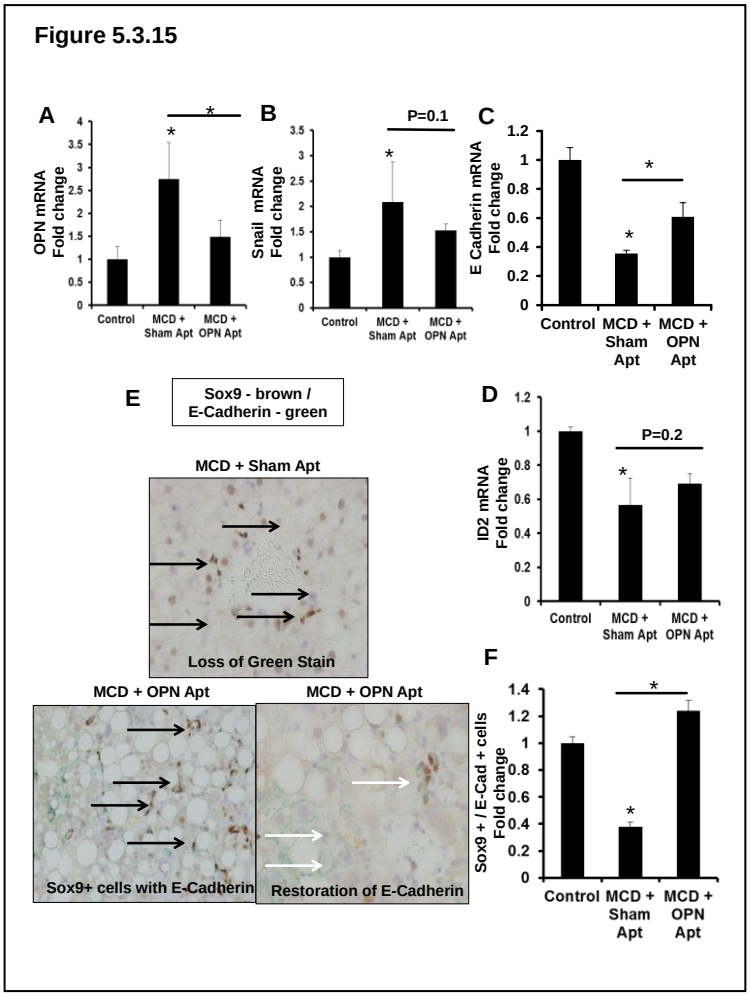

Figure 5.3.15: OPN aptamers upregulate epithelial and repress mesenchymal genes in MCD diet-fed mice

Mice were treated as described in Figure 5.3.9. (A) OPN mRNA. (B) Snail mRNA. (C) E-Cadherin mRNA. (D) Id2 mRNA. Results were expressed as fold change relative to control-treated mice and graphed as mean ± SEM. *p<0.05 vs. control mice. Livers were stained for Sox9 (Brown) and E-Cadherin (Green) (E-F). (E) (Top) Sox9 / E-Cadherin double staining (loss of E-Cadherin staining) in sham aptamer-treated mice; (Bottom left) Re-expression of E-Cadherin in Sox9+ cells in OPN aptamer treated mice; (Bottom right) Re-expression of membranous-E-Cadherin in OPN aptamer-treated mice. (F) Sox9 / E-Cadherin quantification by cell counting; number of double positive cells per HPF. Results are expressed as fold change relative to control mice and graphed as mean ± SEM. *p<0.05 vs. control mice. Black arrows indicate Sox9 positive cells which co-express (or should co-express) E-Cadherin. White arrows indicate membranous expression of E-Cadherin

DDC model:

Biliary-type fibrosis was induced by the DDC-supplemented diet (81). Increased SR staining and liver hydroxyproline content (**Fig 5.3.16A**) was similarly associated with a greater than 10-fold enrichment in the number of αSMA+ cells (**Fig 5.3.16B**) and an upregulation in αSMA, Collagen 1αI, and TGF-β1 mRNA **(Fig 5.3.16C – E)**. There was an accumulation of OPN+ and Sox9+ cells (over 10-fold) (**Fig 5.3.17A, B),** and OPN/Sox9 double-positive cells (up to 6-fold) (**Fig 5.3.17C**). These changes were accompanied by upregulation in OPN (~14-fold) **(Fig 5.3.17D),** and Sox9 mRNA (~40% increase) **(Fig 5.3.17E).**

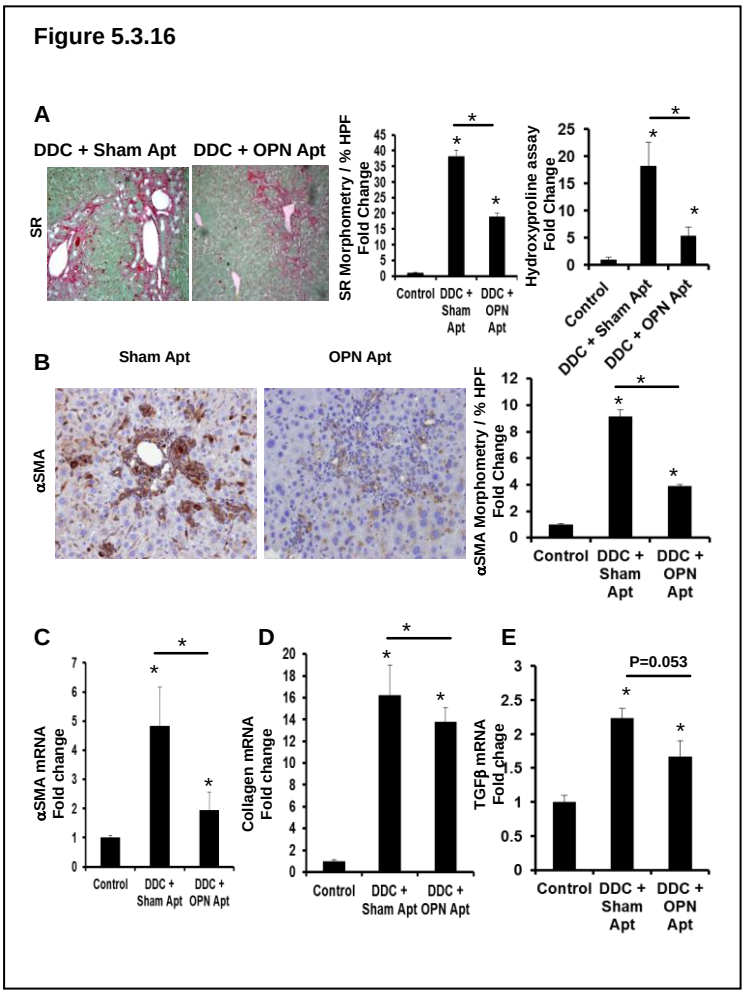

Fig. 5.3.16: OPN aptamers attenuate fibrogenesis in DDC-fed mice
Mice were fed control chow or the DDC-diet for 3 weeks to induce biliary-type fibrosis (n= 10; 5/group). Another group of mice which received DDC-diet were injected with sham aptamers or OPNaptamers by tail-vein injections (4 injections / mouse) in the final week of DDC treatment. Mice were sacrificed 24 h after final dose of aptamers, and livers harvested for IHC, QRTPCR, and the hydroxyproline assay. (A) Representative SR staining with corresponding quantification by morphometric analysis and the hepatic hydroxyproline assay (B) Representative αSMA staining and morphometry (20x fields for analysis). (C) αSMA mRNA (D) Collagen 1αI mRNA. (E) TGF-β mRNA. Results were expressed as fold change relative to control-treated mice and graphed as mean ± SEM. *p<0.05 vs. control mice, or as indicated.

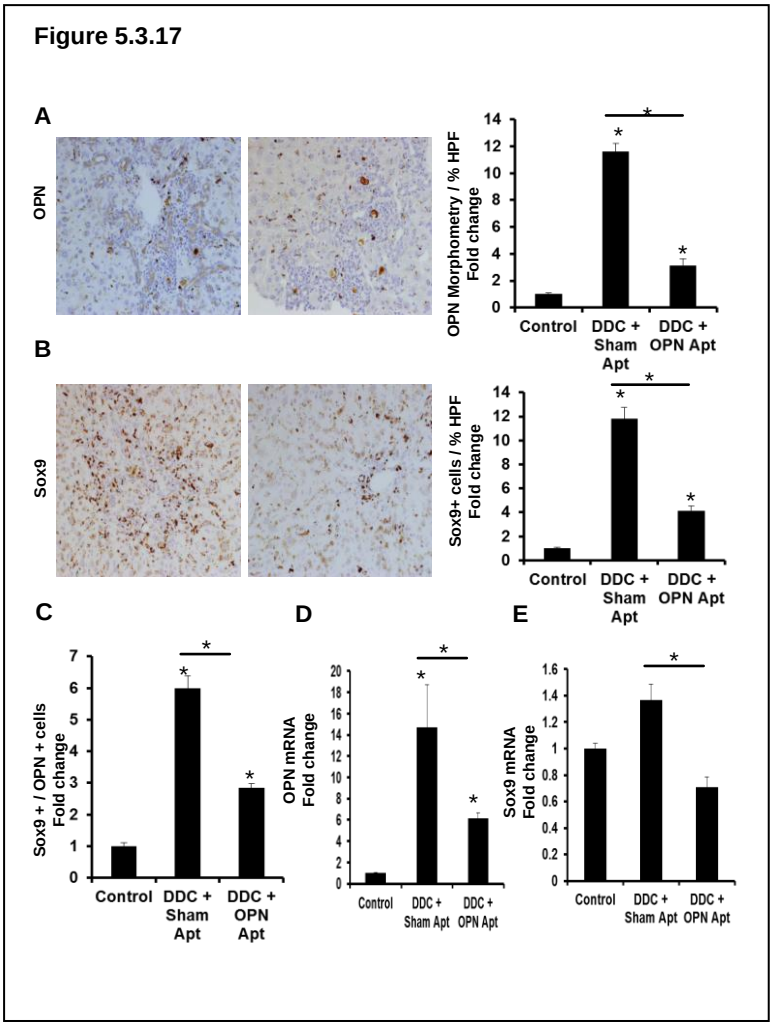

Fig. 5.3.17: OPN aptamers inhibits the LPC response in DDC-fed mice
Mice were fed control chow or the DDC-diet, as described in 5.3.16. Livers were harvested for IHC and QRTPCR. Representative staining are shown. (A) OPN staining and OPN quantification by morphometric analysis. (B) Sox9 staining and Sox9 quantification by cell counting; % of positive cells per HPF. (C) Morphometric analysis of Sox9-OPN double-staining. (D) Sox9 mRNA. (E) OPN mRNA. Results are expressed as fold change relative to control mice and graphed as mean ± SEM. *p<0.05 vs. control mice, or as indicated.

OPN neutralization attenuates the LPC response and ameliorates fibrogenesis (interventional)

CCl_4 and MCD models

Fibrosis:

Aptamers were administered during the final week of liver injury. No mice died. OPN neutralization ameliorated liver fibrosis in both CCl_4-treated, and MCD-fed mice. OPN aptamers significantly repressed hepatic hydroxyproline content and the amount of SR-stained fibrils **(Fig 5.3.9A, B)** by 4-5 fold, reduced αSMA+ cells by 50-80% **(Fig 5.3.9C, D),** and downregulated αSMA (80-90%), Collagen 1αI (50-100%), and TGF-β1 (50-90%) mRNA **(Fig 5.3.10).**

Liver progenitors:

Inhibited fibrogenesis was accompanied by fewer liver progenitors **(Fig 5.3.11, Fig 5.3.12, Fig 5.3.13).** OPN+ cells and Sox9+ cells were ~4-fold and ~2-3-fold fewer, respectively, after OPN-neutralization **(Fig 5.3.11A, B; Fig 5.3.12A, B).** There was parallel repression of Sox9 and K19 mRNA levels **(Fig 5.3.13).**

Liver progenitor re-programming:

OPN-neutralization also downregulated mesenchymal markers, OPN and Snail **(Fig 5.3.14A, B; Fig 5.3.15A, B)** while upregulating epithelial markers, E-cadherin and Id2 **(Fig 5.3.14C, D; Fig 5.3.15C, D).** Immunostaining further revealed the restored-expression of membranous-E-Cadherin, and greater number of Sox9/E-Cadherin double-positive cells in OPN aptamer-treated mice, to near normal levels **(Fig 5.3.14E, F; Fig 5.3.15E, F).** This was mirrored by a reduction in Sox9/OPN double positive cells to basal levels **(Fig 5.3.11C; Fig 5.3.12C),** thus confirming reversal of the fibrogenic phenotype.

DDC model:

Comparable outcomes were noted in DDC-fed mice: OPN aptamer treatment led to ~4 fold less hepatic hydroxyproline, ~2-fold less SR stained fibrils **(Fig 5.3.16A),** ~3-fold fewer αSMA+ cells (**Fig 5.3.16B**), and repression of αSMA (3-fold), Collagen 1αI (~25%), and TGF-β (~30%) mRNA (**Fig 5.3.16C – E**). This was accompanied by an attenuated LPC response: fewer OPN+ (~4-fold) (**Fig 5.3.17A)**, Sox9+ (~3-fold) (**Fig 5.3.17B**), and Sox9/OPN double positive cells (~2-fold) (**Fig 5.3.17C**). There was a comparable downregulation in OPN (3-fold), and Sox9 (2.5-fold) mRNA **(Fig 5.3.17D, E).** By contrast, Sox9/E-Cadherin double positive cells increased nearly 2-fold (**Fig 5.3.18**) during OPN-neutralization.

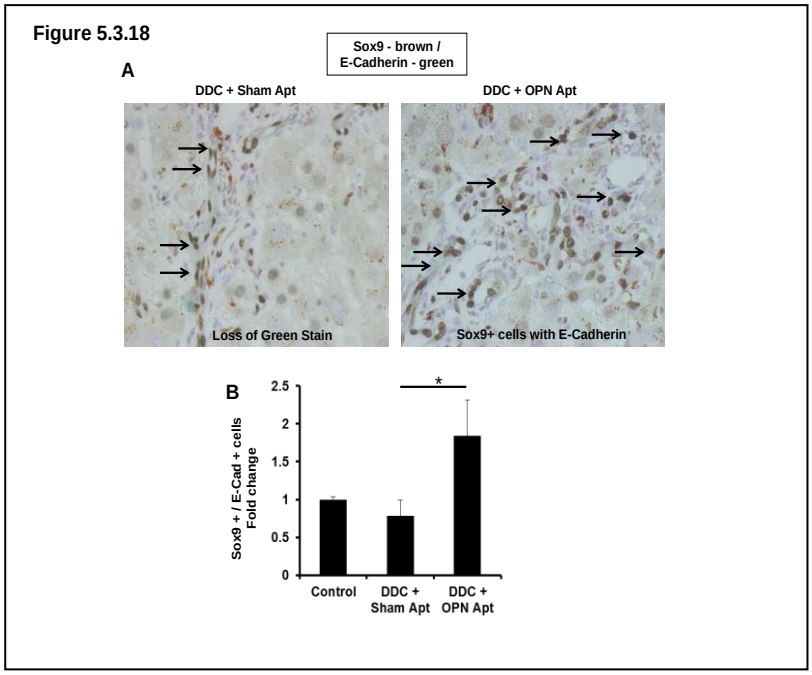

Fig. 5.3.18: OPN aptamers upregulate E-Cadherin in DDC-fed mice
Mice were treated as described in 5.3.16. Livers were stained for Sox9 (Brown) and E-Cadherin (Green). (A) Loss of E-Cadherin staining in DDC-fed mice with sham aptamers, and upregulation of E-Cadherin in Sox9+ cells in OPN aptamer-treated mice. (B) Sox9/E-Cadherin quantification by cell counting; number of double positive cells/HPF. Results are expressed as fold change relative to control mice and graphed as mean ± SEM. *p<0.05 vs. control mice. Black arrows indicate Sox9 positive cells which co-express (or should co-express) E-Cadherin.

The outcomes of OPN aptamer-studies were verified using OPN neutralizing antibodies. MCD-fed mice that received OPN antibodies accumulated 4-5 fold less SR-stained fibrils **(Fig 5.3.19A),** 60% fewer αSMA+ cells **(Fig 5.3.19B),** and downregulated αSMA, Collagen 1αI, TGF-β1 mRNA by up to 60% **(Fig 5.3.19C – E).** This was associated with fewer OPN+ and Sox9+ cells (~80%) **(Fig 5.3.20A, B),** and reduced OPN and Sox9 mRNA (~50%) **(Fig 5.3.20C, D).**

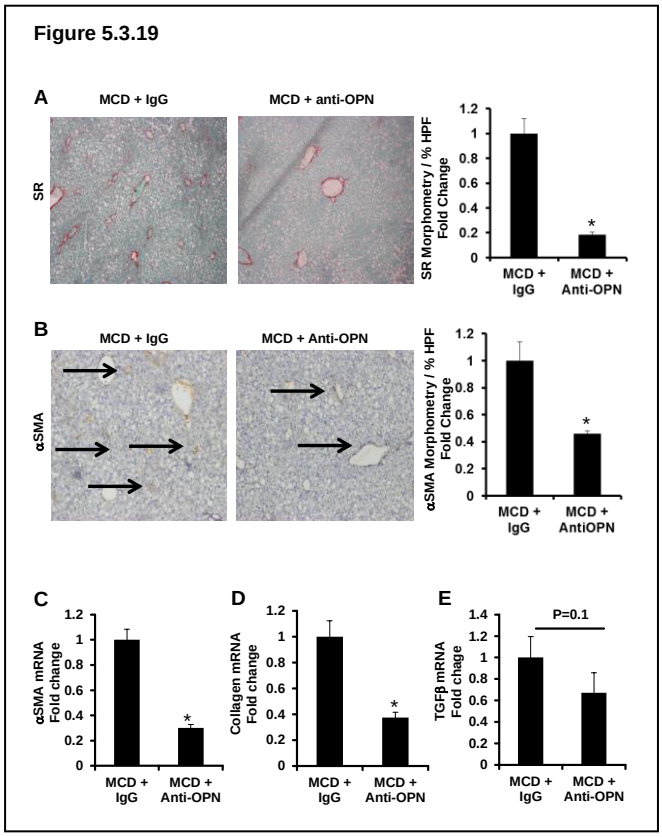

Fig. 5.3.19: OPN neutralizing antibodies inhibit fibrogenesis in MCD diet-fed mice
To verify results of aptamer studies, a further study was performed using OPN neutralizing antibodies. MCD diet-fed mice (n= 10; 5/group) were injected either control (IgG) or anti OPN in the final week, as described in Methods (i.e. 4 injections via tail-vein injections per mouse; 50ug per injection). Mice were sacrificed 24 h after the final injection, and livers harvested for IHC and QRTPCR. (A) Representative Sirius Red staining and quantification by morphometric analysis. (B) Representative αSMA staining and αSMA morphometry (20x fields chosen for analysis by the Metaview software). Black arrows denote cells expressing respective antigens. (C) αSMA mRNA. (B) Collagen 1αI mRNA. (C) TGF-β mRNA. Results were expressed as fold change relative to IgG-treated mice and graphed as mean ± SEM. *p<0.05 vs. IgG-treated mice

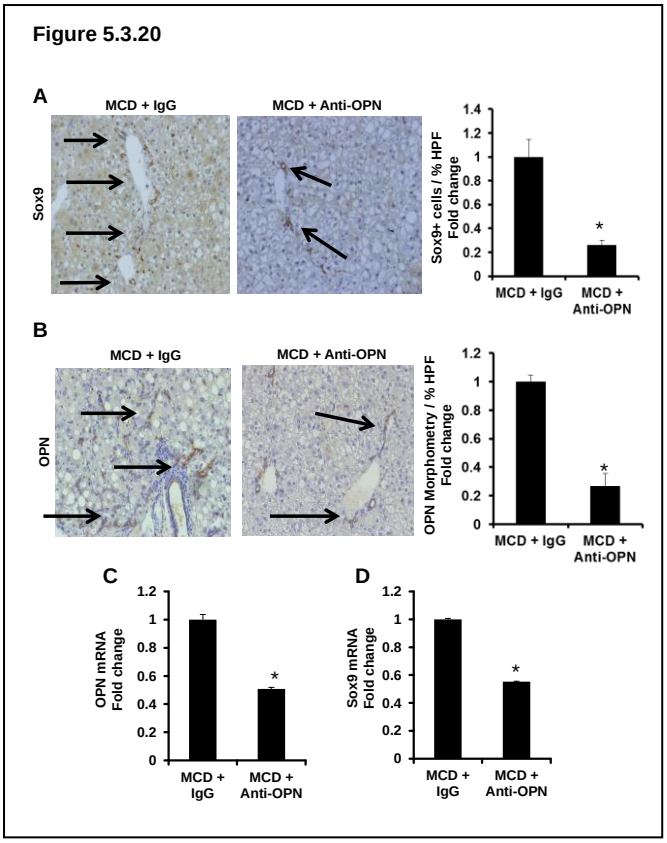

Fig. 5.3.20: OPN neutralizing antibodies attenuate the LPC response in MCD diet-fed mice
MCD diet-fed mice were injected either control (IgG) or anti-OPN as described in 5.3.19. Livers were harvested for IHC and QRTPCR. (A) Sox9 staining and Sox9 quantification by cell counting; % of positive cells per HPF. (B) Representative OPN staining and morphometric analysis (20x fields chosen for analysis by the Metaview software). (C) OPN mRNA. (D) Sox9 mRNA. Results were expressed as fold change relative to IgG-treated mice and graphed as mean ± SEM. *p<0.05 vs. IgG-treated mice. Black arrows denote cells expressing respective antigens.

In summary, targeting OPN using two neutralizing approaches, and in three liver disease models, led to an attenuated liver progenitor-cell response, and an amelioration of murine liver fibrosis.

5.4. Role of OPN in Liver Inflammation

NKT associated OPN drive fibrogenesis in NAFLD (Syn WK et al. Gut. 2012 Sep; 61(9):1323-9)

The liver contains a large number of NKT cells, which provide intravascular immune surveillance (134, 135). NKT cells respond to glycolipid antigens presented by MHC class 1-like molecule, CD1d, and when activated, secrete both Th1 (pro-inflammatory / anti-fibrotic) and Th2 (anti-inflammatory / pro-fibrotic) cytokines (135 – 138). In the hepatitis B virus-transgenic mouse (139), NKT-derived IL4 and IL13 were reported to be responsible for the fibrogenic outcomes. Conversely, CD1d knockout (CD1d-/-) mice, which lack NKT cells, were protected from xenobiotic-induced hepatic inflammation, injury and fibrosis (140). These findings complement human studies showing NKT accumulation in primary biliary cirrhosis (141, 142) and chronic viral hepatitis C (143).

The role of NKT cells in NAFLD progression is only beginning to emerge. NKT cells are generally depleted in fatty livers (144 – 146), but appear to accumulate in livers with NASH-related fibrosis (146, 147). Recently, we reported that Hh mediated accumulation of NKT cells contributes to development and progression of NASH in mice and humans (16). Mice with an overly active Hh pathway express higher levels of the NKT cell chemokine, CXCL16, the adhesion molecule VCAM-1, and IL15, a factor that promotes NKT viability (148). These mice accumulate more hepatic NKT cells, and develop worse NASH fibrosis. Consistent with this, we found that individuals with NASH-cirrhosis harbored 4 fold more NKT cells than those with healthy livers.

In addition to secreting the classical cytokines, IL4 and IL13, NKT cells can also secrete OPN, a cytokine and matricellular protein that exacerbates Concavalin A induced hepatitis (24), and promotes NAFLD progression **(Results: 5.1).** Recently, we showed that NKT cells also secrete the fetal morphogen, Shh (17). Shh induces the transition of quiescent HSC into activated, collagen-producing MF (48), and amplifies the ‘repair-associated inflammatory response’ (15).

Intriguingly, inhibition of the Hh pathway *in vivo* leads to the amelioration of fibrosis in mice with cholestatic liver injury (149).

In this study, we evaluated the hypothesis that fibrosis progression in NASH is NKT cell-dependent. We fed mice that were genetically deficient in NKT cells (Jα18-/- and CD1d-/-) MCD diets to induce NASH, evaluated if NKT depletion protected against NASH fibrosis, and assessed if NKT cell-mediated fibrogenesis required OPN. Findings in mice and cultured HSC were then corroborated by evaluating similar endpoints in patients with NASH.

5.4.1. NKT-deficient mice develop less fibrosis than WT mice after MCD diets

Compared to WT mice that were fed normal chow (n= 10), MCD diet-treated mice (n= 10) developed significant steatohepatitis and fibrosis after 8 weeks **(Fig 5.4.1A)**. The latter was demonstrated by increased SR staining **(Fig 5.4.1B, C),** and hepatic hydroxyproline quantification **(Fig 5.4.1D)**. Collagen deposition was accompanied by the accumulation of α–SMA-immunoreactive cells **(Fig 5.4.2A, B)**, and induction of pro-fibrogenic genes, including α-sma, collagen 1α1, and TGFβ **(Fig 5.4.2C, D; Fig 5.4.3A).**

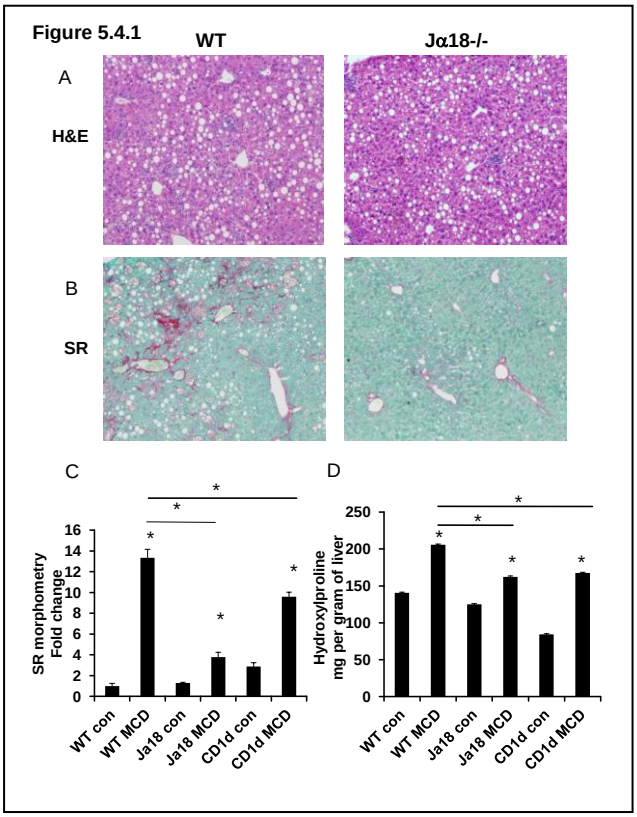

Fig. 5.4.1: NKT-deficient mice develop less fibrosis after the MCD diet
WT, Jα18-/- and CD1d-/- mice were fed control chow (n= 10/strain) or MCD diet (n= 10/strain) for 8 weeks, and then sacrificed. (A) Representative H&E and (B) SR staining after MCD diet. (C) SR quantification by morphometric analysis; results are expressed as fold change relative to WT control chow-fed mice, and graphed as mean ± SEM. (D) Hepatic hydroxyproline content at the end of the treatment period. *P<0.05 vs. control chow-fed mice.

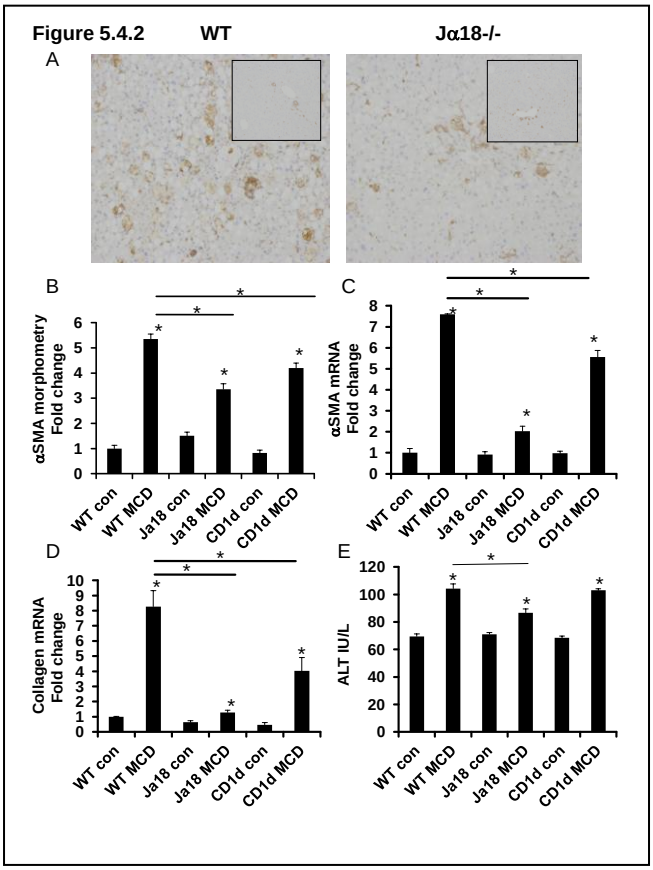

Fig. 5.4.2: NKT-deficient mice exhibit attenuated fibrogenic response compared with WT mice
Mice were fed control chow and MCD diets as described in 5.4.1. (A) αSMA immunoreactivity and (B) αSMA morphometry. Sections from 4 animals were used and 15 randomly selected, 20x fields chosen for analysis by the Metaview software. Small inserts in (A) show representative staining from chow-fed mice. Whole liver tissues were harvested for RNA analysis by QRTPCR. (C) αSMA mRNA, (D) Collagen Iα1 mRNA, and (E) ALT IU/L. Results are expressed as fold change relative to WT control chow-fed mice and graphed as mean ± SEM. *P<0.05 vs. control chow-fed mice

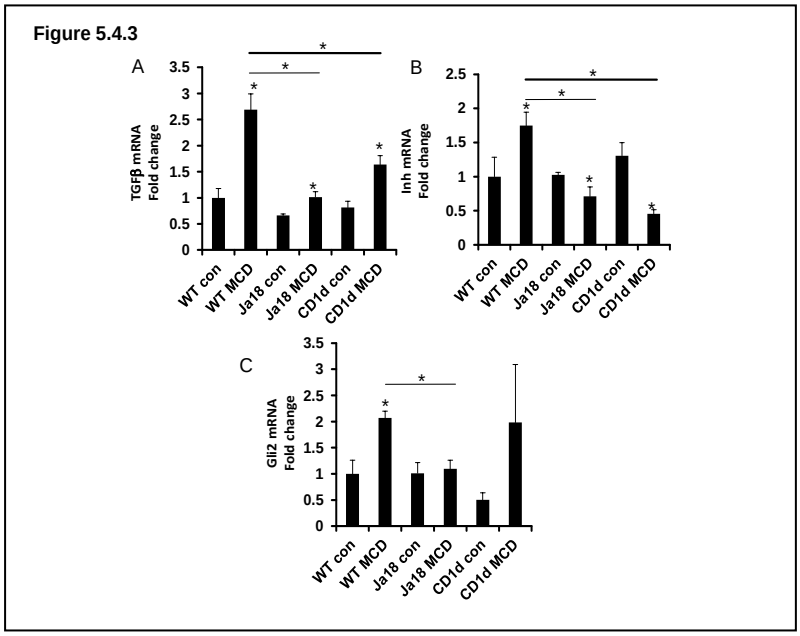

Fig. 5.4.3: NKT-deficient mice exhibit reduced TGF-β and attenuated Hh signaling after MCD diet induced NASH.
Mice were fed control chow and MCD diets as described in 5.4.1. Whole liver tissue was harvested for RNA analysis by QRTPCR. (A) TGFβ, (B) Indian Hedgehog (Inh), (C) Gli2 mRNA. Results are expressed as fold change relative to WT control chow-fed mice and graphed as mean ± SEM. *P<0.05 vs. WT control chow-fed mice

Jα18-/- mice which lack invariant NKT cells, developed significantly less hepatic fibrosis **(Fig 5.4.1B – D; Fig 5.4.2A – D)** and injury **(Fig 5.4.2E)** than WT mice after MCD diet. This finding in mice that lack invariant NKT cells is consistent with our previous report that CD1d-/- mice (which lack all NKT subsets) exhibited reduced fibrogenic responses after diet induced NASH (16) **(Fig 5.4.1C, D; Fig 5.4.2B – D; Fig 5.4.3A).**

We reported that Hh pathway activation induces the transition of quiescent HSC to collagen-producing MF (48), and promotes fibrogenic repair in NASH (14). Consistent with this, Indian Hh (a Hh ligand), and Gli2 (a Hh-regulated transcription factor) were significantly induced during diet-induced NASH (**Fig 5.4.3B, C)**. Conversely, NKT-deficient mice, which developed less fibrosis, exhibited attenuated Hh signaling **(Fig 5.4.3B, C).**

5.4.2. NKT-deficient mice express less OPN during MCD diet-induced NASH than WT mice

In **Result Section 5.1**, we showed that OPN acts in paracrine and autocrine fashions to promote HSC activation and fibrogenesis. After MCD diet, OPN-/- mice exhibited reduced fibrosis, while mice that overexpressed OPN developed worse fibrosis. Here, we show that livers from MCD fed WT mice upregulate OPN protein expression by nearly 5 fold **(Fig 5.4.4A, C).** In contrast, livers of both NKT cell deficient strains that developed less fibrosis than WT mice after diet-induced NASH had significantly reduced levels of OPN **(Fig 5.4.4A, C; Fig 5.4.5).** These findings raise the possibility that NKT cell associated factors modulate OPN expression and resultant liver fibrosis.

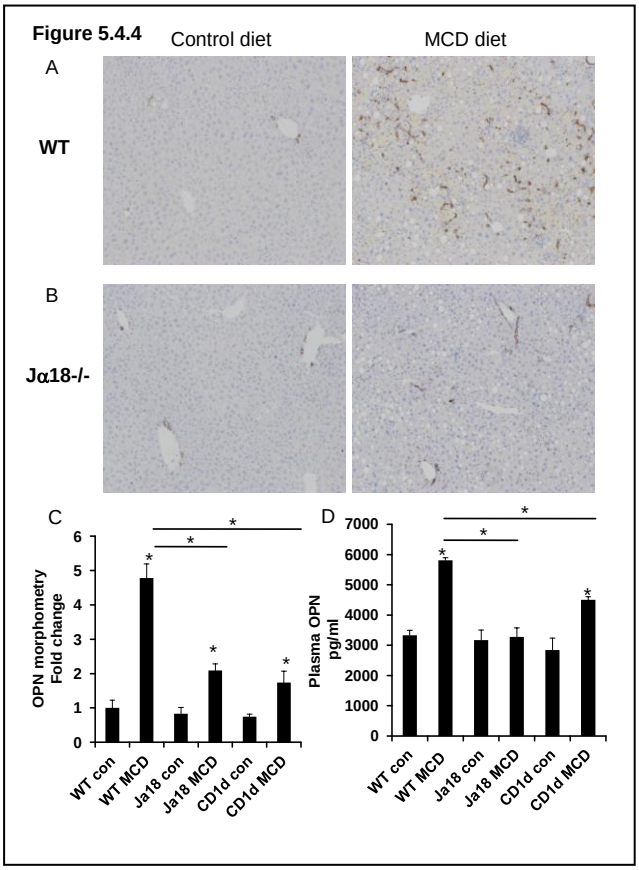

Fig. 5.4.4: NKT-deficient mice harbor less liver and plasma OPN than WT mice after MCD diet-induced NASH

Mice were fed as described in 5.4.1. Matched plasma was collected for OPN ELISA. (A-C) Representative OPN immunostaining after control chow or MCD diets in WT and Jα18-/- mice (final magnification 200X), and quantification by morphometry. Sections from 10 animals were used per group and 10 randomly selected, 200X fields chosen for analysis by the Metaview software. Results are expressed as fold change (% positive staining) relative to WT control mice, and graphed as mean ± SEM. (D) Plasma OPN. Plasma from 10 animals per group were used for OPN ELISA, and displayed as pg/ml. Each sample was run in duplicate. *P<0.05 vs. WT control mice

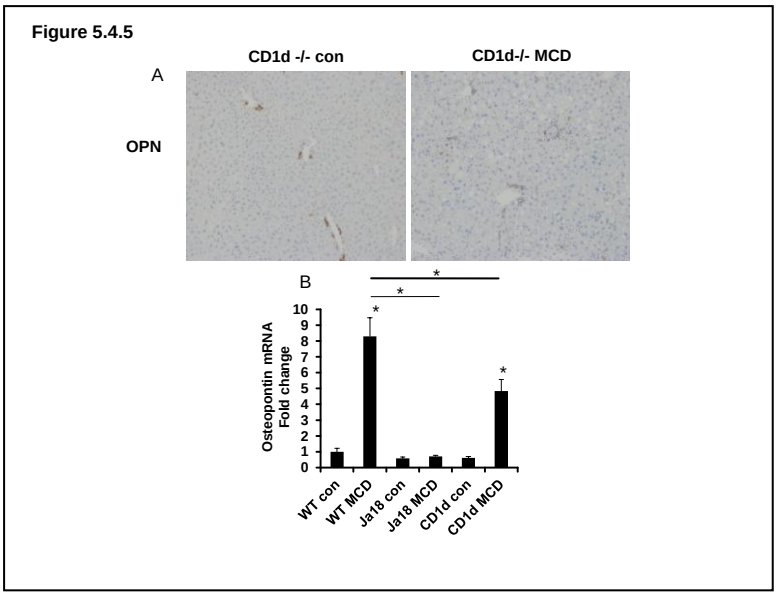

Fig. 5.4.5: Livers from NKT-deficient mice contain less OPN than WT mice after MCD diet.
Mice were fed as described in 5.4.1. (A) Representative OPN immunostaining after control chow or MCD diets in CD1d-/- mice (final magnification 200X). Whole liver RNA was analyzed by QRTPCR. (B) OPN mRNA. Results are expressed as fold change relative to WT control chow-fed mice and graphed as mean ± SEM. *P<0.05 vs. WT control chow-fed mice

Previously, others reported that plasma OPN levels correlated with severity of liver fibrosis in subjects with chronic hepatitis B and C (150, 151). In this study, plasma from WT mice with NASH fibrosis contained nearly 2 fold more OPN by ELISA than chow fed controls **(Fig 5.4.4D).** Consistent with reduced hepatic OPN expression, plasma OPN levels were 2 fold lower in NKT cell deficient mice after diet-induced NASH. The aggregate data, therefore, suggest that elevated plasma OPN levels may be a biomarker of advanced NASH fibrosis.

5.4.3. Primary mouse liver NKT cell associated OPN promotes MF activation of primary HSC

In addition to HSC and cholangiocytes (**Results: 5.1 and 5.3**), OPN is expressed by activated immune cells (24)**.** Therefore, we examined if activated liver NKT cells generate OPN that acts in a paracrine fashion to promote HSC fibrogenesis. Primary LMNC were isolated from healthy mice and incubated with αGC (which specifically activates iNKT cells) or vehicle overnight; LMNC-CM was then collected for OPN ELISA. αGC-activated LMNC-CM contained 4 fold more OPN protein than vehicle treated LMNC-CM, and similar levels of OPN as CM from cholangiocytes, which are known to be a source of OPN in liver **(Fig 5.4.6A).** To ascertain if activated LMNC *in vivo* also express higher amounts of OPN, we harvested primary LMNC from chow or MCD fed WT mice (n=4/group), and OPN expression was analyzed by QRTPCR. Primary LMNC from MCD fed mice harbored 12 fold more OPN mRNA than LMNC from chow fed mice **(Fig 5.4.6B).** αGC-activated

LMNC-CM was then added to primary cultures of mouse HSC with either OPN aptamers or sham aptamers for 48 h. The addition of OPN aptamers to neutralize OPN activity in LMNC-CM resulted in a significant repression of HSC fibrogenic genes (OPN, Collagen) **(Fig 5.4.6C, D)**.

To ascertain if differences in the fibrogenic outcomes observed in **Fig 5.4.1** could be attributed to fewer NKT cells, and hence, reduced NKT derived OPN, we isolated primary LMNC from WT, Jα18-/- and CD1d-/- mice, and incubated them with αGC or vehicle overnight, and LMNC-CM was collected for OPN ELISA, or added to primary cultures of HSC. We found that WT-LMNC mice secreted 5 fold more OPN protein **(Fig 5.4.6E)** and induced greater collagen expression in HSC than NKT deficient-LMNC **(Figure 5.4.6F).** These findings, in concert, support the hypothesis that activated NKT cell associated OPN promotes HSC activation in a paracrine fashion.

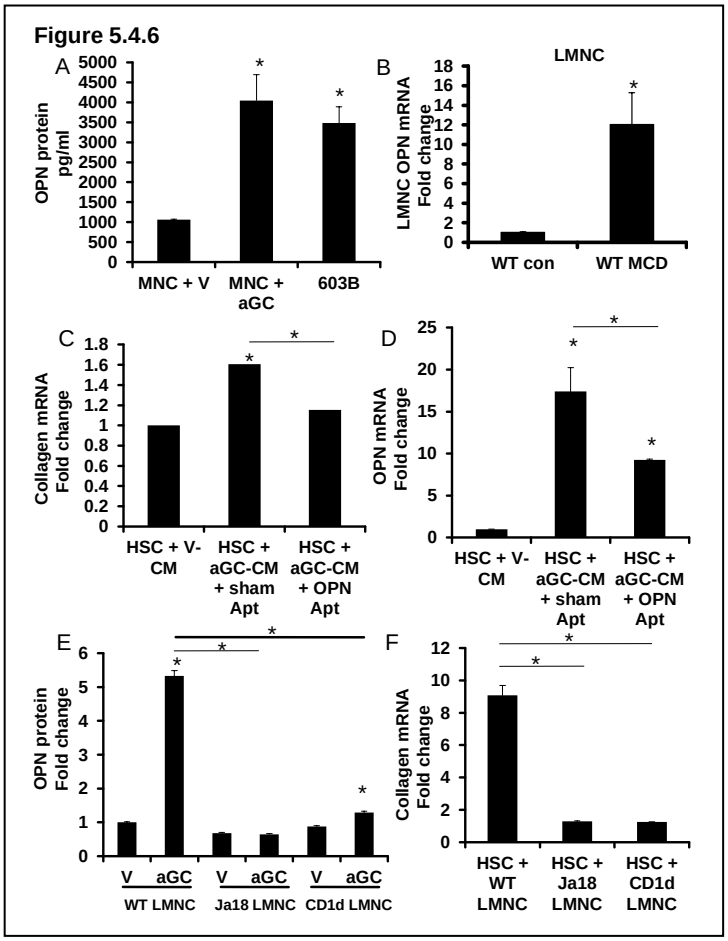

Fig. 5.4.6: αGC-activated liver NKT cell associated OPN promotes HSC activation

Primary LMNC (1 x 10^5) from WT mice were cultured in complete NKT media, and treated with vehicle (V) or αGC (to activate NKT cells) for 24 h. CM was collected for OPN ELISA; 603B mouse cholangiocyte-CM was used as a positive control. (A) OPN protein was quantified by ELISA. Each LMNC-CM sample was run in duplicate and expressed as pg/ml. (B) LMNC were isolated from WT mice that were fed control chow (n= 4) or MCD diet (n= 4) for 8 weeks, and OPN mRNA expression was analyzed by QRTPCR. Results are expressed as fold change relative to control chow derived LMNC. (C-D) Mouse primary HSC were cultured with CM from αGC-activated WT LMNC(αGC-CM) + OPN aptamers or sham aptamers for 48 h; HSC expression of collagen I α1(C) and OPN (D) mRNA were assessed by QRTPCR. Results are expressed as fold change relative to HSC that were treated with CM from vehicle-treated WT LMNC (V-CM). (E) OPN was quantified by ELISA in CM from LMNC that were harvested from WT, Jα18-/- or CD1d-/-mice and treated with either vehicle (V) or αGC to activate NKT cells. Results are expressed as fold change relative to vehicle (V)-treated WT LMNC. Mouse primary HSC were cultured for 48 h in LMNC-CM harvested from WT, Jα18-/-, and CD1d-/- mice and treated with vehicle or αGC to activate NKT cells. HSC expression of collagen I α1 mRNA was assessed by QRT PCR (F). Results are expressed as fold change relative to HSC that were cultured with CM from respective vehicle-activated LMNC. Mean ± SEM of duplicate experiments are graphed. *P<0.05

5.4.4. NASH progression in humans in accompanied by increased liver and plasma OPN

Herein, we demonstrate that fibrogenesis in mice with diet-induced NASH depends upon hepatic NKT cells, and show the mechanism involves NKT cell-mediated production of OPN**.** As NKT cells comprise a much greater proportion of the resident hepatic immune cells in mice than humans (152, 153), we next examined livers from patients with NASH to assess the relationship between hepatic NKT cell accumulation, OPN expression, and fibrosis in humans.

Human livers with advanced NASH (stage 3-4 fibrosis) contained 3 fold more OPN, particularly in the fibrous septa, than those with early NASH (no fibrosis or stage 1-2 fibrosis) **(Fig 5.4.7A, B)**. Previously, we reported that the hepatic content of cells that co-express CD57 and CD3 or CD56 and CD3 (i.e., NKT cells) is increased significantly in patients with NASH-related cirrhosis (16). Here we show that NKT cells that accumulate during NASH fibrosis express OPN protein **(Fig. 5.4.8A – C).** Moreover, we found that increased hepatic OPN expression was mirrored by higher plasma OPN levels in NASH patients with advanced fibrosis than those with mild fibrosis **(Fig 5.4.7C).** Overall plasma OPN levels in NASH were approximately 2 fold higher than levels detected in healthy volunteers (mean OPN level, normal: 3000pg/ml) (150). The findings in

humans with NASH, therefore, are similar to those in mice with NASH and together suggest that OPN may be a useful biomarker of advanced NASH fibrosis.

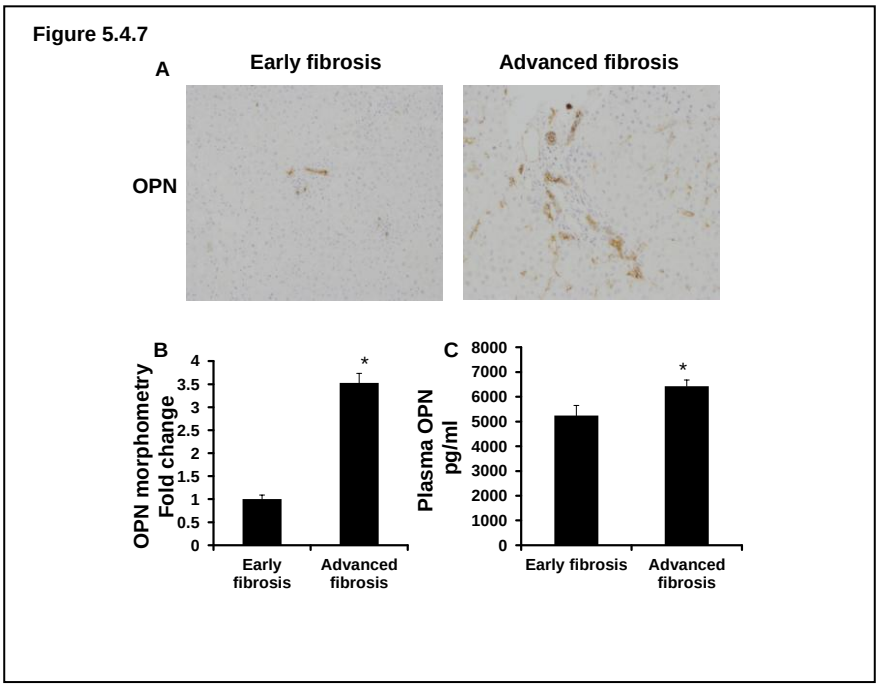

Fig. 5.4.7: NASH progression in humans is accompanied by upregulation of liver and plasma OPN (A-B) Coded liver sections from 10 patients with early and advanced NASH fibrosis were stained for OPN, and OPN expression was quantified by computer-assisted morphometry. (A) Representative photomicrographs from patients with early and advanced NASH fibrosis. (B) Quantitative analysis of liver OPN positive cells in all patients. Numbers of OPN positive cells are expressed as percentage of stained cells per high-powered field. (C) Plasma was collected from individuals with early or advanced NASH (n=25/group) and plasma OPN measured by ELISA. Plasma samples were run in duplicate. Mean ± SEM are graphed; * $p<0.001$ vs early fibrosis.

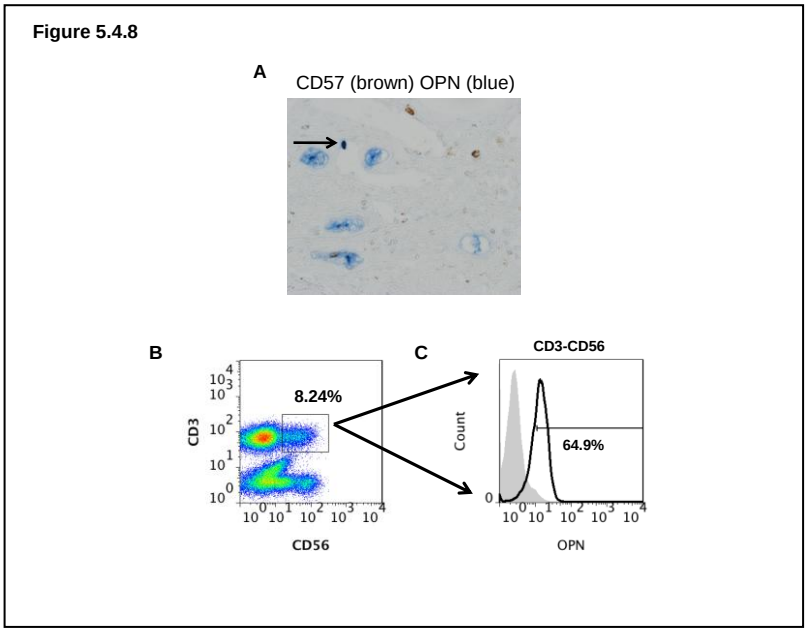

Fig. 5.4.8: NASH progression in humans is associated with the accumulation of OPN expressing NKT cells

Coded liver sections from patients with NASH fibrosis were double stained for CD57 / OPN. LMNC from a non-diseased liver were stained for CD3, CD56, OPN, and analyzed by FACS analysis. (A) CD57 (brown) – OPN (blue) double staining. (B) CD3-CD56 double positive NKT cells, (C) Proportion of CD3-CD56 NKT cells which expressed intracellular OPN

Chapter 6: Discussion

Chapter 6

Osteopontin is induced by Hedgehog Pathway Activation and Promotes Fibrosis Progression in Nonalcoholic Steatohepatitis

*(Syn WK et al. **Hepatology. 2011 Jan; 53(1):106-15**.)*

Previously, we demonstrated that dying hepatocytes produce Hh ligands (11, 12), which engage various types of Hh-responsive cells, including HSC, ductular cells / LPCs, and NKT cells, to trigger fibrogenic responses (13, 14, 17). We observed that Hh pathway activity correlated with MF accumulation and fibrosis stage in NAFLD patients and rodent models of NAFLD, and suggested that inter-individual differences in Hh signaling influenced intensity of fibrogenic responses during NASH (14). The present studies provide further support for this concept because they identify OPN as a proximal effector of Hh mediated fibrogenesis, and demonstrate that livers of OPN-/- mice are significantly protected from NASH fibrosis.

A recent analysis of the OPN gene revealed binding sites for Gli transcription factors, suggesting that OPN transcription is likely to be regulated by Hh signaling (18). By demonstrating co-localization of Gli and OPN in liver cells, and proving that expression of OPN mRNA is increased by a Smoothened agonist, but decreased by a Smoothened antagonist, our results support and advance this concept. In addition, our data demonstrate that changes in OPN gene expression are paralleled by changes in OPN protein content and biological activity because OPN aptamers reverse the pro-fibrogenic actions of OPN. The latter studies also verify that OPN is a significant downstream target of Hh signaling (rather than vice versa) because neutralizing OPN had no effect on cellular expression of the Hh target, Gli2, but significantly diminished fibrogenic gene expression, even in Ptc+/- cells with supra-normal Hh pathway activity. Coupled with the evidence that OPN-/- mice are significantly protected from NASH fibrosis, the data explain why we noted that hepatic content of Gli2(+) cells and OPN (+) cells increased in parallel as liver fibrosis advanced in patients with NAFLD.

OPN may also dictate the fibrogenic response in other chronic liver diseases, as it is significantly overexpressed in livers from cirrhotic ALD, AIH, PBC and PSC, and a recent study reported that

plasma OPN levels correlate with hepatic inflammation and fibrosis in chronic hepatitis C (151). Although more work is needed to delineate the interactions between OPN and other putative pro-fibrogenic factors (81), this concept suggests that OPN levels may provide a useful biomarker for liver fibrosis in NASH, and that OPN neutralization might be useful for preventing progressive hepatic fibrosis in NASH patients.

Osteopontin is a proximal effector of leptin-mediated non-alcoholic steatohepatitis (NASH) fibrosis
(Coombes JD ….Syn WK. Biochim Biophys Acta. 2016 Jan; 1862(1):135-44)

OPN is an important downstream effector of leptin-induced fibrogenesis. The loss of OPN using OPN aptamers or OPN knockdown abrogates HSC activation despite the presence of exogenous leptin, and these *in vitro* observations were recapitulated in the *ex vivo* liver slice model. These results are consistent with findings from studies on Hh signaling in liver fibrosis. Both OPN and Hh are leptin regulated, and are key effectors of leptin-induced liver fibrosis. An over-activation of the Hh pathway leads to tissue fibrosis and cancer, while the loss of Hh signaling impairs wound healing (i.e. less fibrosis) (154, 155). In the liver, we and others recently reported that over-activation of the Hh pathway occurs during human NASH progression (14), and that blocking Hh with the commercially available inhibitor, GDC0449 or cyclopamine ameliorates NASH and reduces liver fibrosis in mice (156).

The prevalence of NAFLD and NASH is increasing in parallel with the rising tide of obesity and type 2 diabetes mellitus. Studies show that obese individuals and those who harbour additional metabolic risk factors are at a much higher risk of developing NASH and /or NASH fibrosis (157). Therefore, targeting ‘modifiable’ mediators in these ‘at-risk’ individuals could help alleviate NASH / fibrosis burden. Leptin is an adipose tissue-derived hormone whose physiological role is to induce satiety, but levels of leptin are significantly higher in the obese, and in some with NAFLD (110, 111). To date, studies have evaluated the potential utility of leptin replacement in those with hypoleptinemia-NASH. In one study, leptin administration improved steatosis, but not fibrosis stage (158), and as leptin is directly pro-fibrogenic, it is possible that supplementation of

exogenous leptin may inadvertently lead to worsening fibrosis. On the other hand, leptin neutralization in those with advanced NASH-fibrosis (and excess leptin) may be a useful anti-fibrotic strategy (as observed in ob/ob mice), although the likely increase in food intake and body weight (and metabolic risk) may well cancel out any potential clinical benefit.

Like leptin, plasma OPN levels are increased in the obese and in patients with type 2 diabetes mellitus, hypertension, and ischemic heart disease (159). More recently, serum OPN was also found to be associated with the onset of diabetic nephropathy and cardiac events (160). Thus, high levels of OPN occur in those with the metabolic syndrome, a risk factor for progressive NASH. Importantly, OPN neutralization reduces infiltration of macrophages and immune subsets into adipose tissues, reduces obesity-induced inflammation, and improves systemic glucose tolerance (25, 161 – 163). In concert with the current findings, these data suggest that OPN could be an important target in the treatment of obese patients with NASH (and the metabolic syndrome), by reducing insulin resistance and limiting NASH-fibrosis (in spite of high prevailing leptin levels).

In summary, our analyses show that OPN is leptin-regulated, and is a key effector of leptin-induced, NASH fibrosis. Future studies will be necessary to evaluate the utility of OPN neutralization in various models of obesogenic NASH (such as the high-fat, high fructose / sucrose-fed model), and evaluate if extended periods of treatment could lead to even better anti-fibrotic outcomes.

Osteopontin Neutralization Abrogates the Liver Progenitor Cell Response and Fibrogenesis in Mice
(Coombes JD …. Syn WK. Gut. 2015 Jul; 64(7):1120-31)

This is the first study to show that OPN neutralization is effective in treating murine liver fibrosis. Treatment with OPN aptamers or OPN neutralizing antibodies attenuated the LPC response, and repressed fibrogenesis to levels comparable with control chow-fed mice, suggesting that one week

of ‘anti OPN’ treatment is safe, and effective in reversing fibrogenic outcomes. Mechanistically, we show that OPN is an important viability factor for LPCs, and directly regulates LPC phenotype by up-regulating mesenchymal genes while repressing epithelial ones. Importantly, OPN neutralization significantly inhibited LPC migration in wound healing and transmigration assays, key features of EMT (130).

EMT describes the process by which epithelial progenitors acquire a more mesenchymal phenotype that facilitates their migration into the stroma (164). This process is critical for development and is characteristic of invasive cancers. Fate-mapping studies in three distinct mouse-strains and in two models of chronic liver injury provide compelling evidence that EMT occurs during liver regeneration and repair (40, 41, 165). Comparable features of EMT are detected in human diseased livers (13, 14). In this study, OPN neutralization led to fewer Sox9+ LPC, and significantly less hepatic K19 and Sox9 mRNA (i.e. attenuated liver progenitor response) than sham treated mice. Importantly, Sox9+ LPC lost E-Cadherin expression with fibrosis progression, but regained epithelial type expression during OPN neutralization. Sox9+ LPC also lost expression of the mesenchymal marker, OPN, during fibrosis regression. The collective in vitro and in vivo data support the hypothesis that OPN regulates LPC-wound healing responses.

The liver progenitor niche comprises the LPC (oval cell), bone marrow-derived progenitors, and HSC (166). Previously, we showed that co-cultures of LPC with HSC led to enhanced progenitor cell proliferation and EMT (13) while LPC-derived Hh ligands and OPN activate HSC into myofibroblast (**Result: 5.1**). Here, we showed that OPN neutralization resulted in a ‘less fibrogenic’ LPC-secretome in vitro and a ‘less-fibrogenic’ progenitor cell microenvironment in vivo, highlighting the importance of OPN within the progenitor niche. This finding is particularly relevant given our recent study identifying HSC as a resident multi-potent progenitor (40, 41), and provides an explanation for their shared phenotype (i.e. LPC and HSC express similar progenitor markers, and undergo EMT) (14, 48). Thus, LPC and HSC interact to replenish the progenitor pool (41), and identify OPN as a key modulator of the LPC-associated response during injury.

OPN binds to multiple receptors (19). As such, it is likely that OPN neutralization has other effects, apart from modulating LPC and HSC responses. Preliminary studies show that OPN can promote immune cell entry into the liver and perpetuate hepatic injury, while others have reported that OPN can directly regulate immune cell functions (167). OPN and its family members are also known to bind to MMPs (168). Collectively, these observations explain in part, how OPN neutralization could lead to such impressive reversibility in fibrosis. Further studies however, will be needed to evaluate how OPN modulates MMP activities and whether OPN regulates specific immune subset recruitment and function (fibrosis-promoting vs. fibrosis-regressing) in vivo (169).

TGF-β is a pro-fibrogenic cytokine, and promotes progenitor-cell EMT (129). Given that OPN also regulates the liver progenitor-response and EMT, it is not surprising that TGF-β and OPN may interact. Previously, we showed that TGF-β mRNA expression is Hh regulated (14). In this study, we confirmed that OPN neutralization in mice led to reduced TGF-β1 mRNA. Intriguingly, OPN neutralization also decreased levels of phospho-Smad-2/3-complexes in LPC. This was mirrored by increased Ski and SnoN, two potent transcriptional co-repressors of the TGF-β pathway (131). Under basal conditions, Ski and SnoN inhibit gene transcription; TGF-β stimulation leads to Ski and SnoN degradation, thereby, allowing phospho-Smad-2/3 to bind to target genes. The results imply that OPN may be a novel regulator of SnoN and Ski levels during fibrogenic liver repair, and OPN neutralization decreases levels of phospho-Smad-2/3 which, in turn, triggers proteosomal-degradation of Ski and SnoN (170). This is consistent with observations that Ski and SnoN over-expression are associated with amelioration of renal fibrosis, and resistance to renal-tubular EMT (171). Our preliminary studies further suggest that OPN mediated effects may occur via OPN-CD44 and OPN-αvβ3 interactions (putative OPN-receptors). The aggregate findings show that OPN effects are mediated in part, by modulating TGF-β signaling, complementing and extending earlier evidence which positioned both OPN and TGF-β downstream of Hh during liver fibrogenesis (14; **Results: 5.1**).

To date, studies have utilized OPN knockout (genetically deficient) mice (14, 81, 95). Despite their usefulness in providing proof-of-concept, translating findings from these animals to humans are limited, as genetic modifications may result in contradictory outcomes when subjected to chronic injury. These disparities could be explained by the presence of distinct OPN isoforms (intracellular and extracellular/soluble) which exhibit overlapping, but also differing functions (19). Soluble OPN behaves as a cytokine while intracellular OPN is an important viability and cytoskeletal protein that regulates intracellular protein functions. In support, our cell culture data show that the reduction of intracellular OPN expression (in 603B-shOPN) leads to similar but non-identical outcomes. In vivo, OPN knockout mice developed more fibrosis after chronic CCL_4 (95), but less fibrosis in dietary-induced NASH (14). Similar divergent outcomes have been reported in OPN knockout mice with lung or rheumatological disease (172, 173). OPN aptamers or OPN neutralizing antibodies used in this study is potentially safer because it negates the excess circulating OPN without directly abolishing the expression of intracellular OPN necessary for key cellular function (133). Furthermore, in clinical practice, individuals are more likely to need treatment for advanced-fibrosis, as opposed to prophylactic anti-fibrotics; therefore, the administration of OPN neutralizing therapies once fibrosis has developed is more likely to be clinically relevant (1).

Although no mice died in this study, future studies need to specifically evaluate the potential risks of OPN neutralization. OPN overexpression however, occurs during tissue inflammation and fibrosis (skin, lung, kidneys, bone marrow), and in individuals with metabolic risk factors such as obesity, endothelial dysfunction, and diabetes (19, 174). Thus, neutralizing and lowering excess extracellular OPN under such circumstances could be beneficial. This concept and therapeutic safety is supported by a recent phase 1/2 study of OPN-neutralization in patients with advanced rheumatoid arthritis (126).

In summary, our analyses in cell culture, mice and humans show that OPN upregulation during liver injury is a conserved repair response, and influences LPC function by modulating TGF-β signaling. OPN neutralization using two neutralizing modalities, and in three different models of

mice abrogated the LPC response and liver fibrosis. Future studies will be necessary to evaluate the importance of alternative mechanisms by which OPN modulates fibrogenesis, and to evaluate if extended periods of treatment could lead to even better anti-fibrotic outcomes. As humanized antibodies to OPN and OPN aptamers are currently being developed, future studies will also be needed in humans to evaluate the safety and efficacy of anti OPN treatment.

NKT associated OPN drive fibrogenesis in NAFLD
(Syn WK et al. Gut. 2012 Sep; 61(9):1323-9)

This study shows that hepatic NKT cells are critical drivers of fibrogenesis in NASH, and demonstrates that the mechanism involves NKT cell mediated increase in the liver content of OPN. Importantly, plasma levels of OPN reflect the activity of this process in liver and thus, may prove to be a useful non-invasive marker of advanced NASH.

Previously, we reported that Hh pathway activity correlates with severity of NAFLD liver injury (14), and showed that Hh signaling enhances hepatic accumulation of immune cells, including CD1d-restricted NKT cells (16). Here, we prove that fibrogenesis in mice with diet-induced NASH directly depends upon NKT cells. Compared with WT mice, two strains of NKT cell deficient mice (Jα18-/- and CD1d-/-) exhibited dramatically attenuated fibrosis after 8 weeks of MCD diets. NKT cell deficient mice also demonstrated blunted Hh pathway activity (less expression of Hh ligand and the Hh-regulated transcription factor, Gli2), and reduced expression of OPN, a Hh-regulated cytokine which acts in both paracrine and autocrine manners to promote HSC activation and fibrogenesis **(Results 5.1).**

In the present study, LMNC from WT mice with diet-induced NASH expressed 12 fold higher levels of OPN mRNA than chow diet-fed controls. CM from WT mice-derived LMNC that were treated with αGC to activate resident NKT cells stimulated cultured HSC to express collagen mRNA, whereas similarly treated LMNC from two different strains of NKT cell deficient mice did not. These results indicate that activated liver NKT cells promote the production of factors that drive fibrogenic

responses in HSC, and suggest that one of these pro-fibrogenic factors might be OPN. Indeed, ELISA demonstrated that CM from αGC-activated WT LMNC contained four times more OPN than CM from similarly-treated LMNC populations from NKT cell deficient mice. Moreover, neutralizing OPN activity with OPN aptamers significantly abrogated the HSC fibrogenic responses to WT LMNC-derived factors, reducing HSC expression of collagen mRNA to basal levels. The aggregate findings, therefore, complement and extend earlier evidence that liver NKT cells are capable of producing OPN by showing that important fibrogenic actions of NKT cells are directly mediated by OPN (17, 24).

Our studies in human subjects support the pathophysiological relevance of excessive OPN production during NASH fibrogenesis. Notably, we provide evidence that the upregulation of liver OPN production in advanced NASH is mirrored by increased plasma OPN levels. Recent reports suggest that high plasma OPN levels may also be predictive of cirrhosis in patients with chronic hepatitis B and C (150, 151). In addition, elevated plasma OPN levels are associated with cancer development, recurrence, and bad prognosis (175, 176). Given these observations, it is conceivable that plasma OPN levels might be used to identify NASH patients who are at high risk of bad outcomes. Further studies, in a larger cohort of individuals with NAFLD, will be necessary to confirm the clinical utility of this novel biomarker.

Chapter 7: Conclusions

Chapter 7

1. OPN is upregulated by Hh pathway activation in chronic liver injury and promotes liver fibrosis

OPN gene and protein expressions are upregulated in animal models of CLD and in liver tissues obtained from patients with advanced liver disease (cirrhosis). Importantly, excess OPN has a direct pathogenic role as it can directly promote HSC activation. OPN neutralization conversely, prevents this.

By manipulating Hh pathway activity with pharmacologic agents in cell cultures, we confirmed that Hh signaling regulates OPN gene and protein expression. These findings were supported by observations in primary HSC from mice with an overly active Hh pathway. OPN neutralization attenuated the fibrogenic responses despite persistent Hh pathway activation, therefore confirming that OPN is a downstream effector of the Hh pathway.

2. OPN is proximal effector of leptin mediated liver fibrosis

Both OPN and leptin promote liver fibrosis and are regulated by the Hh pathway. In HSC and total liver, leptin induces OPN expression. Through genetic and pharmacologic approaches, we further show that leptin fibrogenic effects are OPN dependent and that regulation of OPN expression occurs via leptin induced PI3K/Akt signaling.

3. OPN enhances the LPC response in CLD

OPN increases LPC proliferation, promotes EMT, and enhances the wound healing response in different models of study (two mouse LPC lines and in three mouse models of liver fibrosis). Conversely, OPN neutralization abrogates the LPC response in vitro and in vivo, and reduces liver

fibrosis. Specifically, OPN effects are achieved by modulating levels of Ski and SnoN, two corepressors of the TGF-β signaling pathway.

4. NKT cell derived OPN promotes NASH fibrosis

NKT cells are the key immune cells which drive liver fibrosis, as confirmed in different models (αGC-activated primary MNC / NKT cells and two genetic mouse models of NKT deficiency). NKT cells secrete OPN which promotes HSC activation. Mice deficient in NKT numbers exhibit a global reduction in liver OPN and develop less fibrosis.

Final Conclusion:

This body of research shows that OPN is upregulated during CLD and promotes fibrogenesis by activating HSC and LPCs. OPN is secreted by multiple cell types including HSCs, LPCs, and recruited NKT cells, which amplify the fibrogenic responses. In vivo, OPN neutralization abrogates the LPC response and reduces liver fibrosis, thus demonstrating that targeting OPN is a potentially attractive anti-fibrotic strategy.

Chapter 8: Bibliography

Chapter 8

1. Friedman SL, Sheppard D, Duffield JS, Violette S. Therapy for fibrotic diseases: nearing the starting line. Sci Transl Med 2013; 5: 167sr161
2. Bataller R, Brenner DA. Liver fibrosis. J. Clin. Invest 2005; 115**,** 209 –218
3. Trautwein C, Friedman SL, Schuppan D, Pinzani M. Hepatic fibrosis: Concept to treatment. J. Hepatol 2015; 62: S15-24
4. Adams LA, Lindor KD. Nonalcoholic fatty liver disease. Ann Epidemiol 2007; 17: 863–869
5. Kanwal F , Kramer JR, Duan Z, Yu X, White D, El-Serag HB. Trends in the Burden of Nonalcoholic Fatty Liver Disease in a United States Cohort of Veterans. Clin. Gastroenterol. Hepatol 2016; 14: 301-308
6. Diehl AM, Chute J. Underlying potential: cellular and molecular determinants of adult liver repair. J Clin Invest 2013;123(5): 1858-60
7. Syn WK, Diehl AM. Fibrosis progression: putative mechanisms and molecular pathways. In: Williams R and Taylor-Robinson SD, eds. Clinical dilemmas in Non-alcoholic fatty liver disease, 1st ed. John Wiley & Sons, Ltd, 2016; 61 -71
8. Holt AP, Salmon M, Buckley CD, Adams DH. Immune interactions in hepatic fibrosis. Clin Liver Dis. 2008; 12(4): 861-82
9. Hirose Y, Itoh T, Miyajima A. Hedgehog signal activation coordinates proliferation and differentiation of fetal liver progenitor cells. Exp Cell Res 2009; 315(15): 2648–57.
10. Briscoe J, Thérond PP. The mechanisms of Hedgehog signalling and its roles in development and disease. Nat Rev Mol Cell Biol 2013; 14(7): 416–29.

11. Jung Y, Witek RP, Syn WK, Choi SS, Omenetti A, Premont R, Guy CD, Diehl AM. Signals from dying hepatocytes trigger growth of liver progenitors. Gut 2010; 59(5): 655–65.

12. Rangwala F, Guy CD, Lu J, Suzuki A, Burchette JL, Abdelmalek MF, Chen W, Diehl AM. Increased production of sonic hedgehog by ballooned hepatocytes. J Pathol 2011; 224(3): 401–10.

13. Omenetti A, Porrello A, Jung Y, Yang L, Popov Y, Choi SS, Witek RP, Alpini G, Venter J, Vandongen HM, Syn WK, Baroni GS, Benedetti A, Schuppan D, Diehl AM. Hedgehog signaling regulates epithelial mesenchymal transition during biliary fibrosis in rodents and humans. J Clin Invest 2008; 118(10): 3331–42.

14. Syn WK, Jung Y, Omenetti A, Abdelmalek M, Guy CD, Yang L, Wang J, Witek RP, Fearing CM, Pereira TA, Teaberry V, Choi SS, Conde-Vancells J, Karaca GF, Diehl AM. Hedgehog-mediated epithelial-to-mesenchymal transition and fibrogenic repair in nonalcoholic fatty liver disease. Gastroenterology 2009; 137(4): 1478–1488 e8.

15. Omenetti, A., Syn WK, Jung Y, Francis H, Porrello A, Witek RP, Choi SS, Yang L, Mayo MJ, Gershwin ME, Alpini G, Diehl AM. Repair-related activation of hedgehog signaling promotes cholangiocyte chemokine production. Hepatology 2009; 50(2): 518–27.

16. Syn WK, Oo YH, Pereira TA, Karaca GF, Jung Y, Omenetti A, Witek RP, Choi SS, Guy CD, Fearing CM, Teaberry V, Pereira FE, Adams DH, Diehl AM. Accumulation of natural killer T cells in progressive nonalcoholic fatty liver disease. Hepatology 2010; 51(6): 1998–2007.

17. Syn WK, Witek RP, Curbishley SM, Jung Y, Choi SS, Enrich B, Omenetti A, Agboola KM, Fearing CM, Tilg H, Adams DH, Diehl AM. Role for hedgehog pathway in regulating growth and function of invariant NKT cells. Eur J Immunol 2009; 39(7): 1879–92.

18. Das S, Harris LG, Metge BJ, Liu S, Riker AI, Samant RS, Shevde LA. The hedgehog pathway transcription factor GLI1 promotes malignant behavior of cancer cells by up-regulating osteopontin. J Biol Chem 2009; 284(34): 22888-97

19. Uede T. Osteopontin, intrinsic tissue regulator of intractable inflammatory diseases. Pathol Int 2011; 61(5): 265-80.

20. Liaw L, Birk DE, Ballas CB, Whitsitt JS, Davidson JM, Hogan BL. Altered wound healing in mice lacking a functional osteopontin gene (spp1). J Clin Invest 1998; 101(7): 1468–78.

21. Rangaswami H, Bulbule A, Kundu GC. Osteopontin: role in cell signaling and cancer progression. Trends Cell Biol 2006; 16(2): 79–87.

22. Banerjee A, Burghardt RC, Johnson GA, White FJ, Ramaiah SK. The temporal expression of osteopontin (SPP-1) in the rodent model of alcoholic steatohepatitis: a potential biomarker. Toxicol Pathol 2006; 34(4): 373-84.

23. Banerjee A, Apte UM, Smith R, Ramaiah SK. Higher neutrophil infiltration mediated by osteopontin is a likely contributing factor to the increased susceptibility of females to alcoholic liver disease. J Pathol 2006; 208(4): 473-85.

24. Diao H, Kon S, Iwabuchi K, Kimura C, Morimoto J, Ito D, Segawa T, Maeda M, Hamuro J, Nakayama T, Taniguchi M, Yagita H, Van Kaer L, Onóe K,

Denhardt D, Rittling S, Uede T. Osteopontin as a mediator of NKT cell function in T cell-mediated liver diseases. Immunity 2004; 21(4): 539-50.

25. Kiefer FW, Zeyda M, Gollinger K, Pfau B, Neuhofer A, Weichhart T, Säemann MD, Geyeregger R, Schlederer M, Kenner L, Stulnig TM. Neutralization of osteopontin inhibits obesity-induced inflammation and insulin resistance. Diabetes 2010; 59(4): 935–46.

26. Kiefer FW, Zeyda M, Todoric J, Huber J, Geyeregger R, Weichhart T, Aszmann O, Ludvik B, Silberhumer GR, Prager G, Stulnig TM. Osteopontin expression in human and murine obesity: extensive local up-regulation in adipose tissue but minimal systemic alterations. Endocrinology 2008;149(3):1350-7

27. Giachelli CM, Bae N, Almeida M, Denhardt DT, Alpers CE, Schwartz SM. Osteopontin is elevated during neointima formation in rat arteries and is a novel component of human atherosclerotic plaques. J Clin Invest 1993; 92(4): 1686-96

28. Uchinaka A, Hamada Y, Mori S, Miyagawa S, Saito A, Sawa Y, Matsuura N, Yamamoto H, Kawaguchi N. SVVYGLR motif of the thrombin-cleaved N-terminal osteopontin fragment enhances the synthesis of collagen type III in myocardial fibrosis. Mol Cell Biochem 2015; 408(1-2): 191-203

29. Takemoto M, Yokote K, Yamazaki M, Ridall AL, Butler WT, Matsumoto T, Tamura K, Saito Y, Mori S. Enhanced expression of osteopontin by high glucose. Involvement of osteopontin in diabetic macroangiopathy. Ann N Y Acad Sci 2000; 902:357-63

30. Feldstein AE, Canbay A, Angulo P, Taniai M, Burgart LJ, Lindor KD, Gores GJ. Hepatocyte apoptosis and fas expression are prominent features of human nonalcoholic steatohepatitis. Gastroenterology 2003; 125(2): 437–43.

31. Wieckowska A, Zein NN, Yerian LM, Lopez AR, McCullough AJ, Feldstein AE. In vivo assessment of liver cell apoptosis as a novel biomarker of disease severity in nonalcoholic fatty liver disease. Hepatology 2006; 44(1): 27–33.

32. Yang S, Koteish A, Lin H, Huang J, Roskams T, Dawson V, Diehl AM. Oval cells compensate for damage and replicative senescence of mature hepatocytes in mice with fatty liver disease. Hepatology 2004; 39(2): 403–11.

33. Roskams, T. and V. Desmet, Ductular reaction and its diagnostic significance. Semin Diagn Pathol 1998; 15(4): 259–69

34. Richardson MM, Jonsson JR, Powell EE, Brunt EM, Neuschwander-Tetri BA, Bhathal PS, Dixon JB, Weltman MD, Tilg H, Moschen AR, Purdie DM, Demetris AJ, Clouston AD. Progressive fibrosis in nonalcoholic steatohepatitis: association with altered regeneration and a ductular reaction. Gastroenterology 2007;133(1): 80-90

35. Feldstein AE, Wieckowska A, Lopez AR, Liu YC, Zein NN, McCullough AJ. Cytokeratin-18 fragment levels as noninvasive biomarkers for nonalcoholic steatohepatitis: a multicenter validation study. Hepatology 2009; 50(4):1072-8.

36. Machado MV, Michelotti GA, Pereira TA, Boursier J, Kruger L, Swiderska-Syn M, Karaca G, Xie G, Guy CD, Bohinc B, Lindblom KR, Johnson E, Kornbluth S, Diehl AM. Reduced lipoapoptosis, hedgehog pathway activation and fibrosis in caspase-2 deficient mice with non-alcoholic steatohepatitis. Gut 2015; 4(7):1148-57

37. Witek RP, Stone WC, Karaca FG, Syn WK, Pereira TA, Agboola KM, Omenetti A, Jung Y, Teaberry V, Choi SS, Guy CD, Pollard J, Charlton P, Diehl AM. Pan-caspase inhibitor VX-166 reduces fibrosis in an animal model of nonalcoholic steatohepatitis. Hepatology 2009; 50(5): 1421-30

38. Santoni-Rugiu E, Jelnes P, Thorgeirsson SS, Bisgaard HC. Progenitor cells in liver regeneration: molecular responses controlling their activation and expansion. APMIS 2005; 113(11-12): 876-902.

39. Roskams T. Relationships among stellate cell activation, progenitor cells, and hepatic regeneration. Clin Liver Dis 2008; 12(4): 853-60

40. Michelotti GA, Xie G, Swiderska M, Choi SS, Karaca G, Krüger L, Premont R, Yang L, Syn WK, Metzger D, Diehl AM. Smoothened is a master regulator of adult liver repair. J Clin Invest 2013; 123(6): 2380-94.

41. Swiderska-Syn M, Syn WK, Xie G, Krüger L, Machado MV, Karaca G, Michelotti GA, Choi SS, Premont RT, Diehl AM. Myofibroblastic cells function as progenitors to regenerate murine livers after partial hepatectomy. Gut 2014; 63(8): 1333-44.

42. Kordes C, Sawitza I, Götze S, Häussinger D. Stellate cells from rat pancreas are stem cells and can contribute to liver regeneration. PLoS One 2012; 7(12): e51878

43. Kordes C, Sawitza I, Götze S, Herebian D, Häussinger D. Hepatic stellate cells contribute to progenitor cells and liver regeneration. J Clin Invest 2014; 124(12): 5503-15

44. Xie G, Choi SS, Syn WK, Michelotti GA, Swiderska M, Karaca G, Chan IS, Chen Y, Diehl AM. Hedgehog signalling regulates liver sinusoidal endothelial cell capillarisation. Gut 2013; 62(2): 299-309

45. Canbay A, Feldstein AE, Higuchi H, Werneburg N, Grambihler A, Bronk SF, Gores GJ. Kupffer cell engulfment of apoptotic bodies stimulates death ligand and cytokine expression. Hepatology 2003; 38(5):1188-98.

46. Wree A, Eguchi A, McGeough MD, Pena CA, Johnson CD, Canbay A, Hoffman HM, Feldstein AE. NLRP3 inflammasome activation results in hepatocyte pyroptosis, liver inflammation, and fibrosis in mice. Hepatology 2014; 59(3): 898-910.

47. Pusterla T, Nèmeth J, Stein I, Wiechert L, Knigin D, Marhenke S, Longerich T, Kumar V, Arnold B, Vogel A, Bierhaus A, Pikarsky E, Hess J, Angel P. Receptor for advanced glycation endproducts (RAGE) is a key regulator of oval cell activation and inflammation-associated liver carcinogenesis in mice. Hepatology 2013; 58(1): 363-73.

48. Choi SS, Omenetti A, Witek RP, Moylan CA, Syn WK, Jung Y, Yang L, Sudan DL, Sicklick JK, Michelotti GA, Rojkind M, Diehl AM. Hedgehog pathway activation and epithelial-to-mesenchymal transitions during myofibroblastic transformation of rat hepatic cells in culture and cirrhosis. Am J Physiol Gastrointest Liver Physiol 2009; 297(6): G1093-106.

49. Pereira Tde A, Witek RP, Syn WK, Choi SS, Bradrick S, Karaca GF, Agboola KM, Jung Y, Omenetti A, Moylan CA, Yang L, Fernandez-Zapico ME, Jhaveri R, Shah VH, Pereira FE, Diehl AM. Viral factors induce Hedgehog pathway activation in humans with viral hepatitis, cirrhosis, and hepatocellular carcinoma. Lab Invest 2010; 90(12): 1690-703

50. Dooley S, ten Dijke P. TGF-β in progression of liver disease. Cell Tissue Res. 2012; 347(1): 245-56

51. Iredale JP, Murphy G, Hembry RM, Friedman SL, Arthur MJ. Human hepatic lipocytes synthesize tissue inhibitor of metalloproteinases-1. Implications for regulation of matrix degradation in liver. J Clin Invest 1992; 90(1): 282-7.

52. Arthur MJ, Stanley A, Iredale JP, Rafferty JA, Hembry RM, Friedman SL. Secretion of 72 kDa type IV collagenase/gelatinase by cultured human lipocytes. Analysis of gene expression, protein synthesis and proteinase activity. Biochem J1992; 287 (Pt 3): 701-7.

53. Garcia-Bañuelos J, Siller-Lopez F, Miranda A, Aguilar LK, Aguilar-Cordova E, Armendariz-Borunda J. Cirrhotic rat livers with extensive fibrosis can be safely transduced with clinical-grade adenoviral vectors. Evidence of cirrhosis reversion. Gene Ther 2002; 9(2): 127-34.

54. Lalor PF, Adams DH. The liver: a model of organ-specific lymphocyte recruitment. Expert Rev Mol Med. 2002; 4(2):1-16

55. Shetty S, Lalor PF, Adams DH. Lymphocyte recruitment to the liver: molecular insights into the pathogenesis of liver injury and hepatitis. Toxicology 2008; 254(3):136-46.

56. Ramachandran P[1], Pellicoro A, Vernon MA, Boulter L, Aucott RL, Ali A, Hartland SN, Snowdon VK, Cappon A, Gordon-Walker TT, Williams MJ, Dunbar DR, Manning JR, van Rooijen N, Fallowfield JA, Forbes SJ, Iredale JP. Differential Ly-6C expression identifies the recruited macrophage phenotype, which orchestrates the regression of murine liver fibrosis. Proc Natl Acad Sci U S A 2012; 109(46): E3186-95.

57. Bäckhed F, Ding H, Wang T, Hooper LV, Koh GY, Nagy A, Semenkovich CF, Gordon JI.The gut microbiota as an environmental factor that regulates fat storage. Proc Natl Acad Sci U S A. 2004; 101(44): 15718-23.

58. De Minicis S, Rychlicki C, Agostinelli L, Saccomanno S, Candelaresi C, Trozzi L, Mingarelli E, Facinelli B, Magi G, Palmieri C, Marzioni M, Benedetti A, Svegliati-Baroni G. Dysbiosis contributes to fibrogenesis in the course of chronic liver injury in mice. Hepatology 2014; 59(5): 1738-49.

59. Klaus S. Adipose tissue as a regulator of energy balance. Curr Drug Targets. 2004; 5(3): 241-50

60. Choi SS, Syn WK, Karaca GF, Omenetti A, Moylan CA, Witek RP, Agboola KM, Jung Y, Michelotti GA, Diehl AM. Leptin promotes the myofibroblastic phenotype in hepatic stellate cells by activating the hedgehog pathway. J Biol Chem 2010; 285(47): 36551-60.

61. Kumar P, Smith T, Rahman K, Mells JE, Thorn NE, Saxena NK, Anania FA. Adiponectin modulates focal adhesion disassembly in activated hepatic stellate cells: implication for reversing hepatic fibrosis. FASEB J 2014; 28(12): 5172-83.

62. van Beuge MM, Prakash J, Lacombe M, Post E, Reker-Smit C, Beljaars L, Poelstra K. Enhanced effectivity of an ALK5-inhibitor after cell-specific delivery to hepatic stellate cells in mice with liver injury. PLoS One 2013; 8(2): e56442.

63. Henderson NC, Arnold TD, Katamura Y, Giacomini MM, Rodriguez JD, McCarty JH, Pellicoro A, Raschperger E, Betsholtz C, Ruminski PG, Griggs DW, Prinsen MJ, Maher JJ, Iredale JP, Lacy-Hulbert A, Adams RH, Sheppard D. Targeting of αv integrin identifies a core molecular pathway that regulates fibrosis in several organs. Nat Med 2013; 19(12): 1617-24.

64. Yang L, Wang Y, Mao H, Fleig S, Omenetti A, Brown KD, Sicklick JK, Li YX, Diehl AM. Sonic hedgehog is an autocrine viability factor for myofibroblastic hepatic stellate cells. J Hepatol 2008; 48(1): 98-106.

65. Yoo YA, Kang MH, Kim JS, Oh SC. Sonic hedgehog signaling promotes motility and invasiveness of gastric cancer cells through TGF-beta-mediated activation of the ALK5-Smad 3 pathway. Carcinogenesis. 2008; 29(3): 480-90.

66. Pereira TA, Xie G, Choi SS, Syn WK, Voieta I, Lu J, Chan IS, Swiderska M, Amaral KB, Antunes CM, Secor WE, Witek RP, Lambertucci JR, Pereira FL, Diehl AM. Macrophage-derived Hedgehog ligands promote fibrogenic and angiogenic responses in human schistosomiasis mansoni. Liver Int 2013; 33(1): 149-61.

67. Guy CD, Suzuki A, Zdanowicz M, Abdelmalek MF, Burchette J, Unalp A, Diehl AM; NASH CRN. Hedgehog pathway activation parallels histologic severity of injury and fibrosis in human nonalcoholic fatty liver disease. Hepatology 2012; 55(6): 1711-21.

68. Jung Y, Brown KD, Witek RP, Omenetti A, Yang L, Vandongen M, Milton RJ, Hines IN, Rippe RA, Spahr L, Rubbia-Brandt L, Diehl AM. Accumulation of hedgehog-responsive progenitors parallels alcoholic liver disease severity in mice and humans. Gastroenterology 2008; 134(5): 1532-43.

69. Omenetti A, Yang L, Li YX, McCall SJ, Jung Y, Sicklick JK, Huang J, Choi S, Suzuki A, Diehl AM. Hedgehog-mediated mesenchymal-epithelial interactions modulate hepatic response to bile duct ligation. Lab Invest 2007; 87(5): 499-514.

70. Denhardt DT, Giachelli CM, Rittling SR. Role of osteopontin in cellular signaling and toxicant injury. Annu Rev Pharmacol Toxicol. 2001;41: 723-49

71. Ramaiah SK, Rittling S. Pathophysiological role of osteopontin in hepatic inflammation, toxicity, and cancer. Toxicol Sci 2008;103(1): 4-13

72. Yokasaki Y, Sheppard D. Mapping of the cryptic integrin-binding site in osteopontin suggests a new mechanism by which thrombin can regulate inflammation and tissue repair. Trends Cardiovasc Med 2000; 10(4):155-9

73. Xie Y, Sakatsume M, Nishi S, Narita I, Arakawa M, Gejyo F. Expression, roles, receptors, and regulation of osteopontin in the kidney. Kidney Int. 2001; 60(5): 1645-57

74. Green PM, Ludbrook SB, Miller DD, Horgan CM, Barry ST. Structural elements of the osteopontin SVVYGLR motif important for the interaction with alpha(4) integrins. FEBS Lett 2001; 503: 75–9.

75. Smith LL, Cheung HK, Ling LE, Chen J, Sheppard D, Pytela R, Giachelli CM. Osteopontin N-terminal domain contains a cryptic adhesive sequence recognized by alpha9beta1 integrin. J Biol Chem 1996; 271: 28485–91

76. Weber GF, Ashkar S, Glimcher MJ, Cantor H. Receptor-ligand interaction between CD44 and osteopontin (Eta-1). Science 1996; 271: 509–12.

77. Katagiri YU, Sleeman J, Fujii H, Herrlich P, Hotta H, Tanaka K, Chikuma S, Yagita H, Okumura K, Murakami M, Saiki I, Chambers AF, Uede T. CD44 variants but not CD44s cooperate with beta1-containing integrins to permit cells to bind to osteopontin independently of arginine-glycine-aspartic acid, thereby stimulating cell motility and chemotaxis. Cancer Res 1999; 59(1): 219-26.

78. Morimoto J, Inobe M, Kimura C, Kon S, Diao H, Aoki M, Miyazaki T, Denhardt DT, Rittling S, Uede T. Osteopontin affects the persistence of beta-glucan-

induced hepatic granuloma formation and tissue injury through two distinct mechanisms. Int Immunol 2004; 16(3): 477-88.

79. Sahai A, Malladi P, Melin-Aldana H, Green RM, Whitington PF. Upregulation of osteopontin expression is involved in the development of nonalcoholic steatohepatitis in a dietary murine model. Am J Physiol Gastrointest Liver Physiol 2004; 287: G264-273.

80. Choi SS, Sicklick JK, Ma Q, Yang L, Huang J, Qi Y, Chen W, Li YX, Goldschmidt-Clermont PJ, Diehl AM. Sustained activation of Rac1 in hepatic stellate cells promotes liver injury and fibrosis in mice. Hepatology 2006; 44(5): 1267-77.

81. Fickert P, Stöger U, Fuchsbichler A, Moustafa T, Marschall HU, Weiglein AH, Tsybrovskyy O, Jaeschke H, Zatloukal K, Denk H, Trauner M. A new xenobiotic-induced mouse model of sclerosing cholangitis and biliary fibrosis. Am J Pathol 2007; 171(2):525-36.

82. Mi Z, Guo H, Russell MB, Liu Y, Sullenger BA, Kuo PC. RNA aptamer blockade of osteopontin inhibits growth and metastasis of MDA-MB231 breast cancer cells. Mol Ther 2009; 17(1): 153-61

83. Talbot LJ, Mi Z, Bhattacharya SD, Kim V, Guo H, Kuo PC. Pharmacokinetic characterization of an RNA aptamer against osteopontin and demonstration of in vivo efficacy in reversing growth of human breast cancer cells. Surgery 2011; 150(2): 224-30.

84. Borojevic R, Monteiro AN, Vinhas SA, Domont GB, Mourão PA, Emonard H, Grimaldi G Jr, Grimaud JA. Establishment of a continuous cell line from fibrotic schistosomal granulomas in mice livers. In Vitro Cell Dev Biol. 1985; 21(7): 382-90.

85. Heilmann K, Hoffmann U, Witte E, Loddenkemper C, Sina C, Schreiber S, Hayford C, Holzlöhner P, Wolk K, Tchatchou E, Moos V, Zeitz M, Sabat R, Günthert U, Wittig BM. Osteopontin as two-sided mediator of intestinal inflammation. J Cell Mol Med 2009; 13(6): 1162-74.

86. Yahagi K, Ishii M, Kobayashi K, et al. Primary culture of cholangiocytes from normal mouse liver. In Vitro Cell Dev Biol Anim 1998; 34: 512–514

87. Ishimura N, Bronk SF, Gores GJ. Inducible nitric oxide synthase up-regulates Notch-1 in mouse cholangiocytes: implications for carcinogenesis. Gastroenterology 2005; 128: 1354–1368.

88. Watarai H, Nakagawa R, Omori-Miyake M, Dashtsoodol N, Taniguchi M.Methods for detection, isolation and culture of mouse and human invariant NKT cells. Nat Protoc. 2008; 3(1): 70-8.

89. Croudace JE, Curbishley SM, Mura M, Willcox CR, Illarionov PA, Besra GS, Adams DH, Lammas DA. Identification of distinct human invariant natural killer T-cell response phenotypes to alpha-galactosylceramide. BMC Immunol 2008; 9: 71.

90. Feldstein AE, Papouchado BG, Angulo P, Sanderson S, Adams L, Gores GJ. Hepatic stellate cells and fibrosis progression in patients with nonalcoholic fatty liver disease. Clin Gastroenterol Hepatol 2005; 3: 384-389

91. Ashkar S, Weber GF, Panoutsakopoulou V, Sanchirico ME, Jansson M, Zawaideh S, Rittling SR, Denhardt DT, Glimcher MJ, Cantor H. Eta-1 (osteopontin): an early component of type-1(cell-mediated) immunity. Science 2000; 287: 860-864.

92. Chabas D, Baranzini SE, Mitchell D, Bernard CC, Rittling SR, Denhardt D, Sobel RA, Lock C, Karpuj M, Pedotti R, Heller R, Oksenberg JR, Steinman L.

The influence of the proinflammatory cytokine, osteopontin, on autoimmune demyelinating disease. Science 2001; 294: 1731-1735.

93. Miyazaki K, Okada Y, Yamanaka O, Kitano A, Ikeda K, Kon S, Uede T, Rittling SR, Denhardt DT, Kao WW, Saika S. Corneal wound healing in an osteopontin-deficient mouse. Invest Ophthalmol Vis Sci 2008; 49: 1367-1375.

94. Fujita N, Fujita S, Okada Y, Fujita K, Kitano A, Yamanaka O, Miyamoto T, Kon S, Uede T, Rittling SR, Denhardt DT, Saika S. Impaired angiogenic response in the corneas of mice lacking osteopontin. Invest Ophthalmol Vis Sci 2010; 51: 790-794.

95. Lorena D, Darby IA, Gadeau AP, Leen LL, Rittling S, Porto LC, Rosenbaum J, Desmoulière A. Osteopontin expression in normal and fibrotic liver. Altered liver healing in osteopontin-deficient mice. J Hepatol 2006; 44: 383-390.

96. Lee SH, Seo GS, Park YN, Yoo TM, Sohn DH. Effects and regulation of osteopontin in rat hepatic stellate cells. Biochem Pharmacol 2004; 68:2367-2378

97. Whitington PF, Malladi P, Melin-Aldana H, Azzam R, Mack CL, Sahai A. Expression of osteopontin correlates with portal biliary proliferation and fibrosis in biliary atresia. Pediatr Res 2005; 57: 837-844

98. Omenetti A, Diehl AM. The adventures of sonic hedgehog in development and repair. II. Sonic hedgehog and liver development, inflammation, and cancer. Am J Physiol Gastrointest Liver Physiol 2008; 294: G595-598.

99. Mori R, Shaw TJ, Martin P. Molecular mechanisms linking wound inflammation and fibrosis: knockdown of osteopontin leads to rapid repair and reduced scarring. J Exp Med 2008; 205: 43-51.

100. Berman JS, Serlin D, Li X, Whitley G, Hayes J, Rishikof DC, Ricupero DA, Liaw L, Goetschkes M, O'Regan AW. Altered bleomycin-induced lung fibrosis in osteopontin-deficient mice. Am J Physiol Lung Cell Mol Physiol 2004; 286: L1311-1318.

101. Larter CZ, Yeh MM. Animal models of NASH: getting both pathology and metabolic context right. J Gastroenterol Hepatol 2008; 23: 1635-1648.

102. Lee YA, Wallace MC, Friedman SL. Pathobiology of liver fibrosis: a translational success story. Gut 2015; 64(5): 830-41. Erratum in: Gut 2015;64(8): 1337.

103. Saxena NK, Anania FA. Adipocytokines and hepatic fibrosis. Trends Endocrinol Metab 2015; 26(3): 153-61.

104. Oben JA, Roskams T, Yang S, Lin H, Sinelli N, Torbenson M, Smedh U, Moran TH, Li Z, Huang J, Thomas SA, Diehl AM. Hepatic fibrogenesis requires sympathetic neurotransmitters. Gut 2004; 53(3): 438-45.

105. Saxena NK, Ikeda K, Rockey DC, Friedman SL, Anania FA. Leptin in hepatic fibrosis: evidence for increased collagen production in stellate cells and lean littermates of ob/ob mice. Hepatology 2002; 35(4): 762-71

106. Ikejima K, Takei Y, Honda H, Hirose M, Yoshikawa M, Zhang YJ, Lang T, Fukuda T, Yamashina S, Kitamura T, Sato N. Leptin receptor-mediated signaling regulates hepatic fibrogenesis and remodeling of extracellular matrix in the rat. Gastroenterology 2002; 122(5): 1399-410.

107. Aleffi S, Petrai I, Bertolani C, Parola M, Colombatto S, Novo E, Vizzutti F, Anania FA, Milani S, Rombouts K, Laffi G, Pinzani M, Marra F. Upregulation of proinflammatory and proangiogenic cytokines by leptin in human hepatic stellate cells. Hepatology 2005; 42(6): 1339-48.

108. Elinav E, Ali M, Bruck R Brazowski E, Phillips A, Shapira Y, Katz M, Solomon G, Halpern Z, Gertler A. Competitive inhibition of leptin signaling results in amelioration of liver fibrosis through modulation of stellate cell function. Hepatology 2009; 49(1): 278-86.

109. Honda H, Ikejima K, Hirose M Yoshikawa M, Lang T, Enomoto N, Kitamura T, Takei Y, Sato N. Leptin is required for fibrogenic responses induced by thioacetamide in the murine liver. Hepatology 2002; 36(1): 12-21.

110. Considine RV, Sinha MK, Heiman M, Kriauciunas A, Stephens TW, Nyce MR, Ohannesian JP, Marco CC, McKee LJ, Bauer TL, José F. Caro. Serum immunoreactive-leptin concentrations in normal-weight and obese humans. N Engl J Med 1996; 334(5):292-5.

111. Machado MV, Coutinho J, Carepa F, Costa A, Proença H, Cortez-Pinto H. How adiponectin, leptin, and ghrelin orchestrate together and correlate with the severity of nonalcoholic fatty liver disease. Eur J Gastroenterol Hepatol 2012; 24(10): 1166-72.

112. Kyriakides TR, Bornstein P. Matricellular proteins as modulators of wound healing and the foreign body response. Thromb Haemost 2003; 90(6): 986-92

113. Sahai A, Malladi P, Pan X Paul R, Melin-Aldana H, Green RM, Whitington PF. Obese and diabetic db/db mice develop marked liver fibrosis in a model of nonalcoholic steatohepatitis: role of short-form leptin receptors and osteopontin. Am J Physiol Gastrointest Liver Physiol 2004; 287(5): G1035-43.

114. Machado MV, Michelotti GA, Pereira TA, Xie G, Premont R, Cortez-Pinto H, Diehl AM. Accumulation of duct cells with activated YAP parallels fibrosis progression in NonAlcoholic Fatty Liver Disease. J Hepatol 2015; 63(4): 962-70

115. Saxena NK, Titus MA, Ding X, Floyd J, Srinivasan S, Sitaraman SV, Anania FA. Leptin as a novel profibrogenic cytokine in hepatic stellate cells: mitogenesis and inhibition of apoptosis mediated by extracellular regulated kinase (Erk) and Akt phosphorylation. FASEB J 2004; 18(13): 1612-4.

116. Saxena NK, Sharma D, Ding X, Lin S, Marra F, Merlin D, Anania FA. Concomitant activation of the JAK/STAT, PI3K/AKT, and ERK signaling is involved in leptin-mediated promotion of invasion and migration of hepatocellular carcinoma cells. Cancer Res 2007; 67(6): 2497-507.

117. Olinga P, Schuppan D. Precision-cut liver slices: a tool to model the liver ex vivo. J Hepatol 2013; 58(6): 1252-3.

118. Espanol-Suner R, Carpentier R, Van Hul N, Legry V, Achouri Y, Cordi S, Jacquemin P, Lemaigre F, Leclercq IA. Liver progenitor cells yield functional hepatocytes in response to chronic liver injury in mice. Gastroenterology 2012; 143: 1564-1575

119. Dolle L, Best J, Mei J, Al Battah F, Reynaert H, van Grunsven LA, Geerts A. The quest for liver progenitor cells: a practical point of view. J Hepatol 2010; 52:117-129.

120. Petersen BE, Bowen WC, Patrene KD, Mars WM, Sullivan AK, Murase N, Boggs SS, Greenberger JS, Goff JP. Bone marrow as a potential source of hepatic oval cells. Science 1999; 284: 1168-1170.

121. Oh, S.H., Witek, R.P., Bae, S.H., Zheng D, Jung Y, Piscaglia AC, Petersen BE. Bone marrow-derived hepatic oval cells differentiate into hepatocytes in 2-acetylaminofluorene/partial hepatectomy-induced liver regeneration. Gastroenterology 2007; 132: 1077-1087

122. Wood MJ, Gadd VL, Powell LW, Ramm GA, Clouston AD. The ductular reaction in hereditary haemochromatosis: The link between hepatocyte senescence and fibrosis progression. Hepatology 2014; 59(3): 848-57

123. Carpino G, Renzi A, Onori P, Gaudio E. Role of hepatic progenitor cells in nonalcoholic Fatty liver disease development: cellular cross-talks and molecular networks. Int J Mol Sci 2013; 14: 20112-20130.

124. Takahashi F, Takahashi K, Okazaki T, Maeda K, Ienaga H, Maeda M, Kon S, Uede T, Fukuchi Y. Role of osteopontin in the pathogenesis of bleomycin-induced pulmonary fibrosis. Am J Respir Cell Mol Biol 2001; 24: 264-271

125. Nagao T, Okura T, Irita J, Jotoku M, Enomoto D, Desilva VR, Miyoshi K, Kurata M, Matsui Y, Uede T, Higaki J. Osteopontin plays a critical role in interstitial fibrosis but not glomerular sclerosis in diabetic nephropathy. Nephron Extra 2012; 2: 87-103.

126. Boumans MJ, Houbiers JG, Verschueren P, Ishikura H, Westhovens R, Brouwer E, Rojkovich B, Kelly S, den Adel M, Isaacs J, Jacobs H, Gomez-Reino J, Holtkamp GM, Hastings A, Gerlag DM, Tak PP. Safety, tolerability, pharmacokinetics, pharmacodynamics and efficacy of the monoclonal antibody ASK8007 blocking osteopontin in patients with rheumatoid arthritis: a randomised, placebo controlled, proof-of-concept study. Ann Rheum Dis 2012; 71: 180-185.

127. Nilsson SK, Johnston HM, Whitty GA, Williams B, Webb RJ, Denhardt DT, Bertoncello I, Bendall LJ, Simmons PJ, Haylock DN. Osteopontin, a key component of the hematopoietic stem cell niche and regulator of primitive hematopoietic progenitor cells. Blood 2005; 106: 1232-1239.

128. Furuyama, K., Kawaguchi, Y., Akiyama, H., Horiguchi M, Kodama S, Kuhara T, Hosokawa S, Elbahrawy A, Soeda T, Koizumi M, Masui T, Kawaguchi M, Takaori K, Doi R, Nishi E, Kakinoki R, Deng JM, Behringer RR, Nakamura T, Uemoto S. Continuous cell supply from a Sox9-expressing progenitor zone in adult liver, exocrine pancreas and intestine. Nat Genet 2011; 43: 34-41.

129. Thenappan A, Li Y, Kitisin K, Rashid A, Shetty K, Johnson L, Mishra L. Role of transforming growth factor beta signaling and expansion of progenitor cells in regenerating liver. Hepatology 2010; 51: 1373-1382.

130. Lee JM, Dedhar S, Kalluri R, Thompson EW The epithelial-mesenchymal transition: new insights in signaling, development, and disease. J Cell Biol 2006; 172: 973-981.

131. Deheuninck J, Luo K. Ski and SnoN, potent negative regulators of TGF-beta signaling. Cell Res 2009; 19: 47-57.

132. Hayashi H, Abdollah S, Qiu Y, Cai J, Xu YY, Grinnell BW, Richardson MA, Topper JN, Gimbrone MA Jr, Wrana JL, Falb D. The MAD-related protein Smad7 associates with the TGFbeta receptor and functions as an antagonist of TGFbeta signaling. Cell 1997; 89: 1165-1173.

133. Chiu CC, Sheu JC, Chen CH, Lee CZ, Chiou LL, Chou SH, Huang GT, Lee HS. Global gene expression profiling reveals a key role of CD44 in hepatic oval-cell reaction after 2-AAF/CCl4 injury in rodents. Histochem Cell Biol. 2009; 132(5): 479-89.

134. Geissmann F, Cameron TO, Sidobre S, Manlongat N, Kronenberg M, Briskin MJ, Dustin ML, Littman DR. Intravascular immune surveillance by CXCR6+ NKT cells patrolling liver sinusoids. PLoS Biol 2005; 3:e113.

135. Bendelac A, Savage PB, Teyton L. The biology of NKT cells. Annu Rev Immunol 2007; 25: 297-336.

136. Swain MG. Hepatic NKT cells: friend or foe? Clin Sci (Lond) 2008;114:457-466.

137. Mallevaey T, Fontaine J, Breuilh L, Paget C, Castro-Keller A, Vendeville C, Capron M, Leite-de-Moraes M, Trottein F, Faveeuw C. Invariant and noninvariant natural killer T cells exert opposite regulatory functions on the immune response during murine schistosomiasis. Infect Immun 2007; 75: 2171-2180.

138. Park O, Jeong WI, Wang L, Wang H, Lian ZX, Gershwin ME, Gao B. Diverse roles of invariant natural killer T cells in liver injury and fibrosis induced by carbon tetrachloride. Hepatology 2009; 49: 1683-1694.

139. Jin Z, Sun R, Wei H, Gao X, Chen Y, Tian Z. Accelerated liver fibrosis in hepatitis B virus transgenic mice: involvement of natural killer T cells. Hepatology 2011; 53: 219-229.

140. Ishikawa S, Ikejima K, Yamagata H, Aoyama T, Kon K, Arai K, Takeda K, Watanabe S. CD1d-restricted natural killer T cells contribute to hepatic inflammation and fibrogenesis in mice. J Hepatol 2011; 54: 1195-1204

141. Kita H, Naidenko OV, Kronenberg M, Ansari AA, Rogers P, He XS, Koning F, Mikayama T, Van De Water J, Coppel RL, Kaplan M, Gershwin ME. Quantitation and phenotypic analysis of natural killer T cells in primary biliary cirrhosis using a human CD1d tetramer. Gastroenterology 2002; 123: 1031-1043.

142. Harada K, Isse K, Tsuneyama K, Ohta H, Nakanuma Y. Accumulating CD57 + CD3 + natural killer T cells are related to intrahepatic bile duct lesions in primary biliary cirrhosis. Liver Int 2003; 23: 94-100.

143. Nuti S, Rosa D, Valiante NM, Saletti G, Caratozzolo M, Dellabona P, Barnaba V, Abrignani S. Dynamics of intra-hepatic lymphocytes in chronic hepatitis C: enrichment for Valpha24+ T cells and rapid elimination of effector cells by apoptosis. Eur J Immunol 1998;28: 3448-3455.

144. Guebre-Xabier M, Yang S, Lin HZ, Schwenk R, Krzych U, Diehl AM. Altered hepatic lymphocyte subpopulations in obesity-related murine fatty livers: potential mechanism for sensitization to liver damage. Hepatology 2000; 31: 633-640.

145. Li Z, Soloski MJ, Diehl AM. Dietary factors alter hepatic innate immune system in mice with nonalcoholic fatty liver disease. Hepatology 2005; 42: 880-885.

146. Tajiri K, Shimizu Y, Tsuneyama K, Sugiyama T. Role of liver-infiltrating CD3+CD56+ natural killer T cells in the pathogenesis of nonalcoholic fatty liver disease. Eur J Gastroenterol Hepatol 2009; 21: 673-680.

147. Adler M, Taylor S, Okebugwu K, Yee H, Fielding C, Fielding G, Poles M. Intrahepatic natural killer T cell populations are increased in human hepatic steatosis. World J Gastroenterol 2011; 17: 1725-1731.

148. Li Z, Lin H, Yang S, Diehl AM. Murine leptin deficiency alters Kupffer cell production of cytokines that regulate the innate immune system. Gastroenterology 2002; 123: 1304-1310.

149. Philips GM, Chan IS, Swiderska M, Schroder VT, Guy C, Karaca GF, Moylan C, Venkatraman T, Feuerlein S, Syn WK, Jung Y, Witek RP, Choi S,

Michelotti GA, Rangwala F, Merkle E, Lascola C, Diehl AM. Hedgehog signaling antagonist promotes regression of both liver fibrosis and hepatocellular carcinoma in a murine model of primary liver cancer. PLoS One 2011; 6: e23943.

150. Zhao L, Li T, Wang Y, Pan Y, Ning H, Hui X, Xie H, Wang J, Han Y, Liu Z, Fan D. Elevated plasma osteopontin level is predictive of cirrhosis in patients with hepatitis B infection. Int J Clin Pract 2008; 62: 1056-1062.

151. Huang W, Zhu G, Huang M, Lou G, Liu Y, Wang S. Plasma osteopontin concentration correlates with the severity of hepatic fibrosis and inflammation in HCV-infected subjects. Clin Chim Acta 2010; 411: 675-678.

152. Gao B, Radaeva S, Park O. Liver natural killer and natural killer T cells: immunobiology and emerging roles in liver diseases. J Leukoc Biol 2009; 86(3): 513-28

153. Kronenberg M. Toward an understanding of NKT cell biology: progress and paradoxes. Annu Rev Immunol 2005; 23: 877-900.

154. Michelotti GA, Machado MV, Diehl AM. NAFLD, NASH and liver cancer. Nat Rev Gastroenterol Hepatol 2013; 10(11): 656-65

155. Hu L, Lin X, Lu H, Chen B, Bai Y. An overview of hedgehog signaling in fibrosis. Mol Pharmacol 2015; 87(2): 174-82.

156. Hirsova P, Ibrahim SH, Bronk SF, Yagita H, Gores GJ. Vismodegib suppresses TRAIL-mediated liver injury in a mouse model of nonalcoholic steatohepatitis. PLoS One 2013; 22: 8(7): e70599.

157. Angulo P, Keach JC, Batts KP, Lindor KD. Independent predictors of liver fibrosis in patients with non-alcoholic steatohepatitis. Hepatology 1999; 30: 1356–62

158. Safar Zadeh E, Lungu AO, Cochran EK, Brown RJ, Ghany MG, Heller T, Kleiner DE, Gorden P. The liver diseases of lipodystrophy: the long-term effect of leptin treatment. J Hepatol 2013; 59(1): 131-7.

159. Kahles F, Findeisen HM, Bruemmer D. Osteopontin: A novel regulator at the cross roads of inflammation, obesity and diabetes. Mol Metab 2014; 3(4): 384-93.

160. Gordin D, Forsblom C, Panduru NM, Thomas MC, Bjerre M, Soro-Paavonen A, Tolonen N, Sandholm N, Flyvbjerg A, Harjutsalo V, Groop PH; FinnDiane Study Group. Osteopontin is a strong predictor of incipient diabetic nephropathy, cardiovascular disease, and all-cause mortality in patients with type 1 diabetes. Diabetes Care 2014;37(9): 2593-600.

161. Nomiyama T, Perez-Tilve D, Ogawa D, Gizard F, Zhao Y, Heywood EB, Jones KL, Kawamori R, Cassis LA, Tschöp MH, Bruemmer D. Osteopontin mediates obesity-induced adipose tissue macrophage infiltration and insulin resistance in mice. J Clin Invest 2007; 117(10): 2877-88.

162. Kiefer FW, Neschen S, Pfau B, Legerer B, Neuhofer A, Kahle M, Hrabé de Angelis M, Schlederer M, Mair M, Kenner L, Plutzky J, Zeyda M, Stulnig TM. Osteopontin deficiency protects against obesity-induced hepatic steatosis and attenuates glucose production in mice. Diabetologia 2011; 54(8): 2132-42.

163. Zeyda M, Gollinger K, Todoric J, Kiefer FW, Keck M, Aszmann O, Prager G, Zlabinger GJ, Petzelbauer P, Stulnig TM. Osteopontin is an activator of human adipose tissue macrophages and directly affects adipocyte function. Endocrinology 2011; 152(6): 2219-27.

164. Thiery JP, Sleeman JP. Complex networks orchestrate epithelial-mesenchymal transitions. Nat Rev Mol Cell Biol 2006; 7: 131-142.

165. Yang L, Jung Y, Omenetti A, Witek RP, Choi S, Vandongen HM, Huang J, Alpini GD, Diehl AM. Fate-mapping evidence that hepatic stellate cells are epithelial progenitors in adult mouse livers. Stem Cells 2008; 26: 2104-2113.

166. Roskams T, Katoonizadeh A, Komuta M. Hepatic progenitor cells: an update. Clin Liver Dis 2010; 14: 705-718.

167. Wang KX, Denhardt DT. Osteopontin: role in immune regulation and stress responses. Cytokine Growth Factor Rev 2008; 19(5-6): 333-45

168. Fedarko NS, Jain A, Karadag A, Fisher LW. Three small integrin binding ligand N-linked glycoproteins (SIBLINGs) bind and activate specific matrix metalloproteinases. FASEB J 2004; 18(6): 734-6.

169. Pellicoro A, Ramachandran P, Iredale JP, Fallowfield JA. Liver fibrosis and repair: immune regulation of wound healing in a solid organ. Nat Rev Immunol 2014; 14(3): 181-94.

170. Stroschein SL, Wang W, Zhou S, Zhou Q, Luo K. Negative feedback regulation of TGF-beta signaling by the SnoN oncoprotein. Science 1999; 286: 771-774.

171. Fukasawa H, Yamamoto T, Togawa A, Ohashi N, Fujigaki Y, Oda T, Uchida C, Kitagawa K, Hattori T, Suzuki S, Kitagawa M, Hishida A. Ubiquitin-dependent degradation of SnoN and Ski is increased in renal fibrosis induced by obstructive injury. Kidney Int 2006; 69: 1733-1740

172. Xanthou G, Alissafi T, Semitekolou M, Simoes DC, Economidou E, Gaga M, Lambrecht BN, Lloyd CM, Panoutsakopoulou V. Osteopontin has a crucial role in allergic airway disease through regulation of dendritic cell subsets. Nat Med 2007; 13(5): 570-8

173. Weber GF, Cantor H. Differential roles of osteopontin/Eta-1 in early and late lpr disease. Clin Exp Immunol 2001; 126(3): 578-83.

174. Musso G, Paschetta E, Gambino R, Cassader M, Molinaro F. Interactions among bone, liver, and adipose tissue predisposing to diabesity and fatty liver. Trends Mol Med 2013; 19(9): 522-35

175. Lin F, Li Y, Cao J Fan S, Wen J, Zhu G, Du H, Liang Y. Overexpression of osteopontin in hepatocellular carcinoma and its relationships with metastasis, invasion of tumor cells. Mol Biol Rep 2011; 38(8): 5205-10

176. Sieghart W, Wang X, Schmid K Pinter M, König F, Bodingbauer M, Wrba F, Rasoul-Rockenschaub S, Peck-Radosavljevic M. Osteopontin expression predicts overall survival after liver transplantation for hepatocellular carcinoma in patients beyond the Milan criteria. J Hepatol 2011; 54: 89-97.